

# Drug absorption enhancement capacities and mechanisms of action of *Aloe vera* gel materials

**A Haasbroek**

 **orcid.org 0000-0001-7416-1585**

**B. Pharm**

Dissertation submitted in fulfilment of the requirements for the degree *Master of Science* in *Pharmaceutics* at the North-West University

Supervisor:

Prof JH Hamman

Co-supervisor:

Prof LH du Plessis

Graduation May 2018

Student number: 22692592

Wat julle ook al doen, doen dit van harte soos vir die Here  
en nie vir mense nie.

Kolossense 3:23

Whatever you do, do it from the heart as something done for the Lord  
and not for people.

Colossians 3:23

## ACKNOWLEDGEMENTS

I would not have been able to complete this study without the help of the following:

- My Heavenly Father for giving me the opportunity to get to know Him better and learn more about myself. Without His love, guidance and strength I would not have survived this journey.
- My supervisor, Prof Sias Hamman, for the opportunity to do this project and for your guidance, technical knowledge and expertise. I learnt so much from you.
- My co-supervisor, Prof Lissinda du Plessis, for your guidance and knowledge, and your willingness to help with anything.
- My parents, Bertus and Sarie Haasbroek, for your unconditional love and support. Thank you for always encouraging and supporting me to pursue my dreams. As well as my brother and sister, thank you for putting up with me.
- My best friend, Wihan Pheiffer, thank you for being on my team. Your love, support and encouragement these last couple of months have been invaluable. I would also like to thank you for the proof reading of this manuscript.
- Esmari and Grethe, thank you for your friendship, and for being the best flatmates anyone can ask for. Thank you for the example that you are to me, your hard work and dedication is inspiring.
- To my friends, Corneli, Carmen, Gawie, and Japie, thank you for your support and encouragement, and standing with me even when I withdraw socially.
- Thank you also to my fellow students, Jaco Heyns, Alex Laux and Michelene Swart.
- Carlemi Calitz, thank you for your willingness to help and your technical expertise.
- Dr Clarissa Willers, thank you not only for your patient guidance in the lab, but also everything I could learn from you as a person. Thank you for your assistance and guidance during my experiments.
- Dr Matthew Glyn, thank you for your knowledge and technical assistance with the confocal microscopy experiments and for helping me with this work.
- Prof Suria Ellis, from the Statistical Consultation Services at the NWU for the statistical analysis of my data.
- Mrs Anriette Pretorius, thank you for your help with the polishing of the reference list.
- Mr Chris van Niekerk curator of the NWU Botanical Garden, thank you for the supply of the *Aloe vera* plant for imaging.
- I want to acknowledge the following financial support: this study was made possible with the financial support from the North West University (NWU) and the National Research Foundation (NRF; grant nr 98939) with a grant-linked bursary from my supervisor Prof Sias (JH) Hamman.

**Disclaimer:** Any opinions, findings and conclusions, or recommendations expressed in this material are those of the authors and therefore the NRF does not accept any liability in regard thereto.

## ABSTRACT

Oral drug delivery is one of the most preferred and user friendly routes of drug administration. Macromolecular drugs (such as peptides and proteins) generally have a poor bioavailability when administered orally. Absorption enhancers can be co-administered with macromolecular drugs to increase their bioavailability by either preventing enzymatic degradation or by increasing paracellular permeability (i.e. opening tight junctions). Various natural products have been investigated as possible absorption enhancers. *Aloe vera* ((L.) Burm.f.) leaf materials and *N*-trimethyl chitosan chloride (TMC) are examples of these natural products, which have shown the ability to increase the permeation of macromolecules across Caco-2 cell monolayers.

In this study, the absorption enhancement abilities of *A. vera* gel and whole leaf extract were investigated by conducting *in vitro* transepithelial electrical resistance (TEER) and permeation studies across Caco-2 cell monolayers. For the TEER studies, Caco-2 cell monolayers were treated with different concentrations of *A. vera* gel and whole leaf extract solutions. The positive control used for the TEER study was 0.5% w/v *N*-trimethyl chitosan chloride (TMC; a known absorption enhancer) and the negative control used was media alone. The *in vitro* permeation of different molecular weight FITC-dextran molecules (i.e. 4 000 Da, 10 000 Da, 20 000 Da and 40 000 Da) was determined in the presence of different concentrations *A. vera* gel and whole leaf extract solutions to determine the capacity of absorption enhancement by the aloe leaf materials. In order to determine the mechanism of action of *A. vera* gel and whole leaf extract as drug absorption enhancers across intestinal epithelial cell monolayers, the Caco-2 cell monolayers were incubated with FITC-dextran to visualise the pathway of transport and F-actin was immunofluorescently stained to visualise if F-actin rearrangement occurred as a result of modulation by the aloe leaf materials.

The application of *A. vera* gel and whole leaf extract solutions to Caco-2 cell monolayers resulted in a pronounced decrease in the TEER by all the concentrations of the aloe leaf materials tested in this study. The *in vitro* permeation of FITC-dextran 4 000 Da was markedly higher in the presence of *A. vera* gel and whole leaf extract (in all concentrations tested) compared to that of the control group. For the higher molecular weight FITC-dextran molecules (i.e. 10 000 Da, 20 000 Da and 40 000 Da), no absorption enhancement was seen with the addition of aloe leaf materials, indicating that these larger FITC-dextran molecules have exceeded the absorption enhancement abilities of the aloe leaf materials. With the confocal laser scanning microscopy (CLSM) study, the absorption enhancement of FITC-dextran via the paracellular pathway was confirmed as well as F-actin re-arrangement. The latter confirmed the involvement of tight junction modulation as the mechanism of absorption enhancement by *A. vera* gel and whole leaf extract.

**Keywords:** Absorption enhancement; *Aloe vera*; Caco-2; CLSM; F-actin; FITC-dextran; TEER; tight junctions; paracellular permeability

## UITTREKSEL

Die orale roete is die mees verkose en gebruikervriendelike roete van geneesmiddel toediening. Makromolekulêre geneesmiddels (bv. peptiede en proteïne) het oor die algemeen 'n lae biobeskikbaarheid wanneer dit oraal toegedien word. Om hul biobeskikbaarheid te verhoog kan absorpsiebevorderaars saam met die makromolekules toegedien word. Hierdie verhoging in biobeskikbaarheid kan hoofsaaklik deur twee strategieë teweeggebring word, naamlik die voorkoming van ensiematiese afbraak en verhoogde parasellulêre transport (d.m.v. die modulering van hegte aansluitings tussen selle). Verskeie natuurlike produkte is al ondersoek as absorpsiebevorderaars. Voorbeelde van hierdie natuurlike produkte sluit *N*-trimetiel kitosaanchloried (TMC) en *Aloe vera* ((L.) Burm.f.) in. Hierdie natuurlike produkte besit bewese vermoëns om die *in vitro* transport van makromolekules oor Caco-2 selmonolae te verhoog.

In hierdie studie is die absorpsiebevorderingsvermoë van *A. vera* jel en heel blaar ekstrak ondersoek. Hierdie eienskappe is ondersoek d.m.v. transepiteel elektriese weerstand (TEEW) en *in vitro* transport studies oor Caco-2 selmonolae. Vir die TEEW studies is Caco-2 selmonolae met verskillende konsentrasies *A. vera* jel en heel blaar ekstrak oplossings ge-inkubeer. Die positiewe kontrole wat in hierdie studie gebruik is, het uit 0.5% m/v *N*-trimetiel kitosaanchloried (TMC) ('n bekende absorpsiebevorderaar) bestaan en die negatiewe kontrole was slegs media. Die *in vitro* transport van FITC-dekstraan met verskillende molekulêre massas (o.a. 4 000 Da, 10 000 Da, 20 000 Da en 40 000 Da) is oor Caco-2 selmonolae in die teenwoordigheid van verskeie konsentrasies *A. vera* jel en heel blaar ekstrak ondersoek. Die doel van die *in vitro* eksperiment was om die absorpsiebevorderingskapasiteit van *A. vera* jel en heel blaar ekstrak vas te stel. Om die werkingsmeganisme van absorpsiebevordering deur *A. vera* jel en heel blaar ekstrak te bepaal, is Caco-2 selmonolae met FITC-dekstraan 4 000 Da ge-inkubeer en is die F-aktien immunofluoreserend gekleur. Inkubasie met FITC-dekstraan 4 000 Da is gedoen om die roete van absorpsiebevordering te bevestig en die F-aktien immunofluoreserende verkleuring is gedoen om die herrangskikking van F-aktien te visualiseer, wat a.g.v. hegte aansluiting modulering deur *A. vera* jel en heel blaar ekstrak plaasvind.

'n Drastiese verlaging in die TEEW oor die Caco-2 selmonolae het as gevolg van die blootstelling aan die *A. vera* jel en heel blaar ekstrak oplossings (by alle konsentrasies wat getoets is) plaasgevind. Die *in vitro* transport van FITC-dekstraan 4 000 Da was merkbaar hoër in die teenwoordigheid van *A. vera* jel en heel blaar ekstrak oplossing (in alle konsentrasies) wanneer dit met die kontrole groep van FITC-dekstraan 4 000 Da alleen vergelyk was. Die *in vitro* transport van die FITC-dekstrane met hoë molekulêre massas (bv. 10 000 Da, 20 000 Da en 40 000 Da) het amper geen verandering getoon wanneer dit met die onderskeie kontrole groepe (FITC-dekstraan 10 000 Da, 20 000 Da of 40 000 Da alleen) vergelyk was nie. Die afleiding kan dus

gemaak word dat, hierdie molekules met hoë molekulêre massas, die absorpsiebevorderingsvermoë van *A. vera* jel en heel blaar ekstrak oorskry het. Met die konfokaal laser skanderings mikroskopie (KLSM) studie, is die verhoogde parasellulêre transport van FITC-dekstraan bevestig, asook die herrangskikking van F-aktien is waargeneem. Die laasgenoemde F-aktien herrangskikking het die rol van hegte aansluiting modulering as die werkingsmeganisme waarmee *A. vera* jel en heel blaar ekstrak absorpsiebevordering bewerkstellig, bevestig.

**Sleutelwoorde:** Absorpsiebevordering; *Aloe vera*; Caco-2 selle; F-aktien; FITC-dekstraan; hegte aansluitings; konfokaal mikroskopie; TEEW; parasellulêre deurlaatbaarheid

# TABLE OF CONTENTS

<b>ACKNOWLEDGEMENTS</b> .....	<b>II</b>
<b>ABSTRACT</b> .....	<b>IV</b>
<b>UITTREKSEL</b> .....	<b>VI</b>
<b>LIST OF TABLES</b> .....	<b>XV</b>
<b>LIST OF FIGURES</b> .....	<b>XVII</b>
<b>LIST OF EQUATIONS</b> .....	<b>XXI</b>
<b>LIST OF ABBREVIATIONS</b> .....	<b>XXII</b>
<b>CHAPTER 1: INTRODUCTION</b> .....	<b>1</b>
<b>1.1 Background and motivation</b> .....	<b>1</b>
1.1.1 Oral drug delivery .....	1
1.1.2 Drug absorption enhancement.....	1
1.1.2.1 Aloe vera .....	2
1.1.3 Models to study drug permeability .....	3
1.1.3.1 Caco-2 cell line .....	3
<b>1.2 Research problem</b> .....	<b>3</b>
<b>1.3 Aim and objectives</b> .....	<b>4</b>
1.3.1 Aim .....	4
1.3.2 Objectives.....	4
<b>1.4 Structure of this dissertation</b> .....	<b>5</b>
<b>CHAPTER 2: LITERATURE REVIEW</b> .....	<b>6</b>
<b>2.1 Introduction</b> .....	<b>6</b>
<b>2.2 Gastrointestinal tract drug absorption</b> .....	<b>6</b>
2.2.1 Pathways for gastrointestinal tract drug absorption.....	6

2.2.2	Barriers to gastrointestinal tract drug absorption.....	7
2.2.2.1	The unstirred water layer .....	8
2.2.2.2	Membranes of intestinal epithelial cells.....	8
2.2.2.3	Efflux systems .....	8
2.2.2.4	Tight junctions .....	9
<b>2.3</b>	<b>Drug absorption enhancement .....</b>	<b>9</b>
2.3.1	Chemical modification strategies to enhance drug absorption .....	10
2.3.1.1	PEGylation .....	10
2.3.1.2	Lipidization .....	11
2.3.1.3	Analogue and pro-drug formation .....	11
2.3.2	Pharmaceutical strategies to enhance drug absorption.....	11
2.3.2.1	Enzyme inhibitors .....	11
2.3.2.2	Mucoadhesive systems .....	12
2.3.2.3	Particulate carrier systems.....	12
2.3.2.4	Site-specific delivery systems .....	12
2.3.2.5	Absorption enhancers.....	12
2.3.2.5.1	Absorption enhancers of natural origin .....	13
<b>2.4</b>	<b><i>Aloe vera</i> leaf materials as drug absorption enhancers .....</b>	<b>15</b>
2.4.1	Botany .....	15
2.4.2	Phytochemistry .....	17
2.4.3	Biological activities .....	17
<b>2.5</b>	<b>Experimental models to evaluate intestinal drug permeability .....</b>	<b>19</b>
2.5.1	In vitro models .....	19

2.5.1.1	Membrane-based models .....	19
2.5.1.2	Cell-based models .....	20
2.5.1.2.1	MDCK cell line .....	20
2.5.1.2.2	LLC-PK1 cell line .....	21
2.5.1.2.3	2/4/A1 cell line .....	21
2.5.1.2.4	HT29 cell line.....	21
2.5.1.2.5	TC7 cell line.....	21
2.5.1.2.6	Caco-2 cell line .....	22
2.5.2	<i>Ex vivo</i> models .....	23
2.5.3	<i>In vivo</i> animal models .....	24
2.5.4	<i>In situ</i> models .....	24
2.5.5	<i>In silico</i> models .....	25
<b>2.6</b>	<b>Summary .....</b>	<b>25</b>
 <b>CHAPTER 3: MATERIALS AND METHODS .....</b>		<b>26</b>
<b>3.1</b>	<b>Introduction .....</b>	<b>26</b>
<b>3.2</b>	<b>Materials.....</b>	<b>26</b>
3.2.1	Aloe leaf materials .....	26
3.2.2	Caco-2 cell culturing .....	27
3.2.3	Permeation studies.....	27
3.2.4	Transepithelial electrical resistance studies .....	27
3.2.5	Confocal laser scanning microscopy study .....	27
<b>3.3</b>	<b>Validation of the fluorometric analytical method for FITC-dextran and Lucifer Yellow on the Spectramax® plate reader .....</b>	<b>28</b>

3.3.1	Linearity.....	28
3.3.2	Accuracy and precision.....	29
3.3.2.1	Accuracy.....	29
3.3.2.2	Intra-day precision .....	29
3.3.2.3	Inter-day precision .....	30
3.3.3	Limit of detection and limit of quantification.....	30
3.3.4	Specificity .....	30
<b>3.4</b>	<b>Culturing and seeding of Caco-2 cells for <i>in vitro</i> permeation studies .....</b>	<b>31</b>
3.4.1	Culturing and maintenance of Caco-2 cells.....	31
3.4.2	Seeding onto Transwell® membranes .....	32
3.4.3	Cell monolayer integrity .....	33
<b>3.5</b>	<b><i>In vitro</i> transepithelial electrical resistance (TEER) studies with aloe leaf materials.....</b>	<b>34</b>
3.5.1	Preparation of test solutions .....	34
3.5.2	TEER measurements .....	34
<b>3.6</b>	<b><i>In vitro</i> permeation studies with FITC-dextran to determine the absorption enhancement capacity of aloe leaf materials .....</b>	<b>34</b>
3.6.1	Preparation of test solutions .....	34
3.6.2	Measurement of FITC-dextran permeation .....	35
<b>3.7</b>	<b>Confocal laser scanning microscopy (CLSM) studies to determine the mechanism of drug absorption enhancement of aloe leaf materials.....</b>	<b>35</b>
3.7.1	Preparation of test solutions .....	35
3.7.2	Immunofluorescent staining.....	36
3.7.2.1	Visualisation of transport pathway .....	36

3.7.2.2	Visualization of F-actin filaments in the cytoskeleton .....	36
3.7.2.3	Preparation of samples for confocal laser scanning microscopy .....	37
3.7.2.4	Imaging with confocal laser scanning microscopy.....	37
<b>3.8</b>	<b>Data analysis and statistical evaluation.....</b>	<b>37</b>
3.8.1	Processing of the <i>in vitro</i> permeation data.....	37
3.8.2	Processing of the <i>in vitro</i> transepithelial electrical resistance data.....	38
3.8.3	Statistical evaluation of results.....	38
<b>CHAPTER 4:</b>	<b>RESULTS AND DISCUSSION.....</b>	<b>39</b>
<b>4.1</b>	<b>Introduction .....</b>	<b>39</b>
<b>4.2</b>	<b>Validation of the fluorometric analytical method for FITC-dextran and Lucifer Yellow on the Spectramax® plate reader .....</b>	<b>40</b>
4.2.1	Linearity.....	40
4.2.2	Accuracy and precision.....	41
4.2.2.1	Accuracy.....	41
4.2.2.2	Intra-day precision .....	43
4.2.2.3	Inter-day precision .....	43
4.2.3	Limit of detection (LOD) and limit of quantification (LOQ) .....	44
4.2.4	Specificity .....	46
4.2.5	Conclusion.....	46
<b>4.3</b>	<b>Cell monolayer integrity.....</b>	<b>47</b>
<b>4.4</b>	<b><i>In vitro</i> transepithelial electrical resistance (TEER) studies with aloe leaf materials.....</b>	<b>48</b>
4.4.1	<i>Aloe vera</i> gel .....	48
4.4.2	<i>Aloe vera</i> whole leaf extract.....	50

4.4.3	Conclusions from the transepithelial electrical resistance (TEER) results .....	52
<b>4.5</b>	<b><i>In vitro</i> permeation studies with FITC-dextran to determine the absorption enhancement capacity of aloe leaf materials .....</b>	<b>52</b>
4.5.1	FITC-dextran 4 000 Da .....	52
4.5.1.1	Aloe vera gel .....	52
4.5.1.2	Aloe vera whole leaf extract.....	54
4.5.2	FITC-dextran 10 000 Da .....	56
4.5.2.1	Aloe vera gel .....	56
4.5.2.2	Aloe vera whole leaf extract.....	58
4.5.3	FITC-dextran 20 000 Da .....	60
4.5.3.1	Aloe vera gel .....	60
4.5.3.2	Aloe vera whole leaf extract.....	62
4.5.4	FITC-dextran 40 000 Da .....	64
4.5.4.1	Aloe vera gel .....	64
4.5.4.2	Aloe vera whole leaf extract.....	65
4.5.5	Conclusions form <i>in vitro</i> permeation results .....	67
<b>4.6</b>	<b>Confocal laser scanning microscopy (CLSM) studies to determine the mechanism of drug absorption enhancement of aloe leaf materials.....</b>	<b>68</b>
4.6.1	Visualization of transport pathway .....	68
4.6.2	Visualization of F-actin filaments in the cytoskeleton .....	70
4.6.3	Conclusions from confocal laser scanning microscopy (CLSM) results.....	72
<b>CHAPTER 5: FINAL CONCLUSIONS AND FUTURE RECOMMENDATIONS.....</b>		<b>73</b>
<b>5.1</b>	<b>Final conclusions .....</b>	<b>73</b>
<b>5.2</b>	<b>Recommendations for future studies.....</b>	<b>74</b>

**REFERENCES..... 75**

**APPENDIX A ..... 85**

**APPENDIX B ..... 88**

**APPENDIX C ..... 95**

**APPENDIX D ..... 117**

**APPENDIX E ..... 139**

## LIST OF TABLES

<b>Table 1.1:</b> Summary of drug absorption enhancers of natural origin (Choonara <i>et al.</i> , 2014:1273; Khajuria <i>et al.</i> , 2002:229; Lemmer & Hamman, 2013:106; Li <i>et al.</i> , 2013:12889; Salama <i>et al.</i> , 2006:25; Renukuntla <i>et al.</i> , 2013:79; Werle & Bernkop-Schnürch, 2008:273) .....	2
<b>Table 2.1:</b> Selected absorption enhancers of natural origin and their suggested mechanisms of action (Borska <i>et al.</i> , 2010:864; Isoda <i>et al.</i> , 2001:160; Kang <i>et al.</i> , 2009:1205; Kesarwani & Gupta, 2013:254; Khajuria <i>et al.</i> , 2002:229; Lemmer & Hamman, 2013:106; Li <i>et al.</i> , 2013:12889; Salama <i>et al.</i> , 2006:25; Tatiraju <i>et al.</i> , 2013:56; Werle & Bernkop-Schnürch, 2008:280) .....	14
<b>Table 3.1:</b> Volume of cell suspension required for seeding out Caco-2 cells in the different Transwell® plate systems .....	33
<b>Table 3.2:</b> Required TEER values for the formation of an intact Caco-2 cell monolayer .....	33
<b>Table 3.3:</b> Excitation and emission wavelengths of the dyes and transport marker used in the confocal imaging experiments (Abcam, 2017a; Abcam, 2017b; Kotzé <i>et al.</i> , 1998:38) .....	37
<b>Table 4.1:</b> Linear regression coefficient ( $R^2$ ) values calculated from the standard curves for the selected FITC-dextran molecules and Lucifer yellow .....	41
<b>Table 4.2:</b> Percentage recovery obtained from three different FITC-dextran concentrations ..	42
<b>Table 4.3:</b> Percentage recovery obtained from three different Lucifer yellow concentrations .	42
<b>Table 4.4:</b> Mean fluorescence detection and %RSD values for a specified concentration range of FITC-dextran measured at different time points on the same day .....	43
<b>Table 4.5:</b> Mean fluorescence detection and %RSD values for a specified concentration range of Lucifer yellow measured at different time points on the same day .....	43
<b>Table 4.6:</b> Mean fluorescence detection and %RSD values for a specified concentration range of FITC-dextran measured on three consecutive days .....	44
<b>Table 4.7:</b> Mean fluorescence detection and %RSD values for a specified concentration range of Lucifer yellow measured on three consecutive days .....	44
<b>Table 4.8:</b> Average fluorescence detection and standard deviation values of the blanks (i.e. background noise) as well as slope of the standard curve for FITC-dextran .....	45

**Table 4.9:** Average fluorescence detection and standard deviation values of the blanks (i.e. background noise) as well as slope of the standard curve for Lucifer yellow ..... 45

**Table 4.10:** Percentage recovery of FITC-dextran in the presence of *Aloe vera* gel and *Aloe vera* whole leaf extract ..... 46

## LIST OF FIGURES

<b>Figure 2.1:</b> Illustration of the absorption pathways across the gastrointestinal tract: a) passive paracellular diffusion, b) endocytosis, c) carrier-mediated transport and d) passive transcellular diffusion (Adapted from Nunes <i>et al.</i> , 2016:204; produced using Servier Medical Art, <a href="http://smart.servier.com">http://smart.servier.com</a> ).....	7
<b>Figure 2.2:</b> Schematic illustration of various strategies used for drug absorption enhancement.....	10
<b>Figure 2.3:</b> <i>Aloe vera</i> ((L.) Burm.f.) plant (Courtesy of the NWU Botanical Garden).....	15
<b>Figure 2.4:</b> Anatomical sections of the <i>Aloe vera</i> leaf: a) outermost layer, b) middle layer and c) innermost layer (Courtesy of the NWU Botanical Garden).....	16
<b>Figure 2.5:</b> Flow-chart depicting the different experimental models available for studying intestinal drug permeability.....	19
<b>Figure 2.6:</b> Illustration of a Caco-2 cell monolayer grown on the filter membrane of a Transwell® system (Adapted from Sun <i>et al.</i> (2008:396) and Yang <i>et al.</i> (2017:340); produced using Servier Medical Art, <a href="http://smart.servier.com">http://smart.servier.com</a> ) .....	23
<b>Figure 4.1:</b> Percentage transport of Lucifer yellow across Caco-2 cell monolayers (n = 3) (Error bars represent SD) .....	47
<b>Figure 4.2:</b> Percentage TEER reduction at time 20 min by <i>A. vera</i> gel (0.1% w/v, 0.5% w/v, 1.0% w/v and 1.5% w/v) and TMC (0.5% w/v, positive control group) (n = 3) (Error bars represent SD) (AVG = <i>Aloe vera</i> gel) .....	48
<b>Figure 4.3:</b> Percentage TEER recovery plotted as a function of time after removal of the <i>A. vera</i> gel solutions (0.1% w/v, 0.5% w/v, 1.0% w/v and 1.5% w/v) and TMC (0.5% w/v, positive control group (n = 3) (Error bars represent SD) (AVG = <i>Aloe vera</i> gel) .....	49
<b>Figure 4.4:</b> Percentage TEER reduction at time 20 min by <i>A. vera</i> whole leaf extract (0.1% w/v, 0.5% w/v, 1.0% w/v and 1.5% w/v) and TMC (0.5% w/v, positive control group) (n = 3) (Error bars represent SD) (AVWL = <i>Aloe vera</i> whole leaf extract) .....	50
<b>Figure 4.5:</b> Percentage TEER recovery plotted as a function of time after removal of the <i>A. vera</i> whole leaf extract solutions (0.1% w/v, 0.5% w/v, 1.0% w/v and 1.5% w/v) and TMC (0.5% w/v, positive control group (n = 3) (Error bars represent SD) (AVWL = <i>Aloe vera</i> whole leaf extract) .....	51

**Figure 4.6:** Percentage transport of FITC-dextran (MW = 4 000 Da) plotted as a function of time across Caco-2 cell monolayers in the presence of *Aloe vera* gel solutions with different concentrations (n = 3; error bars represent SD) (AVG = *Aloe vera* gel, FD-4 = FITC-dextran 4 000 Da, MW = molecular weight)..... 53

**Figure 4.7:** Apparent permeability coefficient ( $P_{app}$ ) values of FITC-dextran (4 000 Da) across Caco-2 cell monolayers when applied with *Aloe vera* gel solutions. Bars marked with an asterisk (\*) indicates statistical significant differences from the negative control group ( $p < 0.05$ ) (n = 3; error bars represent SD) (AVG = *Aloe vera* gel, FD-4 = FITC-dextran 4 000 Da) ..... 53

**Figure 4.8:** Percentage transport of FITC-dextran (MW = 4 000 Da) plotted as a function of time across Caco-2 cell monolayers in the presence of *Aloe vera* whole leaf extract solutions with different concentrations (n = 3; error bars represent SD) (AVWL = *Aloe vera* whole leaf extract, FD-4 = FITC-dextran 4 000 Da; MW = molecular weight) ..... 55

**Figure 4.9:** Apparent permeability coefficient ( $P_{app}$ ) of FITC-dextran (4 000 Da) across Caco-2 cell monolayers when applied with *Aloe vera* whole leaf extract solutions. Bars marked with an asterisk (\*) indicates statistical significant differences from the negative control group ( $p < 0.05$ ) (n = 3; error bars represent SD) (AVWL = *Aloe vera* whole leaf extract, FD-4 = FITC-dextran 4 000 Da)..... 55

**Figure 4.10:** Percentage transport of FITC-dextran (MW = 10 000 Da) plotted as a function of time across Caco-2 cell monolayers in the presence of different concentrations *Aloe vera* gel (n = 3; error bars represent SD) (AVG = *Aloe vera* gel, FD-10 = FITC-dextran 10 000 Da, MW = molecular weight) ..... 57

**Figure 4.11:** The effect of different concentrations *Aloe vera* gel on the transport ( $P_{app}$  values) of FITC-dextran (10 000 Da) across Caco-2 cell monolayers in the presence of different concentrations *Aloe vera* gel solutions. Bars marked with an asterisk (\*) indicates statistical significant differences from the negative control group (FD-10 alone) ( $p < 0.05$ ) (n = 3; error bars represent SD) (AVG = *Aloe vera* gel, FD-10 = FITC-dextran 10 000 Da, MW = molecular weight)..... 57

**Figure 4.12:** Percentage transport of FITC-dextran (MW = 10 000 Da) plotted as a function of time across Caco-2 cell monolayers in the presence of *Aloe vera* whole leaf extract solutions with different concentrations (n = 3; error bars represent SD) (AVWL = *Aloe vera* whole leaf extract, FD-10 = FITC-dextran 10 000 Da, MW = molecular weight) ..... 59

**Figure 4.13:** Apparent permeability coefficient ( $P_{app}$ ) values of FITC-dextran (10 000 Da) across Caco-2 cell monolayers in the presence of *Aloe vera* whole leaf extract solutions with different concentrations. Bars marked with an asterisk (\*) indicates statistical significant differences from the negative control group (FD-10 alone) ( $p < 0.05$ ) ( $n = 3$ ; error bars represent SD) (AVWL = *Aloe vera* whole leaf extract, FD-10 = FITC-dextran 10 000 Da)..... 59

**Figure 4.14:** Percentage transport of FITC-dextran (MW = 20 000 Da) plotted as a function of time across Caco-2 cell monolayers in the presence of *Aloe vera* gel solutions in different concentrations ( $n = 3$ ; error bars represent SD) (AVG = *Aloe vera* gel, FD-20 = FITC-dextran 20 000 Da, MW = molecular weight)..... 61

**Figure 4.15:** Apparent permeability coefficient ( $P_{app}$ ) values of FITC-dextran (20 000 Da) across Caco-2 cell monolayers in the presence of different concentrations *Aloe vera* gel solutions. Bars marked with an asterisk (\*) indicates statistical significant differences from the negative control group ( $p < 0.05$ ) ( $n = 3$ ; error bars represent SD) (AVG = *Aloe vera* gel, FD-20 = FITC-dextran 20 000 Da)..... 61

**Figure 4.16:** Percentage transport of FITC-dextran (MW = 20 000 Da) plotted as a function of time across Caco-2 cell monolayers in the presence of different concentrations *Aloe vera* whole leaf extract solutions ( $n = 3$ ; error bars represent SD) (AVWL = *Aloe vera* whole leaf extract, FD-20 = FITC-dextran 20 000 Da, MW= molecular weight) ..... 62

**Figure 4.17:** Apparent permeability coefficient ( $P_{app}$ ) values of FITC-dextran (20 000 Da) across Caco-2 cell monolayers in the presence of *Aloe vera* whole leaf extract solutions with different concentrations. Bars marked with an asterisk (\*) indicates statistical significant differences from the negative control group ( $p < 0.05$ ) ( $n = 3$ ; error bars represent SD) (AVWL = *Aloe vera* whole leaf extract, FD-20 = FITC-dextran 20 000 Da)..... 63

**Figure 4.18:** Percentage transport of FITC-dextran (MW = 40 000 Da) plotted as a function of time across Caco-2 cell monolayers in the presence of *Aloe vera* gel solutions with different concentrations ( $n = 3$ ; error bars represent SD) (AVG = *Aloe vera* gel, FD-40 = FITC-dextran 40 000 Da, MW= molecular weight)..... 64

**Figure 4.19:** Apparent permeability coefficient ( $P_{app}$ ) values of FITC-dextran (40 000 Da) across Caco-2 cell monolayers in the presence of different concentrations *Aloe vera* gel solutions. Bars marked with an asterisk (\*) indicates statistical significant differences from the negative control group ( $p < 0.05$ ) ( $n = 3$ ; error bars represent SD) (AVG = *Aloe vera* gel, FD-40 = FITC-dextran 40 000 Da)..... 65

**Figure 4.20:** Percentage transport of FITC-dextran plotted (40 000 Da) as a function of time across Caco-2 cell monolayers in the presence of *Aloe vera* whole leaf extract solutions with different concentrations (n = 3; error bars represent SD) (AVWL = *Aloe vera* whole leaf extract, FD-40 = FITC-dextran 40 000 Da)..... 66

**Figure 4.21:** Apparent permeability coefficient ( $P_{app}$ ) values of FITC-dextran (40 000 Da) across Caco-2 cell monolayers in the presence of *Aloe vera* whole leaf extract solutions with different concentrations. Bars marked with an asterisk (\*) indicates statistical significant differences from the negative control group ( $p < 0.05$ ) (n = 3; error bars represent SD) (AVWL = *Aloe vera* whole leaf extract, FD-40 = FITC-dextran 40 000 Da)..... 66

**Figure 4.22:** Top-view confocal micrograph images of Caco-2 cell monolayers on which FITC-dextran 4000 Da (FD-4) was applied (**green:** FITC-dextran 4000 Da and **red:** cell nuclei stained with propidium iodide). **a)** Negative control (FD-4 alone), **b)** positive control (0.5% w/v TMC), **c)** *A. vera* gel (1.0% w/v) and **d)** *A. vera* whole leaf extract (1.0% w/v) (Scale bars represents 10  $\mu$ m) ..... 69

**Figure 4.23:** Confocal micrograph images of F-actin distribution in Caco-2 cell monolayers (**green:** F-actin stained with CytoPainter<sup>®</sup> Phalloidin iFluor 488 and **red:** cell nuclei stained with propidium iodide). **a)** Negative control (untreated Caco-2 cell monolayer), **b)** positive control (0.5% w/v TMC), **c)** 1.0% w/v *A. vera* gel and **d)** 1.0% w/v *A. vera* whole leaf extract (Scale bars represents 10  $\mu$ m) ..... 71

## LIST OF EQUATIONS

<b>Equation 1:</b>	$y = mx + c$ .....	28
<b>Equation 2:</b>	$\%RSD = \frac{SD}{Average} \times 100$ .....	29
<b>Equation 3:</b>	$LOD = 3.3 \times \frac{SD}{Slope}$ .....	30
<b>Equation 4:</b>	$LOD = 10 \times \frac{SD}{Slope}$ .....	30
<b>Equation 5:</b>	$C_1 \times V_1 = C_2 \times V_2$ .....	32
<b>Equation 6:</b>	$\%Transport = \frac{\text{Drug concentration at specific time interval}}{\text{Initial FITC-dextran dose}} \times 100$ .....	38
<b>Equation 7:</b>	$P_{app} = \frac{dc}{dt} \frac{1}{(A.60.C_0)}$ .....	38
<b>Equation 8:</b>	$DQ (\%) = \left[ \left( \frac{J^{TM}}{J^H} \right) \times \frac{1}{9} \right] \times 100$ .....	88

## LIST OF ABBREVIATIONS

2/4/A1	Conditionally immortalized rat intestinal cell line
ABC	ATP-binding cassette
ABCB1	ATP-binding cassette subfamily B member 1
ABCB4	ATP-binding cassette subfamily B member 4
AMI	Artificial membrane insert
ANOVA	Analysis of variance
API	Active pharmaceutical ingredient
ATP	Adenosine triphosphate
AUC	Area under the curve
AVG	<i>Aloe vera</i> gel
AVWL	<i>Aloe vera</i> whole leaf extract
BCS	Biopharmaceutics Classification System
Caco-2	Human colon adenocarcinoma cell line
CLSM	Confocal laser scanning microscopy
CYP3A	Cytochrome P450 subfamily 3A
CYP450	Cytochrome P450
Da	Dalton (g/mol)
DMEM	Dulbecco's Modified Eagles Medium
DMSO	Dimethyl sulfoxide
ECACC	European Collection of Cell Cultures
EDTA	Ethylenediaminetetraacetic acid

EGTA	Ethylene glycol tetraacetic acid
F-actin	Filamentous actin
FBS	Foetal bovine serum
FD-4	FITC-dextran 4 000 Da
FD-10	FITC-dextran 10 000 Da
FD-20	FITC-dextran 20 000 Da
FD-40	FITC-dextran 40 000 Da
FITC	Fluorescein isothiocyanate
<sup>1</sup> H-NMR	Proton nuclear magnetic resonance
HEPES	2-[4-(2-hydroxyethyl)piperazin-1-y]ethanesulfonic acid
HT29	Human colon adenocarcinoma cell line with epithelial morphology
ICH	International Conference on Harmonisation
KLSM	Konfokaal laser skanderings mikroskopie
LLC-PK1	Lewis lung carcinoma-porcine kidney 1 cell line
LOD	Limit of detection
LOQ	Limit of quantification
MDCK	Madin-Darby canine kidney cell line
MDR1	Multidrug resistance gene 1
MDR2,3	Multidrug resistance gene 2, 3
MW	Molecular weight
NEAA	Non-essential amino acids
PAMPA	Parallel artificial membrane permeability assay
P <sub>app</sub>	Apparent permeability coefficient

PBS	Phosphate buffered saline
PEG	Polyethylene glycol
PKC	Protein-kinase C
P-gp	P-glycoprotein
R <sup>2</sup>	Regression coefficient
RCF	Relative centrifugal force
RSD	Relative standard deviation
SD	Standard deviation
TC7	Caco-2 cell sub-clone
TEER	Transepithelial electrical resistance
TEEW	Transepiteel elektriese weerstand
TMC	<i>N</i> -trimethyl chitosan chloride / <i>N</i> -trimetiel kitosaanchloried
USP	United States Pharmacopeial Convention
ZO-1	Zonula occludens-1
ZOT	Zonula Occludens toxin

# CHAPTER 1: INTRODUCTION

## 1.1 Background and motivation

### 1.1.1 Oral drug delivery

Oral drug delivery is the route of administration that has the highest patient compliance (Park *et al.*, 2011:280), making it the most popular route for delivering drugs systemically. Even though it is relatively easy to administer drugs via the oral route, there are still a few challenges involved of which the biggest challenge is perhaps the lack of sufficient absorption of certain drugs (e.g. macromolecular drugs) (Park *et al.*, 2011:280). The poor bioavailability of these drugs after oral administration can be attributed to enzymatic degradation and poor membrane permeability due to their unfavourable physico-chemical characteristics such as hydrophilicity and large molecular weight (Beneke *et al.*, 2012:476; Wallis *et al.*, 2014:1087).

There are two main routes of drug permeation across the epithelium of the gastrointestinal tract, namely the paracellular and the transcellular pathways (Rosenthal *et al.*, 2012a:2791). The transcellular pathway is mainly responsible for the absorption of relatively small lipophilic molecules that can permeate through the membranes of the cells (Kotzé *et al.*, 1998:36). Conversely, the paracellular pathway occurs through the tight junctions and intercellular spaces between the cells (Krug *et al.*, 2009:2202). Tight junctions (zonula occludens) represent one of three intercellular complexes that link epithelial cells together and can be described as a multi-protein complex consisting of various transmembrane proteins. The main transmembrane proteins of the tight junctions are occludin, tricellulin and the claudin family (Tscheik *et al.*, 2013:2). Tight junctions are dynamic structures that can be modulated by different stimuli, which can result in increased paracellular absorption of drug molecules in a potentially safe and reversible manner (Lemmer & Hamman, 2013:104).

### 1.1.2 Drug absorption enhancement

Absorption enhancement is the process of improving the bioavailability of orally administered drugs (Hamman *et al.*, 2005:166). Approaches that can be implemented to improve oral peptide and protein drug delivery include chemical and pharmaceutical (i.e. formulation) strategies (Wallis *et al.*, 2014:1087). The chemical approach includes the development of analogues, the formation of pro-drugs and the conjunction with natural or synthetic polymers (Hamman *et al.*, 2005:168). The formulation approach involves the inclusion of absorption enhancers in dosage forms as well as the design of novel preparations that can carry the drug molecules across the epithelial membranes (Beg *et al.*, 2011:693). Absorption enhancers can be defined as substances that are capable of promoting or improving absorption of drugs for increased oral bioavailability without causing tissue damage. The mechanisms by which drug absorption enhancers increase oral

bioavailability include decreasing mucus viscosity, disrupting the structural integrity of the intestinal wall, increasing membrane fluidity and modulating the tight junctions (Renukuntla *et al.*, 2013:79).

Various compounds have been investigated as absorption enhancers, such as fatty acids, bile salts, chelators, surfactants, cationic and anionic polymers, and compounds of natural origin (Kesarwani & Gupta, 2013:256; Renukuntla *et al.*, 2013:79). Absorption enhancers of natural origin can either be derived from plants or animals. A list of compounds of natural origin that have been investigated as drug absorption enhancers is given in Table 1.1.

**Table 1.1:** Summary of drug absorption enhancers of natural origin (Choonara *et al.*, 2014:1273; Khajuria *et al.*, 2002:229; Lemmer & Hamman, 2013:106; Li *et al.*, 2013:12889; Salama *et al.*, 2006:25; Renukuntla *et al.*, 2013:79; Werle & Bernkop-Schnürch, 2008:273)

Plant origin	Animal origin
<i>Aloe vera</i> Capsaicin ( <i>Capsicum</i> ) Genistein Piperine ( <i>Piper longum</i> or <i>P. nigrum</i> ) Quercetin Sinomenine ( <i>Sinomenium acutum</i> ) Turmeric ( <i>Curcuma longa</i> )	Chitosan and its derivatives Zonula Occludens toxin (ZOT)

### 1.1.2.1 *Aloe vera*

The *Aloe vera* ((L.) Burm.f.) (synonym *Aloe barbadensis* (Miller)) plant has been used in traditional medicine for almost 2000 years. *A. vera* has been credited with medicinal properties such as anti-cancer, anti-tumour, anti-fungal and anti-inflammatory activities (Boudreau & Beland, 2006:104). There are three parts of the *A. vera* plant that is used for medicinal purposes namely the gel, whole leaf and latex (Chen *et al.*, 2009:588). The gel is a colourless fraction originating from the innermost part or pulp of fresh *A. vera* leaves (Beneke *et al.*, 2012:476).

Research has been done on the potential pharmacokinetic interactions when *A. vera* products are taken simultaneously with prescription medications. Vinson *et al.* (2005:764) conducted a study to evaluate the effect of *A. vera* liquid preparations on the absorption of vitamin C and E in human subjects and they found that *A. vera* markedly improved the oral bioavailability of both these vitamins. Different mechanisms of action have been suggested by which the aloe leaf materials can enhance absorption of drug molecules such as the opening of the tight junctions, modulation of P-glycoprotein (P-gp) efflux and metabolic inhibition (Beneke *et al.*, 2012:481; Chen *et al.*, 2009:589; Wallis *et al.*, 2016:9). However, Djuv and Nilsen (2008:1626) conducted a variety

of experiments to determine the effect of *A. vera* juice on the inhibition of P-gp transport of digoxin and concluded that the effect was not statistically significant.

### 1.1.3 Models to study drug permeability

The following experimental models exist which are used for research pertaining to intestinal drug permeation (Alqahtani *et al.*, 2013:1; Cabrera-Pérez *et al.*, 2016:17; Yang *et al.*, 2017:338):

- *In vitro* models include cell culture-or membrane-based models. Some cell cultures frequently used for drug permeability studies are Caco-2 (human colon adenocarcinoma) cells, MDCK (Madin-Darby canine kidney) cells, TC7 (a Caco-2 cell sub-clone) cells, and LLC-PK1 (Lewis lung carcinoma-porcine kidney 1) cells.
- *Ex vivo* models involve predominantly excised animal tissue (of different origins) mounted in different devices for permeability experiments.
- *In vivo* models involve whole animals such as pigs, monkeys, dogs, mice, and rats.
- *In situ* models refer to the use of an isolated segment of the intestine that is still part of the animal (usually perfusion studies conducted in anaesthetised animals), e.g. to determine regional differences in intestinal permeation.
- *In silico* models refer to computer software programs that predict oral drug disposition by using *in vivo* and *in vitro* pharmacokinetic data.

#### 1.1.3.1 Caco-2 cell line

The Caco-2 cell line is one of the most frequently used cell cultures for *in vitro* drug transport studies, as it is easily maintained and consists of enterocyte-like and well-characterised epithelial cells (Sun *et al.*, 2008:406). Caco-2 cells grow in culture to form a polarized monolayer, each cell showing a cylindrical morphology with apical microvilli and tight junctions between neighbouring cells. These cells also express small intestinal transporters (i.e. P-gp) and enzymes such as hydrolases, several transferases, cytochrome P450 (CYP450) isoenzymes and aminopeptidase N (Antunes *et al.*, 2013:8; Sambuy *et al.*, 2005:2). Challenges associated with the Caco-2 cell line include the relatively long time it takes to develop tight junctions (generally 21 days), the wide variety of cell passages used in different research groups as well as the relatively low expression of the CYP3A enzyme (Alqahtani *et al.*, 2013:3).

## 1.2 Research problem

Patient compliance can be improved with respect to chronic peptide drug therapy if injections can be replaced with effective oral dosage forms. One promising approach to deliver peptide drugs via the oral route of administration is the inclusion of drug absorption enhancers in dosage forms

together with the active pharmaceutical ingredient. As mentioned before, it has been shown by a number of studies in different models that *A. vera* leaf materials (i.e. gel and whole leaf extract) possess the ability to enhance drug permeation across the intestinal epithelium. However, the capacity of drug absorption enhancement in terms of the size of macromolecular compounds for which permeation can be enhanced across the intestinal epithelium is not yet known. Furthermore, information regarding the exact mechanism of action of *A. vera* leaf materials in terms of drug absorption enhancement across the intestinal epithelium is also lacking.

### **1.3 Aim and objectives**

#### **1.3.1 Aim**

The aim of this study can be divided into the following two main aspects:

- To determine the drug absorption enhancement capacity of *A. vera* gel and whole leaf extract in terms of the molecular size of the compound that can be permeated across the intestinal epithelium,
- To determine the mechanism of action of drug absorption enhancement of *A. vera* gel and whole leaf extract.

#### **1.3.2 Objectives**

The following objectives have been considered necessary in order to reach the main aim:

- a) To culture Caco-2 cell monolayers on the filter membranes of Transwell®-and Snapwell®-plates.
- b) To conduct transepithelial electrical resistance (TEER) studies across Caco-2 cell monolayers in the absence and presence *A. vera* gel and whole leaf extract, as well as a positive control group (*N*-trimethyl chitosan chloride (TMC)).
- c) To conduct permeation studies in the apical-to-basolateral direction with a range of FITC-dextran molecules with varying molecular weights (i.e. 4 000 Da, 10 000 Da, 20 000 Da and 40 000 Da) across Caco-2 cell monolayers in the absence and presence of *A. vera* gel and whole leaf extract.
- d) To visualize Caco-2 cell monolayers treated with FITC-dextran (4 000 Da) in the absence and presence of *A. vera* gel and whole leaf extract by means of confocal laser scanning microscopy (CLSM) in order to determine the pathway of drug absorption enhancement.
- e) To conduct immunofluorescent staining studies on Caco-2 cell monolayers treated with *A. vera* gel and whole leaf extract in order to determine if the opening of tight junctions by means of F-actin filament modulation is the mechanism of drug absorption enhancement.

#### **1.4 Structure of this dissertation**

Chapter 1 outlines the background to place the study in context of the field as well as to state the research problem, the aim and objectives. This is followed by a literature review in Chapter 2, detailing the mechanisms of drug absorption, the different strategies that exist for gastrointestinal absorption enhancement of protein drugs, the role that *A. vera* leaf materials plays in absorption enhancement and different models available for determining intestinal drug permeation. The methods and materials used to execute the experiments in order to collect data for the study are given in Chapter 3. In Chapter 4, the results obtained is reported, interpreted and discussed, with the final conclusions and future recommendations given in Chapter 5.

## CHAPTER 2: LITERATURE REVIEW

### 2.1 Introduction

Drugs can be delivered systemically via various administration methods, for example, the oral, transdermal, intravenous, sublingual and inhalation routes of administration are commonly used to effectively treat patients (Choonara *et al.*, 2014:1271). Of all the routes of drug administration available, oral drug delivery remains the most preferred method with the highest patient compliance (Park *et al.*, 2011:280). Advantages associated with oral drug delivery that promote high compliance for self-treatment in patients include its ease of use and its non-invasive nature (Griffin *et al.*, 2016:368). Further advantages associated with oral drug administration include the financial implications, since lower costs are normally associated with the manufacture of solid oral dosage forms than with sterile dosage forms (Maher & Brayden, 2012:e113). On the other hand, one of the biggest challenges involved in oral drug administration is the low bioavailability of certain drugs (e.g. macromolecular drugs) (Park *et al.*, 2011:280). The relatively low bioavailability of macromolecular drugs (including peptide and protein drugs) can be ascribed to their unfavourable physico-chemical properties such as high molecular weight and hydrophilicity (Park *et al.*, 2011:280), as well as the harsh gastrointestinal environment where enzymatic activity causes extensive degradation (Sánchez-Navarro *et al.*, 2016:1).

Macromolecular drugs can be defined as molecules with a molecular weight greater than 1000 Da (Moroz *et al.*, 2016:109). The large molecular weight of peptides and proteins is considered the main obstacle for delivering them via the oral route of administration as bioavailability decreases substantially for drugs with a molecular weight above 500 Da (Muheem *et al.*, 2016:415; Park *et al.*, 2010:67; Renukuntla *et al.*, 2013:77). Peptides are generally classified into class III (low permeability and high solubility) by the Biopharmaceutic Classification System (BCS) (Wallis *et al.*, 2014:1087).

### 2.2 Gastrointestinal tract drug absorption

#### 2.2.1 Pathways for gastrointestinal tract drug absorption

In order for an orally administered drug to have its desired effect, the drug must reach the systemic circulation via absorption through the intestinal epithelial cells (Zhu *et al.*, 2017:382). Drug transport across intestinal epithelial cells can occur via two main pathways, namely the paracellular and transcellular pathways as illustrated in Figure 2.1 (Cabrera-Peréz *et al.*, 2016:4; Rosenthal *et al.*, 2012a:2791). The paracellular pathway is the transport of drug molecules between epithelial cells and occurs by means of size-limited passive diffusion. The transcellular pathway is the transport of drug molecules through the epithelial cells via passive diffusion, endocytosis or carrier-mediated transport (active or facilitated diffusion) (Cabrera-Peréz *et al.*,

2016:4). Hydrophilic macromolecules such as peptide and protein drugs are mainly transported via the paracellular route since they cannot penetrate cell membranes (Artursson *et al.*, 2012:281; Rosenthal *et al.*, 2012a:2791), but their paracellular movement is severely restricted by the tight junctions between adjacent epithelial cells (Lin *et al.*, 2007:1). Rosenthal *et al.* (2012a:2791) noted that a promising approach to improve the oral absorption of these hydrophilic macromolecules is the co-administration of absorption enhancers.

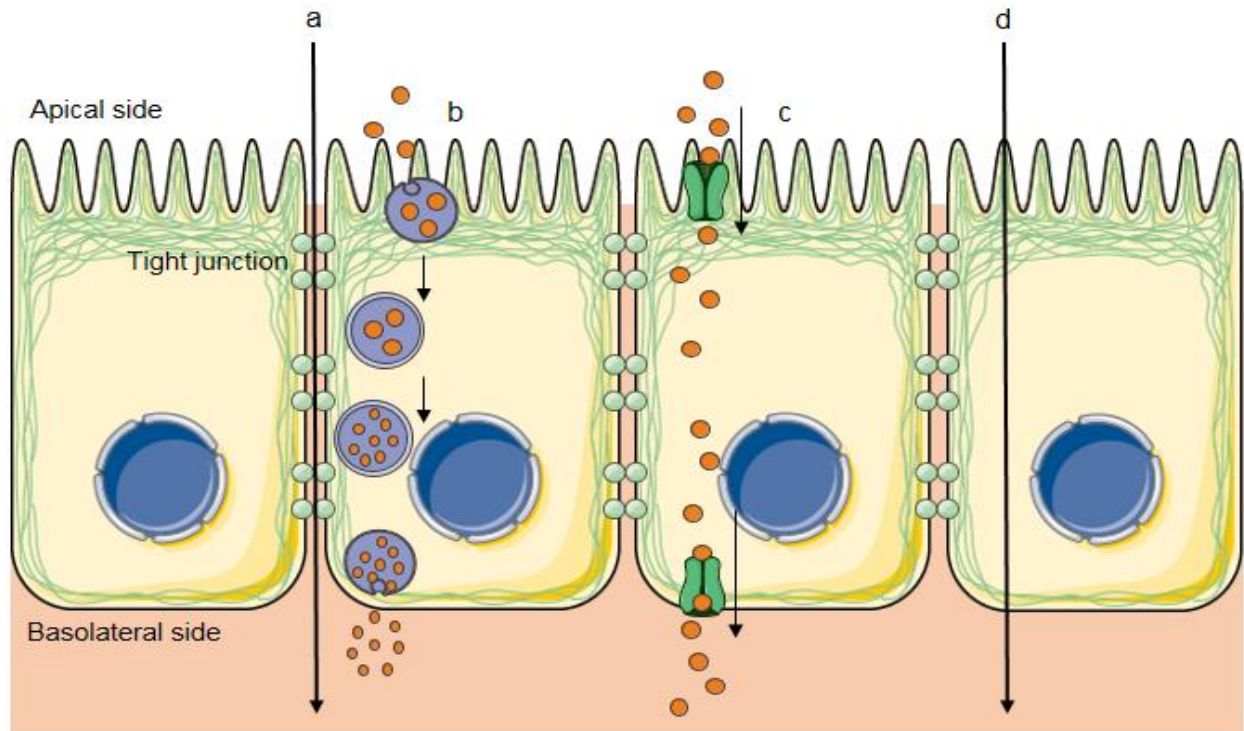


**Figure 2.1:** Illustration of the absorption pathways across the gastrointestinal tract: a) passive paracellular diffusion, b) endocytosis, c) carrier-mediated transport and d) passive transcellular diffusion (Adapted from Nunes *et al.*, 2016:204; produced using Servier Medical Art, <http://smart.servier.com>)

## 2.2.2 Barriers to gastrointestinal tract drug absorption

Peptide drug absorption is limited by several barriers including biochemical and physical obstacles presented by the gastrointestinal tract (Beg *et al.*, 2011:692; Hamman *et al.*, 2005:166). The biochemical barrier is characterized by the degradation of peptides and proteins, which includes metabolic activities by secreted and non-secreted enzymes in the gastrointestinal fluids and epithelia. The biological value of the metabolic activities of these enzymes is to break up proteins into smaller, absorbable oligopeptides and amino acids (Mahato *et al.*, 2003:155). Physical barriers include the poor solubility of macromolecules in the gastrointestinal fluid as well as the size, charge and hydrophobicity limitations that the biological membrane poses (Mahato *et al.*, 2003:155). The physical barriers of the gastrointestinal tract to drug absorption can be divided into four categories namely i) the unstirred water layer, ii) epithelial membranes of

intestinal epithelial cells, iii) efflux systems and iv) tight junctions (Aungst, 2012:12; Kesarwani & Gupta, 2013:254).

### **2.2.2.1 The unstirred water layer**

The epithelial cells of the intestine are covered with an aqueous layer which can be found directly next to the intestinal wall, which comprises of mucus, water, and glycocalyx. It has been shown that the stagnant water layer is of little importance in *in vivo* bioavailability studies, but the mucus layer might cause some difficulty to the absorption of peptides and proteins (Hamman *et al.*, 2005:167). The mucus gel layer is made up of mucins (glycoproteins) with relatively high molecular weights that can interact with drug molecules trying to cross the intestinal wall or by stabilizing the unstirred water layer (Lundquist & Artursson, 2016:259).

### **2.2.2.2 Membranes of intestinal epithelial cells**

For a drug to be absorbed by the transcellular pathway, the molecules should pass through the cell membrane by means of passive diffusion, vesicular transport or carrier-mediated transport. The epithelial cell membranes are semi-permeable as a result of their phospholipid bilayer structure. The transport of lipophilic molecules is favoured across the phospholipid layers of the cell membrane, while hydrophilic molecules are excluded (Mahato *et al.*, 2003:166). Generally, molecular weight and hydrophilic properties of molecules play an important role in the partitioning of molecules into the cell membrane. If large, hydrophilic molecules are not recognised by an active transport carrier system, their transport is restricted to diffusion through the intercellular spaces (i.e. the paracellular pathway). However, the movement of large molecular weight molecules through the intercellular spaces is highly restricted by tight junctions (Hamman *et al.*, 2005:167; Rosenthal *et al.*, 2012b:86; Ward *et al.*, 2000:346).

### **2.2.2.3 Efflux systems**

Efflux active transporter systems such as P-glycoprotein (P-gp) are expressed in a wide variety of human tissues, i.e. the blood-brain barrier, the adrenal gland, the luminal surface of the renal proximal tubule, and intestinal epithelial cells of the colon and small intestine (Amin, 2013:28; Zolnericks *et al.*, 2011:3055). P-glycoprotein (P-gp) is the best characterised member of the ATP-binding cassette (ABC) superfamily and act as a physiological barrier to orally administered drugs (Weinheimer *et al.*, 2017:14; Werle *et al.*, 2009:1644). Two-isoforms of P-gp are expressed in humans, class I isoform (MDR1/ABCB1) are drug transporters, whereas class II isoforms (MDR2,3/ABCB4) are responsible for the transport of phosphatidylcholine into the bile (Amin, 2013:28). Some xenobiotics and toxins that are substrates of P-gp have reduced absorption and oral bioavailability, as P-gp is responsible for the extrusion of these molecules from cells into the

gastrointestinal tract, thereby decreasing intracellular accumulation (Sharom, 2011:163; Weinheimer *et al.*, 2017:14).

#### **2.2.2.4 Tight junctions**

As mentioned before, the paracellular drug absorption pathway is characterized by the transport of drug molecules through the intercellular spaces between neighbouring intestinal cells (Artursson *et al.*, 2012:282; Hamman *et al.*, 2005:167). The intercellular spaces between neighbouring epithelial cells have received growing interest for the delivery of peptides and proteins as a result of their lack of proteolytic activity (Hamman *et al.*, 2005:167; Ward *et al.*, 2000:347). Unfortunately, diffusion of drug molecules through the intercellular spaces is restricted by tight junctions in a charge-specific and molecular-size manner (Hochman & Artursson, 1994:253). Tight junctions (zonula occludens) are one of three intercellular complexes, with adherence junctions (zonula adherens) and desmosomes (macula adherens), that link epithelial cells together. Tight junctions can be described as a dynamic multi-protein complex structures consisting of various transmembrane proteins, with the main proteins being occludin, tricellulin and the claudin family (Lemmer & Hamman, 2013:104; Tscheik *et al.*, 2013:2). The dynamic nature of the tight junctions ensures that it can be modulated by different stimuli, resulting in an increased paracellular absorption in a reversible and potentially safe manner (Lemmer & Hamman, 2013:104).

### **2.3 Drug absorption enhancement**

Oral drug absorption enhancement can be defined as the process of improving the bioavailability of orally administered drugs by increasing the movement of drug molecules across the intestinal epithelium. This improved membrane permeation should be accomplished without damaging the cells or causing toxic effects (Hamman *et al.*, 2005:166). The aim of absorption enhancement strategies is to limit enzymatic degradation and to increase intestinal absorption, thus overcoming the biochemical and physical barriers that exist in the gastrointestinal tract. This can be achieved by means of different chemical modifications or different pharmaceutical (i.e. formulation) strategies as illustrated in Figure 2.2 (Beg *et al.*, 2011:693; Choonara *et al.*, 2014:1273; Renukuntla *et al.*, 2013:87; Wallis *et al.*, 2014:1088).

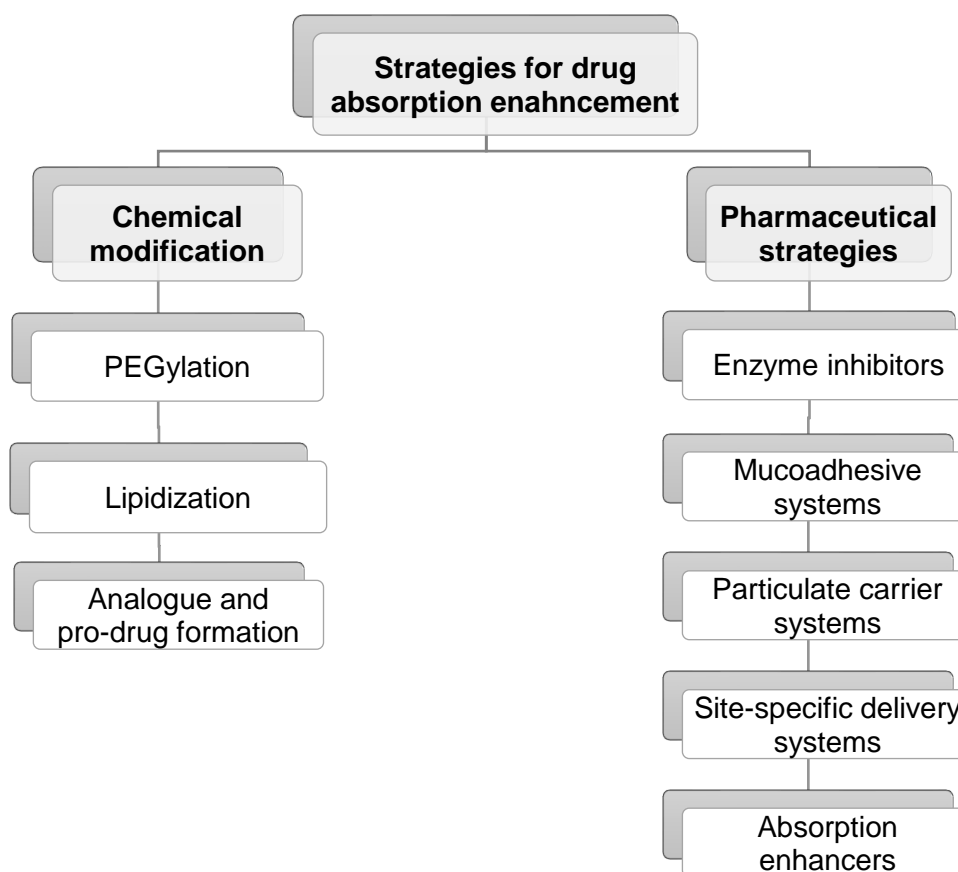


**Figure 2.2:** Schematic illustration of various strategies used for drug absorption enhancement

### 2.3.1 Chemical modification strategies to enhance drug absorption

The aim of chemical strategies to enhance drug absorption is to improve the enzymatic stability, immunogenicity and intestinal permeability of drug molecules by means of changing their chemical structures (Renukuntla *et al.*, 2013:87). This can be achieved through a variety of chemical reactions or processes such as PEGylation, lipidization, formation of analogues and pro-drugs (Choonara *et al.*, 2014:1273; Renukuntla *et al.*, 2013:87; Wallis *et al.*, 2014:1088).

#### 2.3.1.1 PEGylation

The most frequently implemented chemical modification of peptides to render them resistant against enzymatic degradation is the conjugation with polyethylene glycol (PEG) (Aguirre *et al.*, 2016:229). This modification results in a steric shield that protects the protein against some proteolytic activity, resulting in increased enzymatic stability. Subsequently, less frequent drug administration is necessary and lower immunogenicity is experienced (Aguirre *et al.*, 2016:229; Choonara *et al.*, 2014:1274).

### **2.3.1.2 Lipidization**

A common chemical modification that is used to change the characteristics of protein and peptide molecules is lipidization, which is an increase in the lipophilicity of the molecules by means of chemical modification. This usually involves the conjugation of peptides and protein molecules with fatty acids (Renukuntla *et al.*, 2013:87; Wallis *et al.*, 2014:1089). The increased lipophilicity of the proteins result in enhanced passive transcellular permeation, increased metabolic stability and bioavailability (Mahato *et al.*, 2003:177; Renukuntla *et al.*, 2013:87; Wallis *et al.*, 2014:1089).

### **2.3.1.3 Analogue and pro-drug formation**

Pro-drugs are defined as pharmacologically inactive compounds that are converted to active drugs during or directly after the absorption process in the patient (Hamman *et al.*, 2005:168; Renukuntla *et al.*, 2013:88). The aim of the design of pro-drugs is to improve solubility, permeability and stability of the parent drug. The complex macromolecular structure and instability of peptides and proteins as well as lack of novel methodology have hampered the advances made in the pro-drug formation of peptides and proteins (Muheem *et al.*, 2016:419; Renukuntla *et al.*, 2013:88).

## **2.3.2 Pharmaceutical strategies to enhance drug absorption**

Pharmaceutical strategies to enhance drug absorption consist of various formulation approaches, which are aimed at protecting peptide and protein molecules from enzymatic degradation, while increasing their intestinal epithelial permeation. Formulation strategies involve the co-administration of enzyme inhibitors and absorption enhancers, design of mucoadhesive polymeric drug delivery systems that prolong the retention time of the drug delivery system at the site of absorption, multi-particulate carrier systems, and site-specific delivery systems (Choonara *et al.*, 2014:1272; Hamman *et al.*, 2005:171).

### **2.3.2.1 Enzyme inhibitors**

Enzyme inhibitors are co-administered with peptides and proteins to facilitate the stability of these drugs by means of lowering the enzymatic barrier and thereby preventing degradation (Renukuntla *et al.*, 2013:80). The decrease in enzymatic activity is achieved by means of competitive or non-competitive inhibition, or by the inactivation of the target enzyme by reversible or irreversible binding of the enzyme inhibitor to the enzyme. Another mechanism of enzyme inhibitors to exert an effect is by changing the pH and thereby decreasing the optimal environment for enzymatic activity (Choonara *et al.*, 2014:1273).

Since most natural enzyme inhibitors have a low efficacy and is susceptible to enzymatic degradation itself, it has to be co-administered in large quantities, which raises questions on their

safety in chronic use and the effects it might have on the degradation of other functional proteins (Renukuntla *et al.*, 2013:80). It has been suggested that the combination of enzyme inhibitors with absorption enhancers might provide a more feasible option in improving the bioavailability of peptide and protein drugs (Choonara *et al.*, 2014:1273).

#### **2.3.2.2 Mucoadhesive systems**

The ability of mucoadhesive polymers to bind to biological substrates such as mucosal surfaces has stimulated interest in these polymers for use in dosage forms to improve drug delivery (Renukuntla *et al.*, 2013:81). The bonding of the polymers incorporated into the dosage form to the mucin layer on the epithelial mucosa increases the residence time of the drug delivery system in the gastrointestinal tract. This increased residence time can cause higher drug concentration gradients, which may result in increased bioavailability (Park *et al.*, 2011:281; Renukuntla *et al.*, 2013:81; Wallis *et al.*, 2014:1089).

#### **2.3.2.3 Particulate carrier systems**

Several particulate carrier systems are available for improving the delivery of peptide and protein drugs including liposomes, polymeric micelles, micro-emulsions, polymeric micro-particles and nano-particles. These particulate carrier systems offer advantages like protection of drugs against acidic and enzymatic degradation in the gastrointestinal tract (Mahato *et al.*, 2003:180; Park *et al.*, 2010:67; Park *et al.*, 2011:282).

#### **2.3.2.4 Site-specific delivery systems**

Drug absorption is not uniform in all the regions of the gastrointestinal tract because of differences in enzymatic activity, pH, surface area, thickness and composition of the mucus layer (Choonara *et al.*, 2014:1275; Hamman *et al.*, 2005:173). An attractive approach to overcome this problem is to target drug delivery to the colon as the colon-environment has lower enzymatic activity, longer gastrointestinal residence time, and increased sensitivity to absorption enhancers (Choonara *et al.*, 2014:1275; Wallis *et al.*, 2014:1091).

#### **2.3.2.5 Absorption enhancers**

Absorption enhancers are chemical adjuvants that are co-administered with peptides and proteins to increase their bioavailability by reversibly removing or briefly disrupting the intestinal barrier with minimal tissue damage (Hamman *et al.*, 2005:171; Renukuntla *et al.*, 2013:79). The mechanisms through which this can be achieved include i) decreasing mucus viscosity, ii) changing membrane fluidity, iii) disrupting the structural integrity of the intestinal wall, and iv) modulating the tight junctions (Mahato *et al.*, 2003:185; Renukuntla *et al.*, 2013:79).

A relatively large number of compounds have already been investigated for their potential drug absorption enhancing capabilities such as surfactants, chelating agents, fatty acids and derivatives, bile salts, anionic and cationic polymers, and compounds of natural origin (Kang *et al.*, 2009:1204; Kesarwani & Gupta, 2013:256; Renukuntla *et al.*, 2013:79; Park *et al.*, 2011:280). Surfactants disrupt the lipid bilayer in the epithelial cell membrane, thereby making the cell membrane more permeable, increasing transcellular permeation (Muheem *et al.*, 2016:418). Chelating agents (i.e. ethylenediaminetetraacetic acid (EDTA) and ethylene glycol tetraacetic acid (EGTA)) modulate tight junctions, thus increasing paracellular permeation. This is done by forming complexes with calcium ( $\text{Ca}^{2+}$ ) ions, which influence a cascade of biochemical events that eventually cause tight junction opening (Park *et al.*, 2011:281). Fatty acids and its derivatives such as sodium caprate and acyl carnitine increase intercellular  $\text{Ca}^{2+}$  levels through activation of phospholipase C in the plasma membrane, resulting in the contraction of microfilaments associated with tight junctions thereby increasing paracellular permeability (Anilkumar *et al.*, 2011:440). Bile salts (i.e. sodium glycholate and sodium deoxycholate) increase membrane permeability through various mechanisms, such as formation of mixed micelles, decrease of mucus viscosity and peptidase activity as well as phospholipid acyl chain disruption (Choonara *et al.*, 2014:1273).

#### 2.3.2.5.1 Absorption enhancers of natural origin

Various absorption enhancers of natural origin have been identified and can be derived from plants or animals. Different mechanisms of action of absorption enhancement have been suggested for these natural compounds, i.e. regulators of gastrointestinal permeability, enzyme inhibitors and P-gp-efflux pump inhibitors (Isoda *et al.*, 2001:160; Salama *et al.*, 2006:25; Tatiraju *et al.*, 2013:56; Werle & Bernkop-Schnürch, 2008:280). A list of natural compounds that have shown absorption enhancing capabilities are given in Table 2.1.

**Table 2.1:** Selected absorption enhancers of natural origin and their suggested mechanisms of action (Borska *et al.*, 2010:864; Isoda *et al.*, 2001:160; Kang *et al.*, 2009:1205; Kesarwani & Gupta, 2013:254; Khajuria *et al.*, 2002:229; Lemmer & Hamman, 2013:106; Li *et al.*, 2013:12889; Salama *et al.*, 2006:25; Tatiraju *et al.*, 2013:56; Werle & Bernkop-Schnürch, 2008:280)

Suggested mechanism of absorption enhancement	Natural compound
Enzyme inhibitors (i.e. CYP450 and other isozymes)	Gallic acid and ester-derivatives Naringin Quercetin Turmeric ( <i>Curcuma longa</i> )
Efflux transporter (i.e. P-gp) inhibitor	Black cumin ( <i>Cuminum cyminum</i> ) Caraway ( <i>Carum carvi</i> ) Genistein Piperine ( <i>Piper longum</i> or <i>P. nigrum</i> ) Quercetin Sinomenine ( <i>Sinomenium acutum</i> ) Turmeric ( <i>Curcuma longa</i> )
Gastrointestinal function modulators	Ginger ( <i>Zingiber officinale</i> ) Glycyrrhizin ( <i>Glycyrrhiza glabra</i> ) Niaziridin (Drumstick pods)
Tight junction modulators	<i>Aloe vera</i> Capsaicin ( <i>Capsicum</i> ) Chitosan and its derivatives Zonula Occludens toxin (ZOT)

Gastrointestinal function modulation by natural compounds can occur through a number of mechanisms including changes in gastrointestinal cell membrane permeability, tight junction modification, and mucoadhesion (Kesarwani & Gupta, 2013:255; Lemmer & Hamman, 2013:108). Chitosan and its derivatives (amongst others is trimethylated chitosan and thiolated chitosans), which are cationic polysaccharides from animal origin (derived from chitin, naturally occurring in the shells of crustaceans) (Werle & Bernkop-Schnürch, 2008:273). *N*-trimethyl chitosan chloride (TMC) is a water-soluble derivative of chitosan, which has been studied for its ability to increase paracellular permeability by opening tight junctions and its mucoadhesive abilities (Kotzé *et al.*, 1997:1202; Rosenthal *et al.*, 2012a:2792). Zonula occludens toxin (ZOT), cholera toxin and accessory cholera toxin are enterotoxins produced by *Vibrio cholerae* strains (Salama *et al.*, 2006:20). ZOT influences tight junction modulation by a series of intracellular events such as inducing protein kinase C- $\alpha$  (PKC- $\alpha$ ) related polymerization of actin filaments and opening of tight junctions thereby increasing paracellular permeability (Fasano & Nataro, 2004:802). The active component found in red chilli peppers (*Capsicum* genus) is capsaicin, a homovanillic acid derivative (Isoda *et al.*, 2001:155; Tatiraju *et al.*, 2013:59). The absorption enhancing effect of capsaicin was investigated by Isoda *et al.* (2001:160) and found to be a result of the reversible

opening of the paracellular route. It was later confirmed that this opening is a result of tight junction modulation by means of actin filament (F-actin) disruption through zonula occludens-1 (ZO-1) and claudin-1 relocalization (Nagumo *et al.*, 2008:925). *Aloe vera* is another plant with absorption enhancing properties (Lemmer & Hamman, 2013:108; Tatiraju *et al.*, 2013:59; Vinson *et al.*, 2005:764) and is further discussed in the following section.

## 2.4 *Aloe vera* leaf materials as drug absorption enhancers

### 2.4.1 Botany

The *Aloe vera* ((L.) Burm.f.) (synonym *Aloe barbadensis* (Miller)) plant (Figure 2.3) is a succulent perennial xerophyte that was originally found in northern and eastern Africa, but is now commercially cultivated in the United States of America, Aruba, Bonaire, Haiti, India, South Africa and Venezuela (Boudreau & Beland, 2006:105; Sahu *et al.*, 2013:599). To survive in arid regions with little or irregular rainfall, the *A. vera* plant developed water storage mechanisms in the leaves such as the formation of a viscous mucilage. The innermost part of the leaf is made up of clear, moist, soft and slippery tissue that consists of thin-walled parenchyma cells (Eshun & He, 2004:92; Hamman, 2008:1600). As a result, the thick fleshy leaves contain amongst other compounds, storage carbohydrates such as acetylated mannan (acemannan) and cell wall carbohydrates such as cellulose and hemicellulose (Hamman, 2008:1600). An exudate can also be found in the *A. vera* leaves referred to as the latex (a reddish-yellow juice) (Boudreau & Beland, 2006:105; Sánchez-Machado *et al.*, 2017:96).



**Figure 2.3:** *Aloe vera* ((L.) Burm.f.) plant (Courtesy of the NWU Botanical Garden)



**Figure 2.4:** Anatomical sections of the *Aloe vera* leaf: a) outermost layer, b) middle layer and c) innermost layer (Courtesy of the NWU Botanical Garden)

Three anatomical sections can therefore be distinguished in the *A. vera* leaf (Figure 2.4) namely (Sahu *et al.*, 2013:600; Sánchez-Machado *et al.*, 2017:96):

- Outermost layer or the rind that consists of the peel, thorns, bases and tips (Sahu *et al.*, 2013:96; Sánchez-Machado *et al.*, 2017:96).
- Middle layer of yellow sap/juice/latex, produced by the pericyclic tubules found in the vascular bundles located in the leaf pulp just below the rind (Boudreau & Beland, 2006:105; Sánchez-Machado *et al.*, 2017:96; Sahu *et al.*, 2013:600).
- Innermost layer or the fillet contains a clear, slippery mucilaginous gel, which is produced by the thin-walled tubular cells in the innermost part of the leaf referred to as the *A. vera* gel (Boudreau & Beland, 2006:106; Femenia *et al.*, 1999:112; Sahu *et al.*, 2013:600; Sánchez-Machado *et al.*, 2017:96).

## 2.4.2 Phytochemistry

The chemical composition of the *A. vera* leaves is highly dependent on the climate and growing conditions (Boudreau & Beland, 2006:106; Femenia *et al.*, 1999:112; Sánchez-Machado *et al.*, 2017:96). The high water content (99–99.5%) of the *A. vera* gel is one of its main characteristic features (Eshun & He, 2004:92) and the remaining 0.5–1.0% consists of minerals, enzymes, various polysaccharides, organic acids, phenolic compounds, fat- and water-soluble vitamins (Boudreau & Beland 2006:107). Many of the medicinal effects of *A. vera* leaf materials have been attributed to the polysaccharides found in the leaf gel, specifically acemannan (Femenia *et al.*, 1999:190).

The main chemical solutes present in *A. vera* gel are carbohydrates of which the two polysaccharides, acemannan and glucomannan, are the principle components. The biological activities of these polysaccharides depend on their molecular weight, degree of acetylation, type of sugar and glycosidic branching (Sánchez-Machado *et al.*, 2017:96). Immunomodulation, cell proliferation, and anti-viral activity are just some of the biological effects that have been attributed to acemannan (Choi & Chung, 2003:58; Sahu *et al.*, 2013:601), while glucomannan is described as a good moisturizer, contributing to its usefulness in the cosmetic industry (Sánchez-Machado *et al.*, 2017:96).

Other components found in *A. vera* leaf materials that exhibited biological activities are anthraquinones, phytosterols, and glycoproteins. Anthraquinones that have been identified as being pharmacologically active include aloin, barbaloin, aloe-emodin, and emodin. They have shown therapeutic effects such as purgative, anti-inflammatory, and anti-protozoal activities (Choi & Chung 2003:56). The majority of the anti-diabetic and anti-hyperlipidemic activity can be ascribed to the phytosterols such as  $\beta$ -sitosterol (Mukherjee *et al.*, 2014:16; Sánchez-Machado *et al.*, 2017:97). It was suggested that the anti-tumour and anti-ulcer effects of *A. vera* leaf materials is probably the result of glycoproteins (Sahu *et al.*, 2013:602).

## 2.4.3 Biological activities

*Aloe vera* materials and products have long been used in traditional medicine, where the latex has been used for its laxative effects and the gel was mainly used for the treatment of wounds and skin ailments such as psoriasis and genital herpes (Du Plessis & Hamman, 2014:169; Sánchez-Machado *et al.*, 2017:95). Other uses that have also been ascribed to *A. vera* components include anti-bacterial, anti-cancer, anti-diabetic, anti-fungal, anti-obesity, anti-viral effects, and gastric protection against ulcers (Boudreau & Beland, 2006:104; Mascolo *et al.*, 2004:205; Sánchez-Machado *et al.*, 2017:97). Drug absorption enhancing activities have recently been found for *A. vera* leaf materials, gastro-intestinally (Vinson *et al.*, 2005:764), and more specifically across the intestinal epithelium (Beneke *et al.*, 2012:481; Beneke *et al.*, 2013:48;

Chen *et al.*, 2009:589; Lebitsa *et al.*, 2012:304), the skin (Cole & Heard, 2007:16; Fox *et al.*, 2014:104), and the buccal mucosa (Ojewole *et al.*, 2012:356).

Vinson *et al.* (2005:764) conducted a randomized, double-blind, cross-over clinical trial on the effects of two *A. vera* preparations containing gel and whole leaf, respectively, on the bioavailability of vitamins C (ascorbic acid) and E (tocopherol). They found that the co-administration of the *A. vera* products markedly increased the bioavailability of the two selected vitamins, making both *A. vera* products unique in their ability to improve the absorption of both vitamin C (water-soluble) and E (fat-soluble). The mechanisms employed to achieve this improvement in absorption are protection from intestinal degradation in the intestinal tract by flavonoids, this also slowed down the absorption and excretion of the vitamins. The anti-oxidant ability of some flavonoids and polysaccharides are also suspected to contribute to the delayed absorption and excretion of vitamins C and E. Another known influence on absorption rate, is gastric-emptying time. Though it is known that *A. vera* does not affect gastric-emptying time, the polysaccharides do bind to stomach mucosal cells and can also bind to vitamin C and E thus slowing down their absorption. The *A. vera* gel extract was especially effective in increasing and slowing down the absorption of vitamin C, significantly prolonging the plasma concentration.

The P-gp modulating effects of *A. vera* juice was investigated by Djuv and Nilsen (2008:1626). The researchers concluded that the *A. vera* juice did not inhibit the P-gp mediated transport of digoxin in a statistically significant way in any of the concentrations that were tested.

Chen *et al.* (2009:589) investigated the *in vitro* drug absorption enhancing effects of *A. vera* gel and whole leaf extract on insulin across Caco-2 cell monolayers. The transepithelial electrical resistance (TEER) of the Caco-2 cell monolayers was notably decreased by the presence of *A. vera* gel and whole leaf extract, which indicated the opening of the tight junctions between adjacent epithelial cells. This supposed opening of the tight junctions resulted in statistically significantly increased transport of insulin across the Caco-2 cell monolayers.

Other studies confirmed the capability of leaf materials of *A. vera* and other aloe species to enhance drug permeation across *in vitro* intestinal models (Beneke *et al.*, 2012:481) and to improve drug bioavailability *in vivo* in an animal model (Lebitsa *et al.*, 2012:304; Wallis *et al.*, 2016:479). Although P-gp efflux inhibition to some extent was observed for precipitated polysaccharides from *A. vera* gel and a reduction in TEER was observed for both *A. vera* gel and whole leaf extract. This may have indicated the opening of tight junctions. The precise mechanism of action for the drug absorption enhancing effects of *A. vera* gel and whole leaf extract has not yet been elucidated by any of these previous studies.

## 2.5 Experimental models to evaluate intestinal drug permeability

Various experimental models have been used for the prediction of intestinal drug absorption including *in vitro*, *ex vivo*, *in vivo*, *in situ*, and *in silico* models as illustrated in Figure 2.5. Some of these models can be used for high throughput screening and are more cost-effective than *in vivo* pre-clinical (animal) and clinical (humans) studies (Alqahtani *et al.*, 2013:1).

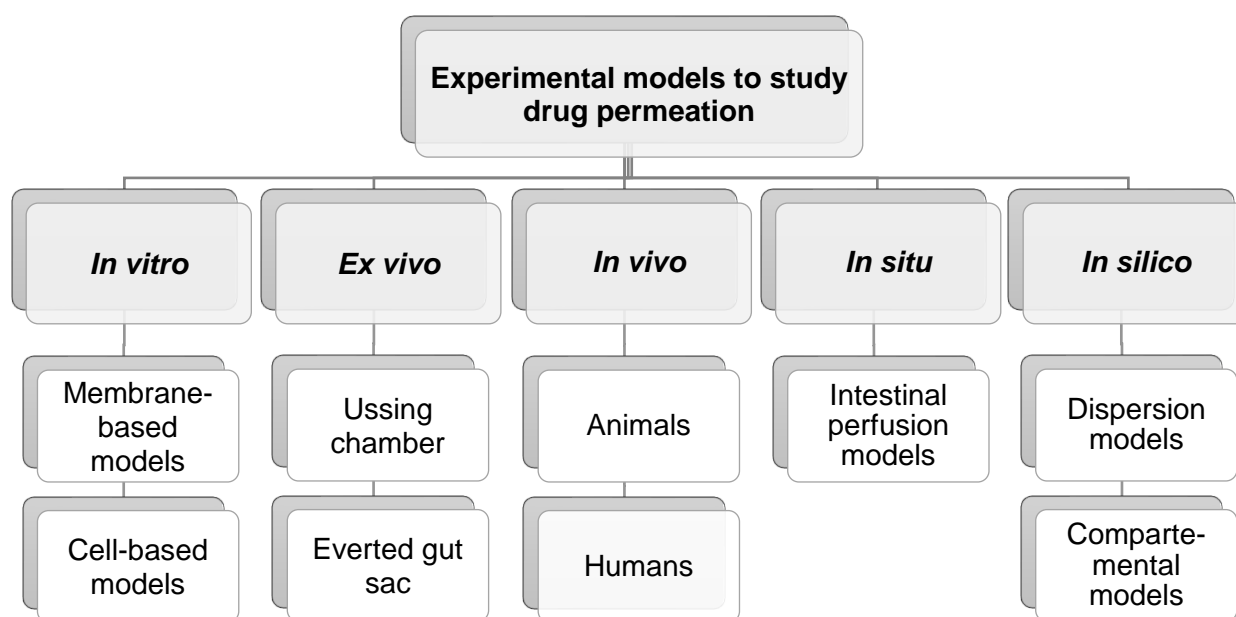


**Figure 2.5:** Flow-chart depicting the different experimental models available for studying intestinal drug permeability

### 2.5.1 *In vitro* models

*In vitro* models can either be membrane-based or cell culture-based (Deferme *et al.*, 2008:187).

#### 2.5.1.1 *Membrane-based models*

Membrane based models make use of artificial membranes with varying lipid compositions to study drug permeation. A widely used application of this model is the parallel artificial membrane permeability assay (PAMPA) and is a filter-supported lipid membrane system (Cabrera-Pérez *et al.*, 2016:14). The composition of the lipid solutions that are added to the filter compartment can be adjusted according to the type of assay required. PAMPA is used as a high throughput screening analysis method, which is used to rapidly screen the permeability characteristics of large numbers of model compounds (Cabrera-Pérez *et al.*, 2016:14; Deferme *et al.*, 2008:188). Disadvantages of this model include an extremely difficult inter-laboratory comparison of results due to the variation in methods that different laboratories apply in the preparation of the

membranes and the execution of the permeation studies. The methods vary specifically with respect to the use of different membrane constituents, permeation times, and sink conditions (Deferme *et al.*, 2008:191).

Recently Berben *et al.* (2018:253) reported the use of an artificial membrane insert (AMI) system as an alternative to other currently available non-cell based or Caco-2 cell permeation models. The fast and high-throughput estimation of passive intestinal permeability, are some of the advantages associated with the AMI-system. Research done on the AMI-system reported a good correlation of the apparent permeability coefficient ( $P_{app}$ ) of a regenerated cellulose membrane (AMI-system) compared to Caco-2 cell models. A shortcoming of this system is its inability to predict enzyme and carrier-mediated intestinal permeation; but investigations for implementing a possible mucus layer in the AMI-system are underway.

### **2.5.1.2 Cell-based models**

Primary cell cultures face certain challenges such as the requirement of expensive culture media, ethical concerns with sourcing cells and it is difficult to form polarised monolayers with these types of cells. Due to these challenges, immortalised cell cultures are more frequently used as *in vitro* models in drug permeability studies (Alqahtani *et al.*, 2013:2; Deferme *et al.*, 2008:192). Perhaps, the most commonly used cell line in drug permeability studies is the Caco-2 cell line, but other cell lines such as MDCK, LLC-PK1, 2/4/A1, HT29, and TC7 have also been used as models for drug permeation studies (Cabrera-Pérez *et al.*, 2016:16; Deferme *et al.*, 2008:193; Yang *et al.*, 2017:338).

#### 2.5.1.2.1 MDCK cell line

Madin-Darby canine kidney (MDCK) cells were derived from the distal tubule of the dog kidney and have gained increasing attention as an alternative cell-based drug permeation model for Caco-2 cells (Alqahtani *et al.*, 2013:3; Deferme *et al.*, 2008:199). MDCK cells can form polarized monolayers and develop tight junctions when it is cultured under standard culture conditions (Le Ferrec *et al.*, 2001:655; Yang *et al.*, 2017:341). The advantage of this cell line is the relatively short culture time that is required to reach confluency and the monolayers have a TEER value closer to that of the human intestine than other cell lines. The main disadvantages of these cells include their non-intestinal (kidney) and non-human (canine) origin. Further disadvantages of these cells are their low expression levels of transporter proteins and low metabolic activity (Deferme *et al.*, 2008:199). MDCK cells have been successfully transfected with the human P-gp gene resulting in a higher expression of this efflux protein. This model has been suggested as an alternative to Caco-2 cells to study drug permeation (Alqahtani *et al.*, 2013:3; Deferme *et al.*, 2008:200).

#### 2.5.1.2.2 LLC-PK1 cell line

Lewis lung carcinoma-porcine kidney 1 (LLC-PK1) cells originates from proximal tubules cells of a porcine kidney (Nielsen *et al.*, 1998:1767). These cells are generally transfected with various P-gp transporters, enabling the expression of human or rat P-gp (Zolnericks *et al.*, 2011:3055). These cells have been used by Adachi *et al.* (2001:1665) to determine the transcellular transport of selected compounds.

#### 2.5.1.2.3 2/4/A1 cell line

This cell-based model has its origin from the foetal rat intestine and is believed to closely mimic the permeability of the human intestinal epithelium, especially with regard to passive paracellular and transcellular transport (Deferme *et al.*, 2008:200; Yang *et al.*, 2017:342). The paracellular pore size on the 2/4/A1 cell monolayers was determined to be around 9.0 Å, which is similar to that found in the human intestine, while the pore size in the Caco-2 cell monolayers are estimated to be approximately 3.7 Å (Tavelin *et al.*, 2003:397).

#### 2.5.1.2.4 HT29 cell line

Wild-type HT29 cells grow in multilayers of undifferentiated cells, which is very unsuitable for permeation studies. When these wild-type cells are cultured in media that contains galactose instead of glucose, they form polarised monolayers (Deferme *et al.*, 2008:200). Various sub-clones of the HT29 cells have been produced that differentiate into enterocytic cells of mucus-secreting goblet cells. HT29-H and HT29-MTX are two of these mucus-secreting clones and has been co-cultured with Caco-2 cells to increase their biorelevance (Deferme *et al.*, 2008:200). This has unfortunately resulted in lower expression of the carriers involved in the intestinal uptake of nutrients and drugs, which is much lower than normally found in the Caco-2 cell line (Pereira *et al.*, 2016:67).

#### 2.5.1.2.5 TC7 cell line

TC7 cells are Caco-2 cell sub-clones with stronger metabolic competence and were obtained through clonal selection (Sarmiento *et al.*, 2012:610). When the TC7 sub-clone is exposed to methotrexate, it maintains a stable expression of CYP3A4, a major CYP3A isoform present in the epithelial cells of the small intestine. Compared to the parent Caco-2 cells, which only expresses CYP3A5, the TC7 cells are superior because they express both the CYP3A4 and CYP3A5 isoforms. This characteristic contributed to the TC7 being the second-most used cell line for the study of intestinal permeation of drug molecules (Pereira *et al.*, 2016:64).

#### 2.5.1.2.6 Caco-2 cell line

Caco-2 cells are derived from human colon adenocarcinoma and are the most widely used cell model for the prediction of intestinal absorption (Artursson *et al.*, 2012:287; Pereira *et al.*, 2016:62). Caco-2 cells differentiate to form a confluent epithelial monolayer with columnar and polarized cells, expressing microvilli on the apical membrane and tight junctions between adjacent cells (Sun *et al.*, 2008:395).

Even though Caco-2 cells have a colonic origin, they express the majority of the functional and morphological characteristics of small intestinal absorptive cells, including enzymes (e.g. disaccharidases and peptidases) normally expressed by enterocytes (Pereira *et al.*, 2016:63). However, CYP3A, the most important intestinal metabolising enzyme, is expressed in very low levels by Caco-2 cells. The expression of P-gp by Caco-2 cells is higher than the levels that are found *in vivo* in the human intestine (Le Ferrec *et al.*, 2001:655; Pereira *et al.*, 2016:63). The tight junctions that form between the cells once confluence is achieved, which is usually after 21 days, has a much smaller pore diameter (approximately 5.0 Å) than what is found in animal or human intestine (8.0–13.0 Å). This can be attributed to the colonic nature of the Caco-2 cells (Sun *et al.*, 2008:395; Tavelin *et al.*, 1999:1220). Further shortcomings associated with the Caco-2 cell model are its inability to produce mucus and a relatively wide variation exists between data generated from various laboratories (Pereira *et al.*, 2016:63).

Caco-2 cells are commonly grown on filter membranes in Transwell® system, enabling the cells to form a polarized monolayer providing an experimental setup to differentiate between the apical and basolateral side of the gastrointestinal tract (as seen in Figure 2.6) (Yang *et al.*, 2017:340). This combined with the fact that the Caco-2 cell line is a well-established and characterised model for studying drug absorption, transport, and metabolism (Cai *et al.*, 2014:175; Yang *et al.*, 2017:339), made the Caco-2 cells the appropriate model for this study.

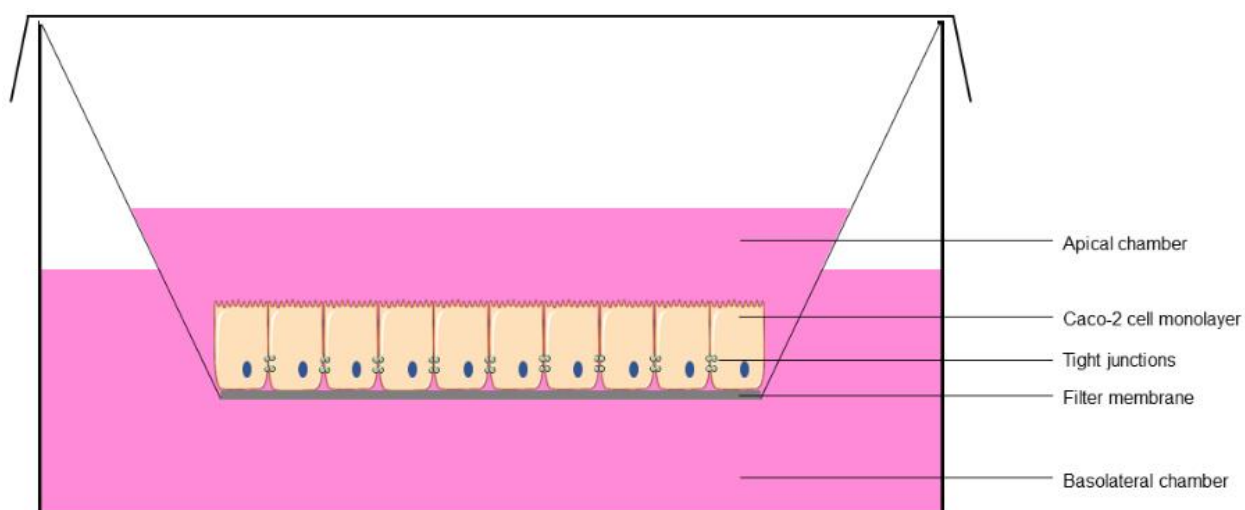


**Figure 2.6:** Illustration of a Caco-2 cell monolayer grown on the filter membrane of a Transwell® system (Adapted from Sun *et al.* (2008:396) and Yang *et al.* (2017:340); produced using Servier Medical Art, <http://smart.servier.com>)

### 2.5.2 *Ex vivo* models

The Ussing chamber apparatus involves a technique where excised animal intestinal tissue segments are mounted between two diffusion half-cells. This setup presents two compartments namely the serosal chamber (on the basolateral side) and the luminal chamber (on the apical side) (Alqahtani *et al.*, 2013:3; Deferme *et al.*, 2008:201). This technique is suitable for evaluation of carrier-mediated or passive transport of compounds and to study inter-species as well as regional differences in intestinal absorption and metabolism (Alqahtani *et al.*, 2013:3; Yang *et al.*, 2017:343).

Another *ex vivo* model that is largely used for drug absorption and metabolism prediction is the everted gut sac model. This model entails the eversion of a freshly isolated piece of animal intestine that is filled with oxygenated medium and tied off at the ends (Le Ferrec *et al.*, 2001:654; Nunes *et al.*, 2016:220). The everted sac is then submerged in the drug-containing solution for the determined time, while samples are withdrawn from the sac at the pre-determined intervals for the measurement of the drug concentration in the sac.

Advantages of this model are that it can be used to determine the role of P-gp in drug absorption and to estimate the first-pass metabolism of the intestinal epithelial cells on drugs in the gastrointestinal tract (Le Ferrec *et al.*, 2001:654; Nunes *et al.*, 2016:221). Further advantages are that it can be used to study substrates of carrier-mediated and efflux transport systems, and regional differences in intestinal drug absorption, as well as its low cost and easiness to use (Alqahtani *et al.*, 2013:5). Shortcomings of this model are that the drug must cross muscle and all the layers of the intestine as well as the relatively short viability period of the tissue. The small volume in the sac may also influence sink conditions, making this model unsuitable for well absorbed compounds (Yang *et al.*, 2017:343).

### 2.5.3 *In vivo* animal models

*In vivo* animal models are commonly used to determine drug bioavailability. Animals that can be used as *in vivo* models for the predictions of drug bioavailability in humans include dogs, pigs, rats, mice, and monkeys (Sjögren *et al.*, 2014:100).

This model involves test compounds being administered to live experimental animals, blood samples are then withdrawn at pre-determined time intervals and analysed to determine the concentration of the administered drug present in each sample. This data is then used to plot plasma level to time curves, from which the area under the plasma curve (AUC) is calculated. To determine the oral bioavailability of the administered test compound, the AUC of the *in vivo* model is compared to the AUC of the intravenous administration of the drug (Alqahtani *et al.*, 2013:5; Yang *et al.*, 2017:347). The presence of an intact gastrointestinal tract with an undisrupted mesenteric circulation, lymphatic absorption, and intestinal membrane are the main advantages of the *in vivo* animal model. Limitations of this model are the difference in the anatomy and physiology of human and animal models, large amounts of resources required, high labour intensity, time-consuming and difficulty in studying drug absorption mechanisms. It is unsuitable for high-throughput screening (Alqahtani *et al.*, 2013:6; Sjögren *et al.*, 2014:100).

### 2.5.4 *In situ* models

*In situ* techniques commonly include the intestinal loop model, where a segment of the small intestine of different animals is used as a model to predict drug absorption and metabolism. In this model, a segment of the small intestine of an animal, such as a rabbit, mouse or rat, is exposed through surgical procedures, perfused with a drug solution, and placed back in the body cavity for the duration of the experiment (Gamboa & Leong, 2013:805). To calculate the drug permeability, the change in the concentration at the beginning and end of the segment is determined. This model is considered a valuable tool in determining the influence of regional differences of intestinal drug permeation and metabolism on drug absorption and dose-dependent pharmacokinetics (Alqahtani *et al.*, 2013:5), since an intact nervous system, blood supply and clearance at the absorption site are present (Antunes *et al.*, 2013:12). Disadvantages associated with the *in situ* perfusion model are the effect of the anaesthetics used in the surgical procedure on the drug absorption, the impracticality for use in high-throughput screening and the overestimation of intestinal drug absorption since this method is dependent on the calculation of the disappearance of drug molecules from the lumen of the intestinal segment (Antunes *et al.*, 2013:12; Yang *et al.*, 2017:344).

Another *in situ* method used specifically for studying segmental intestinal perfusion in humans, is the Loc-I-Gut<sup>®</sup> system. It consists of a multi-channel tube, with two latex balloons approximately 10 cm apart which is orally introduced after local anaesthesia. Tungsten weights at the distal part

of the tube help with the positioning of the tube into the jejunum. After the tube has been positioned, the balloons are inflated, thus closing off a specific part in the small intestine, enabling perfusion of a closed part of the jejunum (Yang *et al.*, 2017:345). This forms a closed system, minimising contamination of distal and proximal fluids into the perfusion section (Lennernäs *et al.*, 1992:1244). The absorption rate, like with the intestinal loop model, is calculated from the disappearance rate of the drug from the perfused section (Lennernäs *et al.*, 1992:1244; Yang *et al.*, 2017:345).

### **2.5.5 *In silico* models**

The use of drug absorption computer simulations and modelling have increased in the last years as it has become an important part of the early screening processes of drug discovery, development and regulation (Alqahtani *et al.*, 2013:8; Antunes *et al.*, 2013:6). These computational models have the ability to take various factors that influence the oral absorption of drugs into account, i.e. physicochemical, bio-pharmaceutical and physiological factors (Alqahtani *et al.*, 2013:8). The early predictions that can be made using *in silico* methods will reduce the time and costs associated with selecting potential candidates for evaluation. These types of predictions also contribute to cost reduction during the screening and optimization processes as there is no need for the synthesis of the compounds required for experiments (Antunes *et al.*, 2013:6). The use of *in silico* models is still restricted regarding the use for simulating intestinal protein absorption, as there is still a need for larger databases with sufficient reliable information on the absorption properties regarding protein drugs. This is further complicated by the molecular and structural complexity of protein drugs, thus real experimental data on permeability and absorption properties will not likely be completely replaced with *in silico* models (Antunes *et al.*, 2013:7).

## **2.6 Summary**

Oral drug administration is the most popular route of drug administration, with higher patient compliance and more affordable therapies when compared to injection therapies. This created the opportunity for the co-administration of absorption enhancers. *A. vera* gel and whole leaf extract has shown an increase in the oral bioavailability of various vitamins and increased permeation across various epithelial cell monolayers. Little is known about the capacity of absorption enhancement (in terms of molecular weight) or the mechanism of action by which *A. vera* gel and whole leaf extract increase gastrointestinal absorption, specifically. The Caco-2 cell line was chosen to investigate the capacity and mechanism of absorption enhancement, as it is a widely studied and well characterized permeation model and is commonly used for mechanistic studies, as well as intestinal absorption and/or transport studies.

## CHAPTER 3: MATERIALS AND METHODS

### 3.1 Introduction

Various categories of experimental models have been used in the determination/prediction of gastrointestinal drug absorption including *in vitro*, *in vivo*, *ex vivo*, *in situ* and *in silico* (Cai *et al.*, 2014:175). *In vitro* experimental models include membrane-based models (e.g. parallel artificial membrane permeability assay), excised tissue models (e.g. pig intestinal tissue) and cell-based models (e.g. Caco-2 cells, MDCK cells, TC7 cells) (Deferme *et al.*, 2008:187). Cell-based *in vitro* techniques are widely used for drug membrane permeability assessments due to cost-effectiveness, less labour-intensiveness, and less ethical considerations compared to other models such as *in vivo* animal models (Sarmiento *et al.*, 2012:607). The Caco-2 cell line was used in this study, which is derived from human colon adenocarcinoma and is well established as a model for studying gastrointestinal epithelial drug permeability (Cai *et al.*, 2011:176; Sun *et al.*, 2008:395).

For the drug permeation and transepithelial electrical resistance (TEER) studies, Caco-2 cells were grown on filter membranes, which enabled the cells to differentiate and form confluent monolayers. The Caco-2 cell monolayer model expresses microvilli on the apical membrane and forms tight junctions between adjacent cells (Sun *et al.*, 2008:395). Caco-2 cell monolayers can also be used to determine the paracellular absorption of drugs, which is usually done by comparing the drug permeability before and after tight junction disruption/modulation. The modulation of tight junctions has been described as one possible mechanism by which intestinal absorption of large hydrophilic molecules can be increased by absorption enhancers (Sun *et al.*, 2008:398). Tight junction modulation can experimentally be confirmed by TEER measurements as well as permeability of paracellular markers. Decreased TEER values and increased permeation of appropriate markers indicate opening of tight junctions. In addition, microscopic examination after staining of cell components and intercellular accumulation of fluorescent probes can be used to indicate opening of tight junctions as a mechanism of paracellular drug absorption enhancement (Matter & Balda, 2003:233; Sun *et al.*, 2008:398).

### 3.2 Materials

#### 3.2.1 Aloe leaf materials

*Aloe vera* dehydrated gel material (Daltonmax700<sup>®</sup>; batch no. 700AQ11PK01) and *Aloe vera* whole leaf material (Daltonmax700<sup>®</sup>; batch no. 715AQ11PK01) were kindly donated by Improve USA, Inc. (De Soto, Texas, USA). Quantitative proton nuclear magnetic resonance (<sup>1</sup>H-NMR) analysis was used to chemically characterise the *A. vera* gel and whole leaf extract, specifically to determine the content of certain marker molecules known to be present in fresh *A. vera* leaf

materials such as aloverose, glucose, malic acid and iso-citric acid, as previously reported by Beneke *et al.* (2012:477) and Du Plessis and Hamman (2014:172). The <sup>1</sup>H-NMR spectra is given in Appendix A.

### **3.2.2 Caco-2 cell culturing**

Caco-2 cells used were procured from the European Collection of Cell Cultures (ECACC) (Catalogue number: 86010202; Cell Line Name: Caco-2, Human Caucasian colon adenocarcinoma; Growth Mode: Adherent) (Sigma Aldrich<sup>®</sup>, Merck, Darmstadt, Germany). Dulbecco's Modified Eagles Medium (DMEM) and phosphate buffered saline (PBS) (Hyclone<sup>™</sup>, GE Healthcare Life Sciences, Logan, Utah, USA) were purchased from Separations (Randburg, South Africa). Foetal bovine serum (FBS) (Gibco<sup>™</sup>, BioSciences, Dublin, Ireland) was purchased from Thermo Fisher Scientific Inc. (Massachusetts, USA). Non-essential amino acids (NEAA) (100X), trypsin-EDTA, L-glutamine (200 mM) and Penicillin/Streptomycin (10 000 U/ml penicillin and 10 000 U/ml streptomycin) (Lonza<sup>™</sup>, Basel, Switzerland) were purchased from Whitehead Scientific (Cape Town, South Africa). Amphotericin B (250 µg/ml) and 2-[4-(2-hydroxyethyl)piperazin-1-y]ethanesulfonic acid (HEPES) (Biochrom<sup>™</sup>, Berlin, Germany) were purchased from The Scientific Group (Randburg, South Africa). Trypan blue solution (0.4% w/v) and Lucifer yellow (Sigma Aldrich<sup>®</sup>) were purchased from Merck.

### **3.2.3 Permeation studies**

Fluorescein isothiocyanate (FITC) dextran with molecular weights of 4000 Da, 10 000 Da, 20 000 Da and 40 000 Da (Sigma-Aldrich<sup>®</sup>) were purchased from Merck. Transwell<sup>®</sup> 6-well plates (Corning Costar<sup>®</sup>) with a surface area of 4.67 cm<sup>2</sup> and a pore size of 0.4 µm were used for the permeation study and purchased from Corning Costar<sup>®</sup> Corporation (Tewksbury, MA, USA).

### **3.2.4 Transepithelial electrical resistance studies**

*N*-trimethyl chitosan chloride (TMC) was synthesised from chitosan (ChitoClear<sup>®</sup>) purchased from Primex (Siglufjordur, Iceland) and characterized by the method previously reported by Hamman *et al.* (2002:237) and Sieval *et al.* (1998:157). Refer to Appendix A for <sup>1</sup>H-NMR spectrum and the calculations of the degree of quaternisation of the TMC used. Transwell<sup>®</sup> 24-well plates (Corning Costar<sup>®</sup>) with 12 membrane inserts (surface area of 0.33 cm<sup>2</sup> and pore size of 0.4 µm) were used for the transepithelial electrical resistance (TEER) study and purchased from Corning Costar<sup>®</sup> Corporation.

### **3.2.5 Confocal laser scanning microscopy study**

Formaldehyde (40% v/v) was purchased from Associated Chemical Enterprises (ACE, Johannesburg, South Africa). Triton X-100 was purchased from Sigma Aldrich<sup>®</sup> (Merck).

CytoPainter® Phalloidin iFluor 488 and Fluoroshield® Mounting Medium with Propidium Iodide was purchased from Abcam® (Biocom Biotech, Centurion, South Africa). Snapwell® 6-well plates (Corning Costar®) (surface area of 1.12 cm<sup>2</sup> and pore size of 0.4 µm) were purchased from Corning Costar® Corporation.

### 3.3 Validation of the fluorometric analytical method for FITC-dextran and Lucifer Yellow on the Spectramax® plate reader

According to the United States Pharmacopeial Convention (USP) (2017b:1781), the validation of an analytical method is the process by which it is established that the procedure meets the requirements for the intended analytical application. A fluorescence analytical procedure/method validation requires the testing of the following parameters: linearity, accuracy, precision, specificity, limit of detection (LOD), and limit of quantification (LOQ) (USP, 2017a:782). The fluorescent analyte used in the *in vitro* experiments of this study was fluorescein isothiocyanate-dextran (FITC-dextran). Complete validation was done on FITC-dextran with a molecular weight of 4000 Da (FD-4), whereas linearity was determined for each of the other FITC-dextrans, namely 10 000 Da, 20 000 Da and 40 000 Da (i.e. FD-10, FD-20 and FD-40, respectively). Lucifer yellow stain was used as an exclusion marker to confirm the integrity of the Caco-2 cell monolayers used in the permeation studies (Bhushani *et al.*, 2016:375).

#### 3.3.1 Linearity

Linearity is the ability of the analytical method to give a response that is directly proportional to the concentration of the analyte within a given concentration range (USP, 2017b:1784). The linearity of the FITC-dextran and Lucifer yellow was determined by doing a linear regression analysis on the fluorescence detection values plotted as a function of the concentration (µg/ml) of the standard/calibration solutions. This plot should give a straight line with an acceptable regression coefficient value ( $R^2 \geq 0.995$ ) (USP, 2017a:783) and can be ascertained by conduction of a regression analysis on the straight line, which is described by the following equation (Shrivastava & Gupta, 2011:24):

$$y = mx + c$$

**Equation 1**

Where y is the fluorescence detection value of the analyte (FITC-dextran or Lucifer yellow) as measured by the plate reader, m is the slope, x is the concentration of the analyte and c is the y-intercept.

The standard/calibration solutions were prepared as follows: FITC-dextran (i.e. FD-4, FD-10, FD-20 and FD-40) stock solutions (250 µg/ml) were prepared from which serial dilutions were made with the following concentrations: 125.00 µg/ml, 62.50 µg/ml, 13.889 µg/ml, 7.813 µg/ml, 4.630 µg/ml, 3.906 µg/ml, 1.543 µg/ml and 0.514 µg/ml. A Lucifer yellow stock solution

(50 µg/ml) was also prepared, which was used to prepare serial dilutions with the following concentrations: 50.00 µg/ml, 25.00 µg/ml, 16.667 µg/ml, 12.50 µg/ml, 6.25 µg/ml, 1.563 µg/ml, 0.781 µg/ml and 0.617 µg/ml.

### **3.3.2 Accuracy and precision**

The accuracy of an analytical procedure is the ability of the method to produce results as close as possible to the true value of the sample. Accuracy can be determined with reference materials that is bought from a supplier and/or manufacturer or by using nine samples over a minimum of three concentrations covering a specified range (International Conference on Harmonisation, ICH, 2005:10; USP, 2017b:1782). Accuracy is measured by the percentage recovery of the analyte in the samples and the criteria stipulated in the USP (2017a:782) for accuracy is a value between 98%–102%.

The precision of an analytical method is the degree of agreement between multiple measurements of an individual sample. Precision can be investigated at different levels namely intra-day and inter-day precision. It is expressed as the percentage standard deviation (%RSD) between a series of measurements (ICH, 2005:10; USP, 2017b:1782) and the suggested requirement to comply with for intra-day precision is a %RSD value  $\leq 2\%$  (USP, 2017a:782) and  $\leq 5\%$  for inter-day precision (ICH, 2005:10). The %RSD was determined by using the following equation:

$$\%RSD = \frac{SD}{Average} \times 100 \quad \text{Equation 2}$$

Where %RSD is the percentage relative standard deviation, SD is the standard deviation between fluorescence detection values and the average of the fluorescence values measured.

#### **3.3.2.1 Accuracy**

Three concentrations of the analyte covering a specified concentration range in three replicates, forming a minimum of nine determinations, were used to determine the accuracy of the analytical procedure (ICH, 2005:10). The FD-4 concentrations used to determine the accuracy included 125 µg/ml, 62.5 µg/ml and 31.25 µg/ml, and the Lucifer yellow concentrations used consisted of 50 µg/ml, 25 µg/ml and 12.5 µg/ml. At least three samples of each concentration were measured on the Spectramax<sup>®</sup> plate reader on the same day.

#### **3.3.2.2 Intra-day precision**

Intra-day precision or repeatability of an analytical procedure is the degree of agreement between measurements of different samples with the same concentration measured over a relatively short period of time (i.e. the same day) by the same analyst on the same equipment (USP,

2017b:1782). The FD-4 and Lucifer yellow solutions (covering a specified range) were prepared and measured by the same analyst on the same Spectramax® plate reader at three different times during the same day (i.e. 11:00, 14:00 and 17:00). The concentration range covered in the solutions measured were 125 µg/ml, 62.5 µg/ml and 31.25 µg/ml for FD-4, and 50 µg/ml, 25 µg/ml and 12.5 µg/ml for Lucifer yellow.

### **3.3.2.3 Inter-day precision**

Inter-day or intermediate precision is the degree of agreement between measurements of different samples with the same concentration measured on different days, and is used to assess the impact of random events on the precision of the analytical procedure (ICH, 2005:10; USP, 2017a:782). Three FD-4 solutions with concentrations of 125 µg/ml, 62.5 µg/ml and 31.25 µg/ml, as well as three solutions for Lucifer yellow with concentrations 50 µg/ml, 25 µg/ml and 12.5 µg/ml were prepared and the fluorescence detection values were measured on the Spectramax® plate reader. This measurement was repeated on three consecutive days.

### **3.3.3 Limit of detection and limit of quantification**

The limit of detection (LOD) and the limit of quantification (LOQ), can be defined as the minimum concentration of the analyte that can be detected or quantified, respectively, with the necessary accuracy and precision (USP, 2017a:1783). LOD and LOQ are expressed as the concentration of the analyte that can be detected and quantified, respectively (ICH, 2005:11).

The following equations were used to calculate the LOD and LOQ (ICH, 2005:11):

$$\text{LOD} = 3.3 \times \text{SD} / \text{Slope} \quad \text{Equation 3}$$

$$\text{LOQ} = 10 \times \text{SD} / \text{Slope} \quad \text{Equation 4}$$

Where, SD is the standard deviation of the blank (i.e. background noise) and Slope is the gradient of the standard/calibration curve.

The standard deviation of the blank was determined from fluorescent detection values of six samples (USP, 2017a:782) of the blank (i.e. the solvent, which is serum-free DMEM).

### **3.3.4 Specificity**

The specificity is the ability of the method to ensure that the analyte's response is accurately measured in the presence of any other component in the sample and to demonstrate the lack of interference from other components that may be present (ICH, 2005:4; USP, 2017a:782). The USP (2017a:782) suggested that the specificity of an analytical procedure can be established by

meeting the criteria for accuracy, i.e. 98%–102% recovery of the analyte in the presence of the other component(s). To determine the specificity of the method for FD-4, different solutions were prepared in serum-free DMEM in the presence of both *A. vera* gel and whole leaf extract (1.5% w/v). This concentration of the *A. vera* gel and whole leaf extract in the specificity test represented the highest concentration used in the solutions for the *in vitro* permeation, TEER and confocal imaging studies.

Lucifer yellow was only used as an exclusion marker for the formation of intact Caco-2 cell monolayers, and as such did not include any aloe leaf materials which could potentially influence the detected fluorescence values.

### **3.4 Culturing and seeding of Caco-2 cells for *in vitro* permeation studies**

#### **3.4.1 Culturing and maintenance of Caco-2 cells**

Caco-2 cells were cultured in growth medium that consisted of high-glucose Dulbecco's Modified Eagles Medium (DMEM) supplemented with 10% v/v foetal bovine serum (FBS), 1% non-essential amino-acid solution (NEAA), 1% penicillin/streptomycin (100 U/ml penicillin and 100 µg/ml streptomycin), 1% amphotericin B (250 µg/ml) and 2 mM L-glutamine. The cells were incubated in an ESCO CellCulture CO<sub>2</sub> incubator (Life Technologies, Fairland, South Africa) at 37°C and exposed to 95% humidified air and 5% CO<sub>2</sub>. Caco-2 cells were cultured and maintained in 75 cm<sup>2</sup> growth flasks, while the growth medium was changed every second day and the flasks were microscopically inspected to determine confluency and to ensure that no contamination or unwanted growth was present (Gouws, 2014:3).

When 50% confluency was reached, the cells were sub-cultured by way of trypsinisation (Natoli *et al.*, 2012:1244). Firstly, the cell culture medium was removed from the flask and the cells were rinsed twice with 10 ml pre-heated PBS. After the washing process, the PBS was decanted and 3 ml of a trypsin-EDTA were added to the flask and gently shaken to ensure that all the cells were covered before the flask was placed back in the CO<sub>2</sub> incubator for a period of 4 min (Natoli *et al.*, 2012:1244). The flask was removed after the 4 min period, tapped once to detach the cells and 6 ml culture medium were added to terminate the trypsin action. The resultant cell suspension was then centrifuged in a 15 ml tube at 140 RCF for 5 min, where after the supernatant was removed and the pellet re-suspended in 5 ml pre-heated culture medium. The cell suspension was gently mixed with a Pasteur pipette to ensure a homogenous mixture and divided into 4 growth flasks. The flasks were made up to volume (15 ml) with pre-heated culture medium and placed back in the incubator.

### 3.4.2 Seeding onto Transwell® membranes

Caco-2 cells were seeded on the membranes of different Transwell®-plates for the different experiments at a seeding density of 20 000 cells/ml under sterile conditions. The Caco-2 cells were detached from the growth flasks by trypsinisation to form a stock cell suspension and the cells were counted using a haemocytometer. The mixture used for counting of the cells consisted of a mixture of 25 µl Trypan blue, 15 µl PBS and 10 µl cell suspension, which was prepared in a 1.5 ml Eppendorf microcentrifuge tube. After 3 min, a volume of 10 µl of the cell counting mixture was added to both counting chambers of the haemocytometer and the cells were counted on 5 of the 9 squares with the aid of a light microscope (Nikon Eclipse TS100/TS100F, Nikon Instruments, Tokyo, Japan). The average cells per square was calculated and multiplied by the dilution factor ( $5 \times 10^4$ ) to determine the concentration of the cells (cells/ml) in the cell suspension. The cell suspension was diluted to obtain a concentration of 20 000 cells/ml, by using the following equation:

$$C_1 \times V_1 = C_2 \times V_2$$

**Equation 5**

Where  $C_1$  is the concentration of the original cell suspension,  $V_1$  is the volume of the original cell suspension needed to prepare the final cell suspension needed,  $C_2$  is the concentration of the final cell suspension (i.e. 20 000 cells/ml) and  $V_2$  is the volume final cell suspension needed to seed onto the required Transwell® membranes.

The Caco-2 cells (passages 51 to 56) were seeded onto the different Transwell®-plates under sterile conditions using specific volumes (Table 3.1) of the cell suspension with the required cell concentration (i.e. 20 000 cells/ml). The Caco-2 cells were maintained on the Transwell® membranes by changing the culture medium every second day and were grown for at least 21 days to form intact epithelial monolayers. Prior to each experiment, TEER was measured to confirm the formation of an intact monolayer (see Table 3.2 for minimum TEER values). Monolayer integrity was also confirmed by determining the percentage transport (Wahlang *et al.*, 2011:278) and apparent permeability coefficient ( $P_{app}$ ) values (Bhushani *et al.*, 2016:375) of Lucifer Yellow, an exclusion transport marker, as described in the next section.

**Table 3.1:** Volume of cell suspension required for seeding out Caco-2 cells in the different Transwell® plate systems

Type of Transwell® plate system	Volume in apical chamber	Volume in basolateral chamber
Transwell® 6-well plates	2.5 ml	2.5 ml
Transwell® 24-well plates (with 12 filter inserts)	0.2 ml	1.0 ml
Snapwell® 6-well plates (detachable filter-ring inserts)	0.5 ml	2.5 ml

**Table 3.2:** Required TEER values for the formation of an intact Caco-2 cell monolayer

Type of Transwell® plate system	TEER value ( $\Omega$ )	TEER value ( $\Omega \cdot \text{cm}^2$ )
Transwell® 6-well plates (area = 4.67 cm <sup>2</sup> ) (Alqahtani <i>et al.</i> , 2013:2)	150	700.5
Transwell® 24-well plates (with 12 filter inserts) (area = 0.33 cm <sup>2</sup> ) (Du Toit <i>et al.</i> , 2016:578)	750	247.5
Snapwell® 6-well plates (detachable filter-ring inserts) (area = 1.12 cm <sup>2</sup> ) (Pick <i>et al.</i> , 2013:10)	179	200

### 3.4.3 Cell monolayer integrity

Lucifer yellow was used as an exclusion transport marker molecule to confirm the integrity of the formed Caco-2 cell monolayers (Bhushani *et al.*, 2016:375). The growth medium was aspirated from the basolateral chambers of the 6-well Transwell® plate and replaced with the appropriate volume of pre-heated serum-free DMEM buffered with HEPES (pH = 7.4) and incubated for 30 min at 37°C. After 30 min, the Transwell® plates were removed from the incubator, the growth medium was aspirated from the apical chambers and replaced with an appropriate volume of a pre-heated Lucifer yellow solution (i.e. 50 µg/ml in serum-free DMEM) (Bhushani *et al.*, 2016:375). The Transwell® plates were incubated with the Lucifer yellow solution for 120 min and samples (200 µl) were withdrawn from the basolateral chamber every 20 min and replaced with equal volume pre-heated serum-free DMEM buffered with HEPES. The Lucifer yellow concentration in the samples was quantified by means of fluorescence spectroscopy at excitation and emission wavelengths of 485 nm and 535 nm, respectively (Wahlang *et al.*, 2011:277). Percentage transport of Lucifer yellow across the Caco-2 cell monolayer should be less than 2% for the two-hour transport period (Wahlang *et al.*, 2011:278). Apparent permeability coefficient

( $P_{app}$ ) values (refer to section 3.8.1 *Data analysis of the in vitro permeation study*) of Lucifer yellow  $\leq 0.2 \times 10^{-6}$  cm/s (Cataluyd *et al.*, 2011:129) or  $0.66\text{--}0.75 \times 10^{-6}$  cm/s (Bhushani *et al.*, 2016:375) were considered indicative of the formation of intact Caco-2 cell monolayers. Based on these studies of Bhushani *et al.*, (2016:375) and Cataluyd *et al.*, (2011:129) the  $P_{app}$  of an intact Caco-2 cell monolayer for this study was considered between  $0.2 - 0.75 \times 10^{-6}$  cm/s.

### **3.5 *In vitro* transepithelial electrical resistance (TEER) studies with aloe leaf materials**

#### **3.5.1 Preparation of test solutions**

For the TEER studies, nine experimental solutions were prepared in serum-free DMEM. The positive control solution consisted of 0.5% w/v TMC (a known tight junction modulator), while the test solutions consisted of *A. vera* gel and whole leaf extract each in four different concentrations, namely 0.1% w/v, 0.5% w/v, 1.0% w/v and 1.5% w/v. Serum-free DMEM alone was used as the negative control group.

#### **3.5.2 TEER measurements**

The TEER measurements of the Caco-2 cell monolayers on filter inserts in 24-well Transwell® plates commenced one hour prior to addition of the test solutions to obtain the TEER values at baseline level. DMEM buffered with HEPES (pH = 7.4) (1 ml) was added to the basolateral chamber and incubated for 30 min prior to the addition of the test solutions (200  $\mu$ l) to the apical chamber on top of the cell monolayers on the filter membranes. The TEER ( $T_0$ ) was measured directly after application of the test solutions to the apical chamber. TEER measurements were then taken at 20 min intervals up to 120 min after addition of test solutions. Subsequently, the cell monolayers were washed with pre-warmed PBS to remove the test compounds (Peng *et al.*, 2007:37) and growth medium was added to the apical chambers. To determine if the tight junction opening effects of the *A. vera* gel and whole leaf extract were reversible, the TEER was subsequently measured at 20 min intervals for another 120 min (Chen *et al.*, 2009:589), thereafter at 3 h, 4 h, 6 h, 12 h, 24 h 48 h and 72 h after test solutions were removed. TEER was measured with a Millicell ERS meter (Millipore, Billerica, Massachusetts, USA) that was connected to a set of chopstick electrodes. The approximate time the recovery of each experimental group took to reach 100% of the initial TEER, was calculated by using Equation 1.

### **3.6 *In vitro* permeation studies with FITC-dextran to determine the absorption enhancement capacity of aloe leaf materials**

#### **3.6.1 Preparation of test solutions**

For the *in vitro* permeation study, four different FITC-dextran (i.e. FD-4, FD-10, FD-20 and FD-40) solutions were prepared. Each of the FITC-dextran test solutions contained FITC-dextran

(125 µg/ml in serum-free DMEM), in addition to four different concentrations of aloe leaf materials (i.e. 0.1% w/v, 0.5% w/v, 1.0% w/v, 1.5% w/v *A. vera* gel and whole leaf extract). Control groups consisted of FITC-dextran in serum-free DMEM without absorption enhancers.

### **3.6.2 Measurement of FITC-dextran permeation**

The *in vitro* permeation of the FITC-dextran molecules with different molecular weights in the absence and presence of the different *A. vera* gel and whole leaf extract solutions was determined in the apical to basolateral (AP-BL, absorptive) direction. The growth medium was aspirated from the basolateral chamber and replaced with 2.5 ml pre-heated serum-free DMEM buffered with HEPES (pH = 7.4) and placed back in the incubator (37°C) to equilibrate for 30 min. After 30 min, the Transwell® plates were removed from the incubator and the growth medium from the apical chamber was aspirated and replaced with 2.5 ml pre-heated test solution after which the initial TEER of each cell monolayer was measured. Samples (200 µl) were extracted from the basolateral chamber at 20 min intervals for a total period of 120 min and replaced with 200 µl pre-heated DMEM buffered with HEPES. The quantification of FITC-dextran concentrations in the samples was done by means of fluorescence spectroscopy at excitation and emission wavelengths of 494 nm and 518 nm, respectively.

### **3.7 Confocal laser scanning microscopy (CLSM) studies to determine the mechanism of drug absorption enhancement of aloe leaf materials**

Confocal laser scanning microscopy (CLSM) was used to visualise selected cell components by immunofluorescent staining in order to identify the mechanism of action of drug absorption enhancement by *A. vera* gel and whole leaf extract. CLSM was also used to obtain fluorescent images of the transport pathway by which the FITC-dextran is transported across the Caco-2 cell monolayer in the presence of the aloe leaf materials.

#### **3.7.1 Preparation of test solutions**

Stock solutions of FITC-dextran (FD-4, 1 mg/ml), *A. vera* gel and *A. vera* whole leaf extract (2.0% w/v), and TMC (1.0% w/v) were each prepared separately in serum-free DMEM. These stock solutions were used to prepare the test solutions, which consisted of combinations of FITC-dextran and each of the other solutions in a 1:1 ratio that were applied to the cell monolayers. The final concentrations of the test solutions were therefore 1.0% w/v *A. vera* gel and *A. vera* whole leaf extract, and 0.5% w/v TMC, while the final concentration of FITC-dextran in the mixture applied to the monolayers was 0.5 mg/ml. Negative control groups consisted of serum-free DMEM without any permeation enhancers.

For the immunofluorescent staining, a 10X CytoPainter® Phalloidin iFluor 488 solution was prepared by diluting 5 µl of a 1000X phalloidin conjugate in dimethyl sulfoxide (DMSO) stock solution with 500 µl PBS containing 1.1% v/v foetal bovine serum (FBS). The 0.1% v/v Triton X-100 solution was prepared by diluting 3 µl of the 100X Triton X-100 solution to 300 µl with PBS.

### **3.7.2 Immunofluorescent staining**

#### **3.7.2.1 Visualisation of transport pathway**

For the transport visualisation experiments, the Caco-2 cells were seeded out and cultured into cell monolayers on the membrane filter inserts of Snapwell® 6-well plates. After 21 days culturing and confirmation of cell monolayer formation, the cell monolayers were incubated with the test solutions for 2 h at 37°C, 5% CO<sub>2</sub> and 95% air.

After the incubation period, the cells were fixed with 4% formaldehyde for 10 min (Abcam, 2017c; Wu *et al.*, 2014:5694) and gently rinsed once with ice-cold PBS (Abcam, 2017a). After fixation, the cell monolayers were prepared on the microscope slides as described in section 3.7.2.3 and images were taken with a confocal laser scanning microscope (Nikon Eclipse TE-3000 inverted microscope, Nikon Instruments, Melville, NY, USA) linked to a Nikon D-Eclipse C1 confocal system with a DSRi1 Nikon digital camera with real time imaging equipped with standard objectives including 60 x and 100 x ApoPlanar oil immersion objectives. The images were taken at room temperature under light exclusion. All experiments were done in triplicate.

#### **3.7.2.2 Visualization of F-actin filaments in the cytoskeleton**

The mechanism of action of the absorption enhancing effects (more specifically, the tight junction opening) of the *A. vera* gel and whole leaf materials was determined by the staining of the F-actin in the cytoskeleton of the Caco-2 cells (Dorkoosh *et al.*, 2004:744; Hsu *et al.*, 2013:792). The cell monolayers in Snapwell® 6-well plates were incubated with test solutions (without FD-4) for 2 h at 37°C, 5% CO<sub>2</sub>, and 95% air. Where after the cell monolayers were fixed with 4% formaldehyde for 10 min and then gently rinsed with ice-cold PBS. Fixation was followed by permeabilization (to increase the permeability of the F-actin for better penetration of the CytoPainter® Phalloidin iFluor 488 stain) with 0.1% Triton X-100 for 3 min after which the cell monolayers were gently rinsed with PBS. Thereafter, F-actin staining was done with 10X CytoPainter® Phalloidin iFluor 488 for 60 min and gently rinsed for 5 min with PBS. After F-actin staining, cell monolayers were ready for microscope slide preparation as described in section 3.7.2.3 and images were taken with a confocal laser scanning microscope as described in section 3.7.2.4. All experiments were done in triplicate.

### 3.7.2.3 Preparation of samples for confocal laser scanning microscopy

Firstly, the filter-ring was removed from the Snapwell<sup>®</sup> insert and placed onto a glass plate to add support before the filter membrane was cut loose with a scalpel. The filter membrane was cut into smaller sections and a section with a size of approximately 1.12 cm x 0.3 cm was transferred to a microscope slide. Three to four drops of Fluoroshield<sup>®</sup> mounting medium containing propidium iodide (Abcam, 2017b) were added and spread out evenly. Care was taken not to touch the cell monolayer on the filter membrane. The propidium iodide contained in the mounting media was used to visualize the cell nuclei. Finally, the excess Fluoroshield<sup>®</sup> mounting medium was removed by gently touching the slide with a piece of paper towel and then a coverslip was added. Slides tended to produce better images when left in a fridge ( $\pm 2^{\circ}\text{C}$ ) overnight.

### 3.7.2.4 Imaging with confocal laser scanning microscopy

The confocal laser scanning microscope mentioned before (refer to section 3.7.2.1) equipped with an Argon Ion laser (emission wavelength of 488 nm or 515 nm), a Helium Neon polarised laser (emission wavelength of 543 nm) and a blue Diode laser (emission wavelength of 409 nm). The excitation and emission wavelengths used for the imaging of FITC-dextran, Phalloidin iFluor and propidium iodide are shown in Table 3.3.

**Table 3.3:** Excitation and emission wavelengths of the dyes and transport marker used in the confocal imaging experiments (Abcam, 2017a; Abcam, 2017b; Kotzé *et al.*, 1998:38)

Compound	Excitation wavelength (nm)	Emission wavelength (nm)
FITC-dextran	494	518
Phalloidin iFluor	493	517
Propidium Iodide	535	615

## 3.8 Data analysis and statistical evaluation

### 3.8.1 Processing of the *in vitro* permeation data

The *in vitro* permeation data was processed by determining the percentage transport at each time interval and calculating the apparent permeability coefficient ( $P_{app}$ ) values for each of the aloe leaf materials and concentrations used.

The percentage transport was calculated from the concentration of FITC-dextran (including 4000 Da, 10 000 Da, 20 000 Da, and 40 000 Da) measured in the basolateral chamber at each time interval relative to the initial dose of FITC-dextran applied to the Caco-2 cell monolayers in the apical chambers. Percentage transport was calculated with the following equation:

$$\% \text{Transport} = \frac{\text{Drug concentration at specific time interval}}{\text{Initial FITC-dextran dose}} \times 100 \quad \text{Equation 6}$$

The apparent permeability coefficient ( $P_{\text{app}}$ ) values were calculated for the transport across the Caco-2 cell monolayers for each of the FITC-dextran molecules (including 4000 Da, 10 000 Da, 20 000 Da, and 40 000 Da) used in the drug absorption enhancement experiments.  $P_{\text{app}}$  is defined as the permeability rate that is normalised by the surface area across which the permeation occurs as well as the concentration, assuming the starting concentration in the receiving chamber is zero (Palumbo *et al.*, 2008:236). The  $P_{\text{app}}$  was calculated by using the following equation (Johnson *et al.*, 2008:263; Kotzé *et al.*, 1998:38):

$$P_{\text{app}} = \frac{dc}{dt} \frac{1}{(A \cdot C_0)} \quad \text{Equation 7}$$

Where  $P_{\text{app}}$  is the apparent permeability coefficient ( $\text{cm/s}^{-1}$ ),  $(dc/dt)$  represents the permeability rate (concentration/min, represented by the slope of the transport curve),  $A$  is the permeation surface area ( $\text{cm}^2$ ) and  $C_0$  is the starting concentration of the permeant.

### 3.8.2 Processing of the *in vitro* transepithelial electrical resistance data

The measured TEER values were normalised to a percentage of the initial TEER value at time 0. To determine the % TEER reduction, these values were then subtracted from 100% (the value at time 0), which expressed quantitatively the effect of each of the experimental materials on the electrical resistance of the Caco-2 cell monolayers (which is an indication of the opening of tight junctions between the cells).

### 3.8.3 Statistical evaluation of results

Data analyses on the *in vitro* permeation results were performed with STATISTICA Ver 12. All data sets were subjected to the Brown-Forsythe test to establish the normality and homogeneity of the data distribution. The parametric tests applied to normally distributed data, were analysis of variance (ANOVA) with Dunnet's post-hoc tests (two-sided). For data sets that weren't normally distributed, non-parametric Kruskal-Wallis testing was applied. Statistically significant differences were accepted when  $p < 0.05$ .

## CHAPTER 4: RESULTS AND DISCUSSION

### 4.1 Introduction

In this study, the intestinal drug absorption enhancement capacity and mechanism of action of *Aloe vera* gel and whole leaf extract were investigated. The Caco-2 cell line, which is an intestinal epithelial cell line, was used as the *in vitro* experimental model to achieve the aim of this study. The Caco-2 cell model is one of the most extensively characterised *in vitro* screening tools in the field of drug permeability studies including drug absorption enhancement (Artursson & Karlsson 1991:881; Rubas *et al.*, 1996:167). Caco-2 cell monolayers grown on Transwell® plate inserts were used for transepithelial electrical resistance (TEER) and permeation studies. For the TEER studies, Caco-2 cell monolayers were incubated for two hours with different concentrations of the aloe leaf materials (i.e. 0.1% w/v, 0.5% w/v, 1.0% w/v and 1.5% w/v of both the *A. vera* gel and whole leaf extract). The positive control was 0.5% w/v *N*-trimethyl chitosan chloride (TMC; a known paracellular absorption enhancer) and the negative control used, was DMEM alone on the Caco-2 cell monolayers. Different molecular weight FITC-dextran (i.e. 4 000 Da, 10 000 Da, 20 000 Da and 40 000 Da) were used to evaluate the drug absorption enhancement capacity of the different *A. vera* gel and whole leaf extract solutions across Caco-2 cell monolayers. The percentage cumulative transport of each FITC-dextran was determined over two hours and the resulting  $P_{app}$  values were calculated and compared to that of the negative control (FITC-dextran alone) for statistical analysis.

The mechanism of action of drug absorption enhancement by the *A. vera* gel and whole leaf extract was investigated by means of confocal laser scanning microscopy (CLSM). CLSM is a technique that has been successfully used to clarify the pathways and mechanisms of drug permeation enhancement (Hsu *et al.*, 2012:6255; Kotzé *et al.*, 1998:44). The Caco-2 cell monolayers were incubated with FITC-dextran (4 000 Da) and the absorption enhancers (1.0% w/v *A. vera* gel and 1.0% w/v *A. vera* whole leaf extract and 0.5% w/v TMC), to visualize the paracellular transport of FITC-dextran. To further determine the mechanism of action of paracellular absorption enhancement, the F-actin in the cytoskeleton of the Caco-2 cells was immunofluorescently stained and then detected by means of CLSM. A rearrangement in the F-actin distribution indicates the modulation of tight junctions (Hsu *et al.*, 2013:792). After Caco-2 cell monolayers were incubated in the absence (negative control) and presence of the absorption enhancers (1.0% w/v *A. vera* gel and 1.0% w/v *A. vera* whole leaf extract and 0.5% w/v TMC), the F-actin was stained with CytoPainter® Phalloidin iFluor 488.

## **4.2 Validation of the fluorometric analytical method for FITC-dextran and Lucifer Yellow on the Spectramax® plate reader**

Validation of the fluorometric analytical method was done to establish that the method complied with the requirements as set out by the USP (2017b:1781) in terms of linearity, accuracy, precision, specificity, limit of detection (LOD) and limit of quantification (LOQ). Fluorescein isothiocyanate-dextran (FITC-dextran) was used as the fluorescently labelled model compound to determine the paracellular permeability modulation effects of the aloe leaf materials (Matter & Balda 2003:232), while Lucifer yellow was used as an exclusion marker confirming the integrity of the Caco-2 cell monolayers used in the *in vitro* permeation studies (Bhushani *et al.*, 2016:375). Fluorescence detection values for FITC-dextran (all selected molecular weights) and Lucifer yellow samples were determined with a Spectramax® plate reader. According to Matter & Balda (2013:232), differently sized fluorescent dextran molecules can be analysed with the same detection method. The excitation and emission wavelengths used when measuring FITC-dextran were 494 nm and 518 nm, and for Lucifer yellow the wavelengths were 485 nm and 535 nm, respectively.

### **4.2.1 Linearity**

In Table 4.1, the calculated regression coefficient ( $R^2$ ) values from the standard curves are listed for each of the FITC-dextran compounds as well as for Lucifer yellow. From Table 4.1, it can be seen that all the model compounds (i.e. FITC-dextran 4 000 Da, 10 000 Da, 20 000 Da and 40 000Da, and Lucifer yellow) complied with the requirement of a  $R^2 \geq 0.995$  USP (2017a:783). Since the analytical method complied with the requirement for linearity for all the marker molecules tested, they showed that the responses were directly correlated to the concentration of the analyte. The linear regression curves for Lucifer yellow and all the FITC-dextran compounds are listed in Appendix B.

**Table 4.1:** Linear regression coefficient ( $R^2$ ) values calculated from the standard curves for the selected FITC-dextran molecules and Lucifer yellow

<b>Model compound</b>	<b>Calculated regression coefficient (<math>R^2</math>)</b>	<b>Compliant with USP (2017a:783) requirements (<math>R \geq 0.995</math>)</b>
FITC-dextran 4 000 Da	0.9991	Yes
FITC-dextran 10 000 Da	0.9995	Yes
FITC-dextran 20 000 Da	0.9971	Yes
FITC-dextran 40 000 Da	0.9958	Yes
Lucifer yellow	0.9997	Yes

## **4.2.2 Accuracy and precision**

### **4.2.2.1 Accuracy**

The percentage recovery values obtained for all three FITC-dextran (4 000 Da) and Lucifer yellow concentrations tested are shown in Table 4.2 and Table 4.3, respectively. This confirmed that the analytical method complied with the criteria for accuracy of 98%–102% recovery as specified in the USP (2017a:782). The analytical procedures therefore produced results that were sufficiently close to the true value of the sample. See Appendix B for fluorescence detection values.

**Table 4.2:** Percentage recovery obtained from three different FITC-dextran concentrations

<b>Theoretical concentration (µg/ml)</b>	<b>Actual concentration (µg/ml)</b>	<b>% Recovery</b>
125.00	125.29	100.23
125.00		
125.00		
62.50	62.22	99.55
62.50		
62.50		
31.25	31.80	101.75
31.25		
31.25		

**Table 4.3:** Percentage recovery obtained from three different Lucifer yellow concentrations

<b>Theoretical concentration µg/ml</b>	<b>Actual concentration</b>	<b>% Recovery</b>
50.00	49.81	99.63
50.00		
50.00		
25.00	25.08	100.33
25.00		
25.00		
12.50	12.73	101.80
12.50		
12.50		

#### 4.2.2.2 Intra-day precision

Table 4.4 and Table 4.5 shows the %RSD values calculated from fluorescence detection values of FITC-dextran (4 000 Da) and Lucifer yellow solutions; covering a specified concentration range over a relatively short period of time (i.e. 11:00, 14:00 and 17:00 on the same day for FITC-dextran and 10:00, 12:00 and 14:00 for Lucifer yellow) as an indication of intra-day precision. The %RSD values were lower than 2% RSD as suggested by the USP (2017a:782), indicating that the analytical method complied with the criteria for intra-day precision. The analytical method therefore showed sufficient short-term repeatability as indicated by the low %RSD values.

**Table 4.4:** Mean fluorescence detection and %RSD values for a specified concentration range of FITC-dextran measured at different time points on the same day

Theoretical concentration (µg/ml)	Mean fluorescence detection value (n = 3)			Average	Standard deviation	%RSD
	11:00	14:00	17:00			
125.00	$7.74 \times 10^{-8}$	$7.98 \times 10^{-8}$	$7.79 \times 10^{-8}$	$7.84 \times 10^{-8}$	$1.04 \times 10^{-7}$	1.32
62.50	$3.93 \times 10^{-8}$	$4.04 \times 10^{-8}$	$4.04 \times 10^{-8}$	$4.00 \times 10^{-8}$	$0.48 \times 10^{-7}$	1.21
31.25	$2.06 \times 10^{-8}$	$2.09 \times 10^{-8}$	$2.12 \times 10^{-8}$	$2.09 \times 10^{-8}$	$0.26 \times 10^{-7}$	1.22

**Table 4.5:** Mean fluorescence detection and %RSD values for a specified concentration range of Lucifer yellow measured at different time points on the same day

Theoretical concentration (µg/ml)	Mean fluorescence detection value (n = 3)			Average	Standard deviation	%RSD
	10:00	12:00	14:00			
50.00	$5.51 \times 10^{-7}$	$5.67 \times 10^{-7}$	$5.50 \times 10^{-7}$	$5.56 \times 10^{-7}$	$7.98 \times 10^{-5}$	1.43
25.00	$2.95 \times 10^{-7}$	$3.04 \times 10^{-7}$	$2.86 \times 10^{-7}$	$2.95 \times 10^{-7}$	$7.02 \times 10^{-5}$	2.38
12.50	$1.47 \times 10^{-7}$	$1.51 \times 10^{-7}$	$1.45 \times 10^{-7}$	$1.48 \times 10^{-7}$	$2.34 \times 10^{-5}$	1.58

#### 4.2.2.3 Inter-day precision

The %RSD values shown in Table 4.6 and Table 4.7 show that the fluorescence analytical method complied with the criteria of %RSD ≤ 5% as set out by the ICH (2005:10) guidelines for inter-day precision, for FITC-dextran and Lucifer yellow.

**Table 4.6:** Mean fluorescence detection and %RSD values for a specified concentration range of FITC-dextran measured on three consecutive days

Theoretical concentration (µg/ml)	Mean fluorescence detection value (n = 3)			Average	Standard deviation	%RSD
	Day 1	Day 2	Day 3			
125.00	$7.24 \times 10^{-8}$	$7.20 \times 10^{-8}$	$7.61 \times 10^{-8}$	$7.35 \times 10^{-8}$	$1.86 \times 10^{-7}$	2.52
62.50	$3.60 \times 10^{-8}$	$3.66 \times 10^{-8}$	$3.81 \times 10^{-8}$	$3.69 \times 10^{-8}$	$0.87 \times 10^{-7}$	2.37
31.25	$2.00 \times 10^{-8}$	$1.97 \times 10^{-8}$	$2.01 \times 10^{-8}$	$1.99 \times 10^{-8}$	$0.19 \times 10^{-7}$	0.95

**Table 4.7:** Mean fluorescence detection and %RSD values for a specified concentration range of Lucifer yellow measured on three consecutive days

Theoretical concentration (µg/ml)	Mean fluorescence detection value (n = 3)			Average	Standard deviation	%RSD
	Day 1	Day 2	Day 3			
50.00	$6.17 \times 10^{-7}$	$6.03 \times 10^{-7}$	$6.21 \times 10^{-7}$	$6.14 \times 10^{-7}$	$7.64 \times 10^{-5}$	1.25
25.00	$3.13 \times 10^{-7}$	$3.20 \times 10^{-7}$	$3.08 \times 10^{-7}$	$3.14 \times 10^{-7}$	$4.95 \times 10^{-5}$	1.58
12.50	$1.62 \times 10^{-7}$	$1.59 \times 10^{-7}$	$1.66 \times 10^{-7}$	$1.62 \times 10^{-7}$	$2.90 \times 10^{-5}$	1.79

#### 4.2.3 Limit of detection (LOD) and limit of quantification (LOQ)

The slope of the linear regression curve and the standard deviation of the blanks for FITC-dextran (4 000 Da) are shown in Table 4.8 and for Lucifer yellow it is shown in Table 4.9. The LOD and LOQ for FITC-dextran were calculated to be 0.038 µg/ml and 0.115 µg/ml, and for Lucifer yellow 0.180 µg/ml and 0.546 µg/ml, respectively. Since the LOD and LOQ were found to be pronouncedly lower than the concentrations in the experimental samples, they are considered acceptable for the application in this study.

**Table 4.8:** Average fluorescence detection and standard deviation values of the blanks (i.e. background noise) as well as slope of the standard curve for FITC-dextran

Fluorescence detection value of the blank	Average	Standard deviation
$2.29 \times 10^{-6}$	$2.22 \times 10^{-6}$	$5.87 \times 10^{-4}$
$2.29 \times 10^{-6}$		
$2.24 \times 10^{-6}$		
$2.15 \times 10^{-6}$		
$2.20 \times 10^{-6}$		
$2.15 \times 10^{-6}$		
<b>SLOPE</b>	<b><math>5.08 \times 10^{-6}</math></b>	

**Table 4.9:** Average fluorescence detection and standard deviation values of the blanks (i.e. background noise) as well as slope of the standard curve for Lucifer yellow

Fluorescence detection value of the blank	Average	Standard deviation
$3.38 \times 10^{-6}$	$3.45 \times 10^{-6}$	$6.46 \times 10^{-4}$
$3.37 \times 10^{-6}$		
$3.51 \times 10^{-6}$		
$3.43 \times 10^{-6}$		
$3.53 \times 10^{-6}$		
$3.51 \times 10^{-6}$		
<b>SLOPE</b>	<b><math>1.18 \times 10^{-6}</math></b>	

#### 4.2.4 Specificity

The specificity of the analytical method was shown to be acceptable (refer to Table 4.10) as the percentage recovery of FITC-dextran (4 000 Da) in the presence of *A. vera* gel and whole leaf extract was within the required range of 98%–102% (USP, 2017a:782). This indicated that the excipients selected as drug absorption enhancers in this study did not interfere with the analysis of the FITC-dextran.

As Lucifer yellow was only employed as an exclusion marker to determine the integrity of the experimental Caco-2 cell monolayers, it was not necessary to establish the percentage recovery of this marker molecule in the presence of aloe leaf materials.

**Table 4.10:** Percentage recovery of FITC-dextran in the presence of *Aloe vera* gel and *Aloe vera* whole leaf extract

<b>Plant materials</b>	<b>Theoretical concentration (µg/ml)</b>	<b>Actual concentration (µg/ml)</b>	<b>% Recovery</b>
<i>A. vera</i> gel (1.5% w/v)	132.5	130.56	98.54
<i>A. vera</i> whole leaf extract (1.5% w/v)	132.5	134.90	101.81

#### 4.2.5 Conclusion

The analytical method complied with the criteria for the validation parameters (i.e linearity, accuracy, precision and specificity). The suitability of the fluorometric analytical method with the Spectramax® plate reader was therefore confirmed for the measurement of FITC-dextran in the *in vitro* permeation study samples and Lucifer yellow in the Caco-2 cell monolayer integrity study samples.

### 4.3 Cell monolayer integrity

The apparent permeability coefficient ( $P_{app}$ ) values of Lucifer yellow were calculated from the transport curve shown in Figure 4.1. The average  $P_{app}$  value for Lucifer yellow ( $0.345937 \times 10^{-6}$  cm/s) in this study was within range of the suggested  $P_{app}$  values for Lucifer yellow when transported across Caco-2 cell monolayers with acceptable integrity, namely  $0.2\text{--}0.75 \times 10^{-6}$  cm/s (Bhushani *et al.*, 2016:375; Cataluyd *et al.*, 2011:129). The percentage transport (Figure 4.1) was also lower than 2% as suggested by Wahlang *et al.* (2011:278). The Lucifer yellow permeation and percentage transport results therefore confirmed the acceptability of the integrity of the Caco-2 cell monolayers used in the permeation studies. Fluorescence detection values used for determining the percentage transport and calculated  $P_{app}$  values, are given in Appendix D.

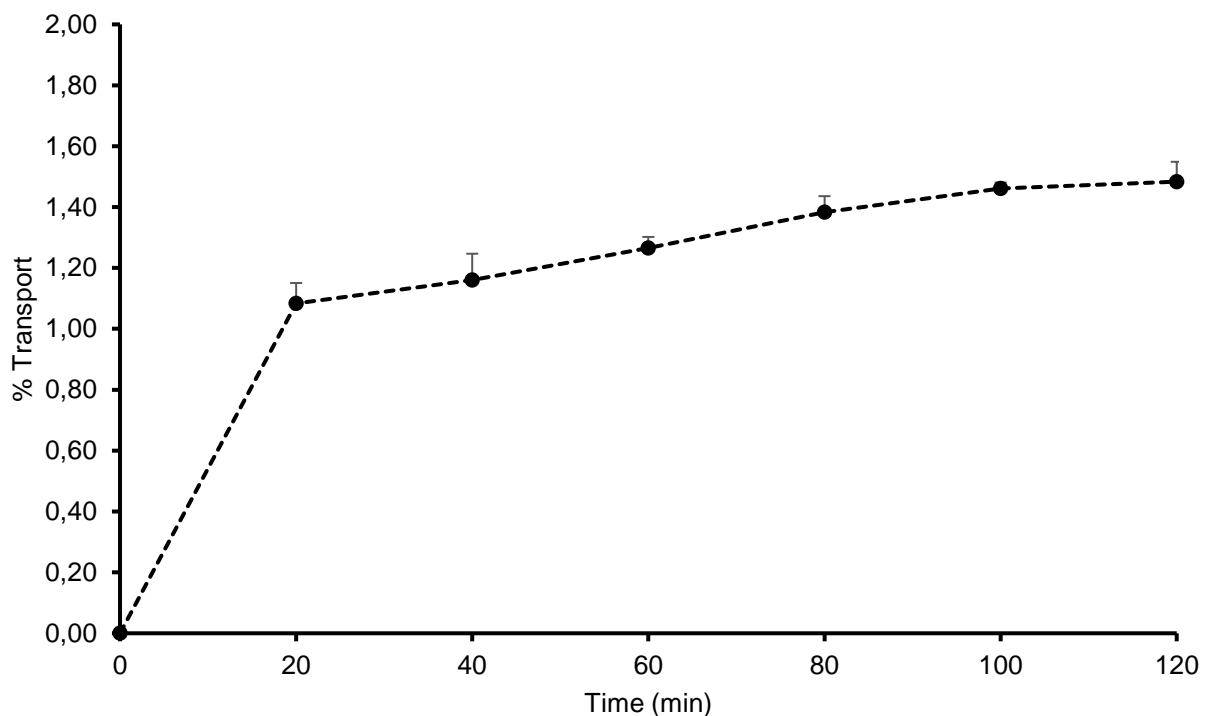


**Figure 4.1:** Percentage transport of Lucifer yellow across Caco-2 cell monolayers (n = 3) (Error bars represent SD)

#### 4.4 *In vitro* transepithelial electrical resistance (TEER) studies with aloe leaf materials

The TEER value of a cell monolayer is indicative of the tight junction integrity and therefore gives an indication of paracellular permeability. A decrease in TEER is related to the opening of tight junctions and therefore also to an increase in the paracellular permeability of the cell monolayer (Hsu *et al.*, 2013:787; Lemmer & Hamman, 2013:107). Prior to each TEER experiment the TEER value of the Caco-2 cell monolayers was measured, as an initial value  $\geq 750 \Omega$  indicated an intact, confluent cell monolayer on the membrane filters of a 24-well Transwell® plate (area of 0.33 cm<sup>2</sup>) (Du Toit *et al.*, 2016:578). Tables with all the experimental TEER data and the relevant calculations can be seen in Appendix C.

##### 4.4.1 *Aloe vera* gel

The percentage TEER reduction at 20 min after application of the *A. vera* gel solutions (i.e. 0.1% w/v; 0.5% w/v; 1.0% w/v and 1.5% w/v) and TMC (0.5% w/v) are shown in Figure 4.2. The percentage TEER of the Caco-2 cell monolayers plotted as a function of time after removal of the *A. vera* gel solutions and TMC (i.e. recovery) is shown in Figure 4.3. The TEER values measured for the negative control group remained at 100% or slightly higher throughout the experimental period (data are not shown, since no TEER reduction occurred).

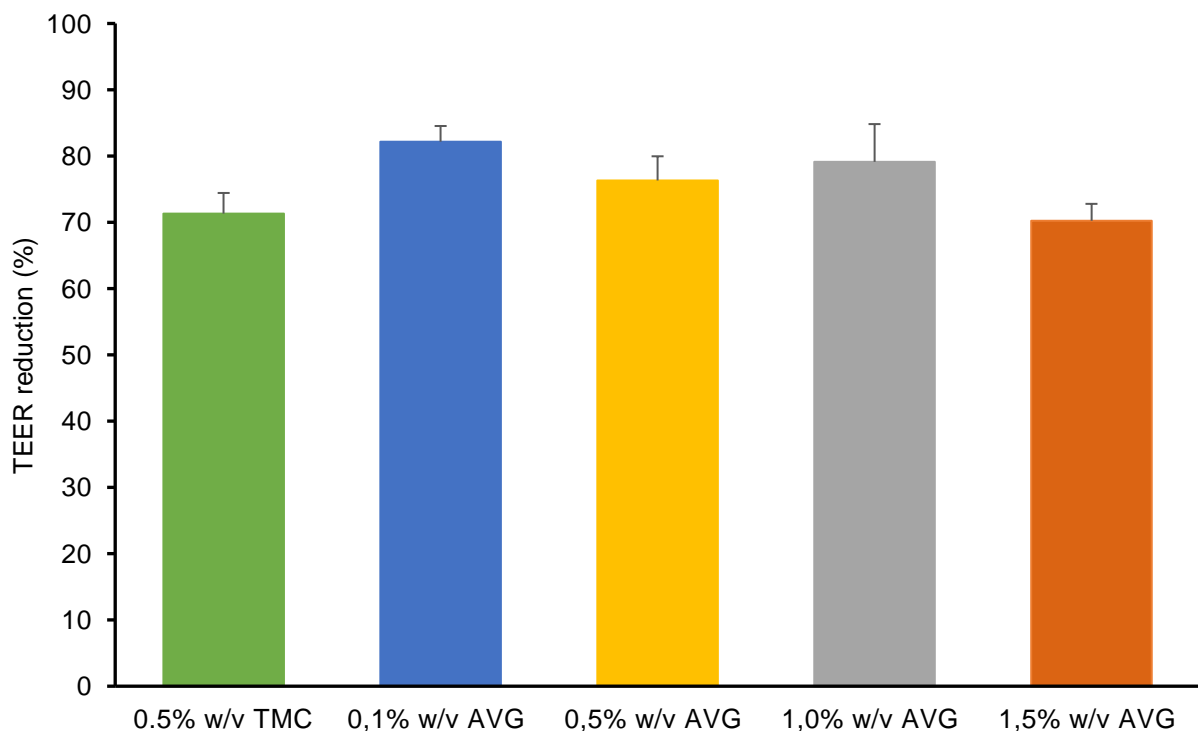


**Figure 4.2:** Percentage TEER reduction at time 20 min by *A. vera* gel (0.1% w/v, 0.5% w/v, 1.0% w/v and 1.5% w/v) and TMC (0.5% w/v, positive control group) (n = 3) (Error bars represent SD) (AVG = *Aloe vera* gel)

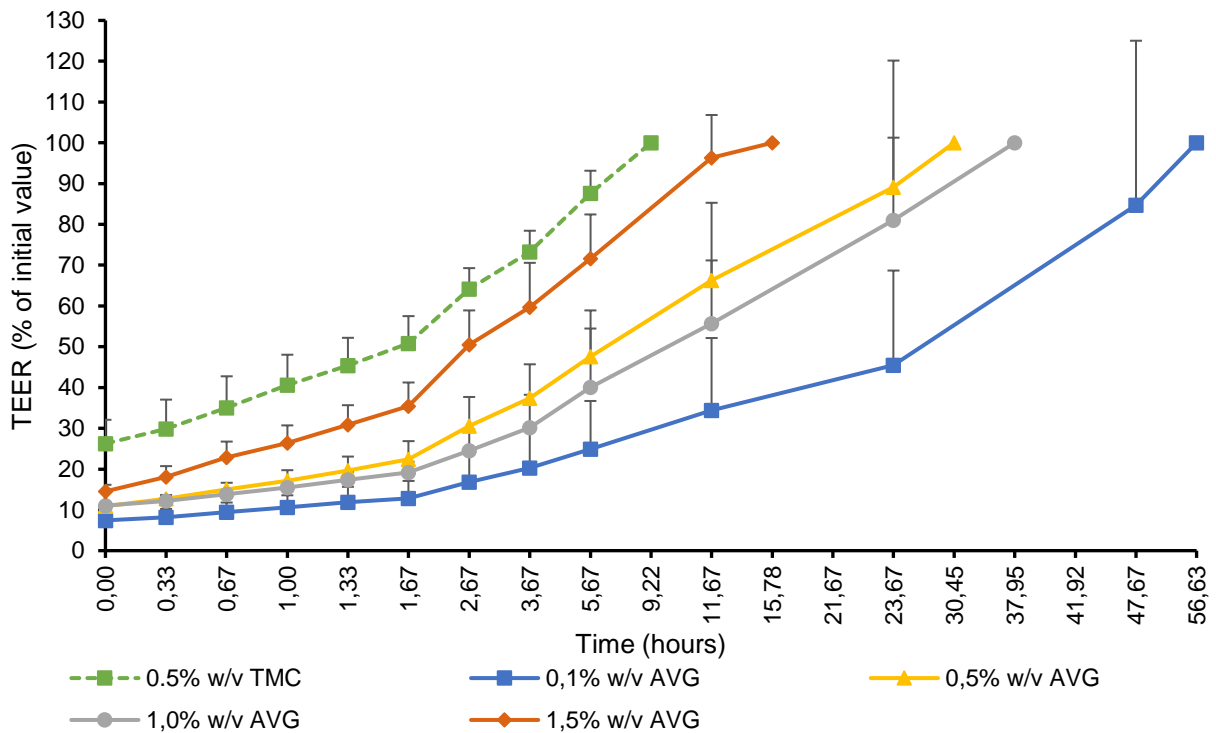


**Figure 4.3:** Percentage TEER recovery plotted as a function of time after removal of the *A. vera* gel solutions (0.1% w/v, 0.5% w/v, 1.0% w/v and 1.5% w/v) and TMC (0.5% w/v, positive control group (n = 3) (Error bars represent SD) (AVG = *Aloe vera* gel)

From Figure 4.2, it is clear that a rapid and relatively large decrease in the percentage TEER occurred after application of the *A. vera* gel solutions. The decrease in TEER caused by *A. vera* gel on the Caco-2 cell monolayers was inversely proportionate to the concentration of *A. vera* gel applied with respect to the 0.1% w/v, 0.5% w/v and 1.5% w/v concentrations, albeit the effect differed relatively little between the solutions with different concentrations. For example, the 1.5% w/v *A. vera* gel solution decreased the TEER to  $29.77 \pm 2.55\%$  of the initial value, while the 0.1% w/v *A. vera* gel solution decreased the TEER to  $17.84 \pm 2.37\%$  of the initial value. The difference can possibly be explained by the viscosity of the *A. vera* gel solutions, the higher concentration solutions could potentially have restricted free movement of ions via the opened tight junctions. Furthermore, the 0.5% w/v *A. vera* gel solution reduced the TEER of the Caco-2 cell monolayers similar to that obtained with the positive control group (i.e. 0.5% w/v TMC that decreased the TEER to  $28.69 \pm 3.11\%$  of the initial value and 1.5% w/v *A. vera* gel solution decreased the TEER to  $70.23 \pm 2.55\%$  of the initial value). Where the rest of the *A. vera* gel solutions (0.1%, 0.5% w/v and 1.0% w/v) decreased the TEER more than the positive control. These TEER reduction results are in accordance with previous findings with *A. vera* gel (Chen *et al.*, 2009:589; Lebitsa *et al.*, 2012:304).

After two hours, the test solutions were removed and the Caco-2 cell monolayers were rinsed with pre-heated phosphate buffered saline (PBS), which caused a slight drop in the TEER. After this decrease in TEER, a steady increase can be noticed toward the initial TEER value (Figure

4.3). The recovery of the TEER values toward 100% of the initial value indicates that the effect of *A. vera* gel on the tight junctions is reversible. Complete recovery to 100% within 24 h can only be seen for the 1.5% w/v *A. vera* gel solution as well as the positive control (0.5% w/v TMC).

#### 4.4.2 *Aloe vera* whole leaf extract

In Figure 4.4, the percentage TEER reduction of Caco-2 cell monolayers at 20 min, after addition of different concentrations *A. vera* whole leaf extract solutions (0.1% w/v, 0.5% w/v, 1.0% w/v and 1.5% w/v) and 0.5% w/v TMC (positive control) is shown. Figure 4.5 demonstrates the percentage TEER recovery plotted as a function of time, after the removal of the *A. vera* whole leaf extract solutions and TMC. The TEER values measured for the negative control group remained at 100% or slightly higher throughout the experimental period (data are not shown, since no TEER reduction occurred).

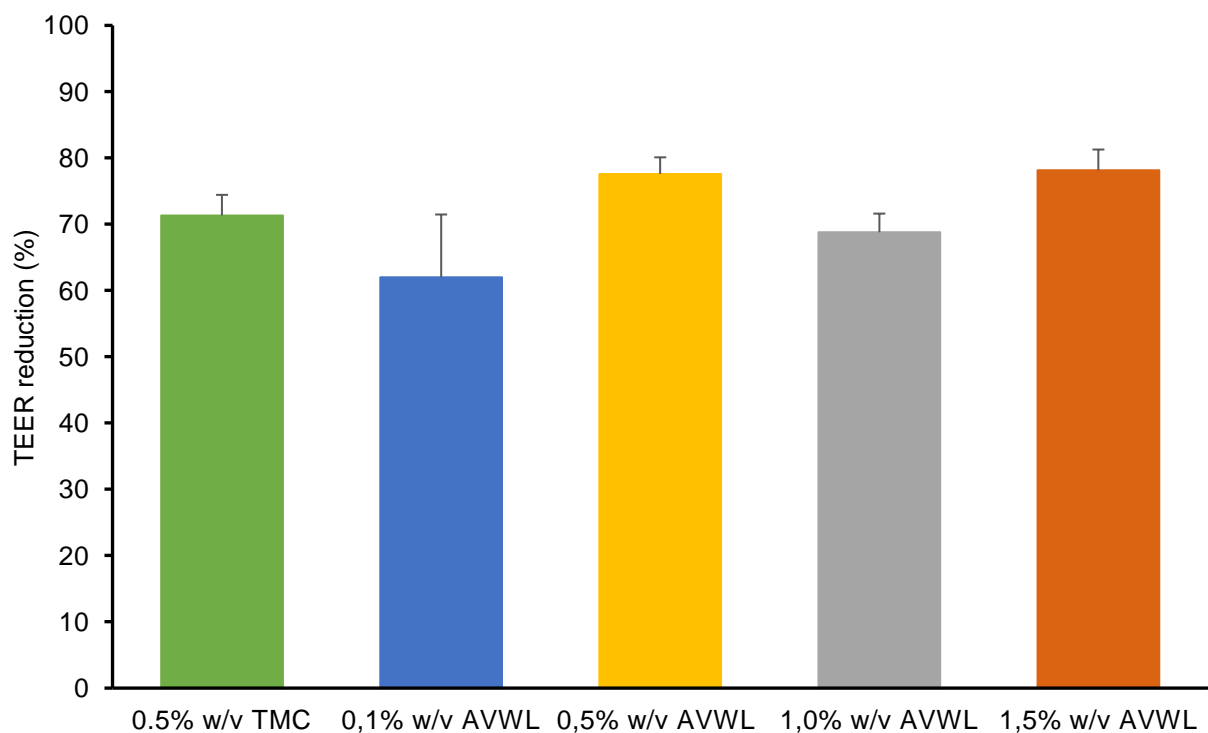


**Figure 4.4:** Percentage TEER reduction at time 20 min by *A. vera* whole leaf extract (0.1% w/v, 0.5% w/v, 1.0% w/v and 1.5% w/v) and TMC (0.5% w/v, positive control group) (n = 3) (Error bars represent SD) (AVWL = *Aloe vera* whole leaf extract)

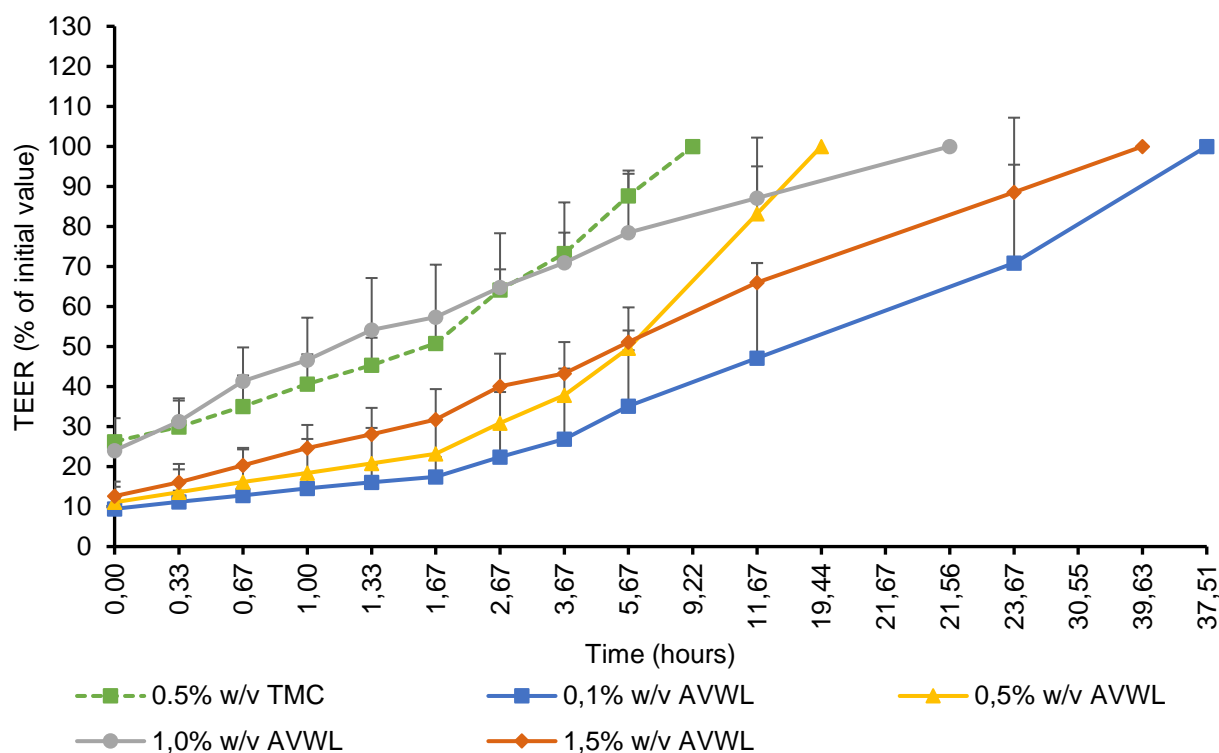


**Figure 4.5:** Percentage TEER recovery plotted as a function of time after removal of the *A. vera* whole leaf extract solutions (0.1% w/v, 0.5% w/v, 1.0% w/v and 1.5% w/v) and TMC (0.5% w/v, positive control group (n = 3) (Error bars represent SD) (AVWL = *Aloe vera* whole leaf extract)

In Figure 4.4, a rapid and relatively large decrease in the percentage TEER of Caco-2 cell monolayers can be seen after the application of all the *A. vera* whole leaf extract solutions. The decrease in TEER caused by the *A. vera* whole leaf extract solutions applied to the Caco-2 cell monolayers was not completely proportionate to the concentration *A. vera* whole leaf extract applied because the 0.5% w/v solution exhibited a TEER reduction value similar to that of the 1.5% w/v solution. The reduction in TEER caused by the *A. vera* whole leaf extract solutions were similar to the TEER reduction observed for the positive control group (i.e. 0.5% w/v TMC that decreased the TEER to  $28.69 \pm 3.11\%$  of the initial value). These results are in accordance with previous studies done with *A. vera* whole leaf extract (Beneke *et al.*, 2012:481; Chen *et al.*, 2009:589).

A slight drop in the percentage TEER was observed after removal of the test solutions and PBS rinse (Figure 4.5). This is followed by a gradual increase in the percentage TEER towards 100% of the initial TEER value. The recovery of the Caco-2 cells monolayer towards 100% of the initial TEER value indicates the reversibility of the effect of the *A. vera* whole leaf extract on the tight junctions. Only the 0.5% w/v *A. vera* whole leaf extract solution and the positive control (i.e. 0.5% w/v TMC) showed a complete recovery to 100% in 24 h.

### **4.4.3 Conclusions from the transepithelial electrical resistance (TEER) results**

Since a reduction in TEER indicates the opening of tight junctions, which is associated with increased paracellular permeability, the results from this TEER study indicated that *A. vera* gel and whole leaf extract are capable of opening tight junctions of epithelial cell monolayers. The capacity of the aloe leaf materials to enhance the *in vitro* permeation of compounds was further investigated by measuring their effects on the permeation of different molecular weight FITC-dextran molecules.

### **4.5 *In vitro* permeation studies with FITC-dextran to determine the absorption enhancement capacity of aloe leaf materials**

The *in vitro* permeation of four FITC-dextran molecules with approximate molecular weights of 4 000 Da (FD-4), 10 000 Da (FD-10), 20 000 Da (FD-20) and 40 000 Da (FD-40) was measured in the presence of four different concentrations of *Aloe vera* gel and whole leaf extract across Caco-2 cell monolayers. The TEER of the Caco-2 cell monolayers was measured prior to each transport experiment because a TEER value  $\geq 150 \Omega$  indicated an intact, confluent cell monolayer on the membrane filter of the 6-well Transwell<sup>®</sup> plates (area of 4.67 cm<sup>2</sup>) (these TEER values are shown in Appendix D) (Alqahtani *et al.*, 2013:2).

#### **4.5.1 FITC-dextran 4 000 Da**

##### **4.5.1.1 *Aloe vera* gel**

The effect of different concentrations of *A. vera* gel solutions on the percentage transport of FITC-dextran 4 000 Da across Caco-2 cell monolayers is shown in Figure 4.6 and the calculated apparent permeability coefficient ( $P_{app}$ ) values are given in Figure 4.7.

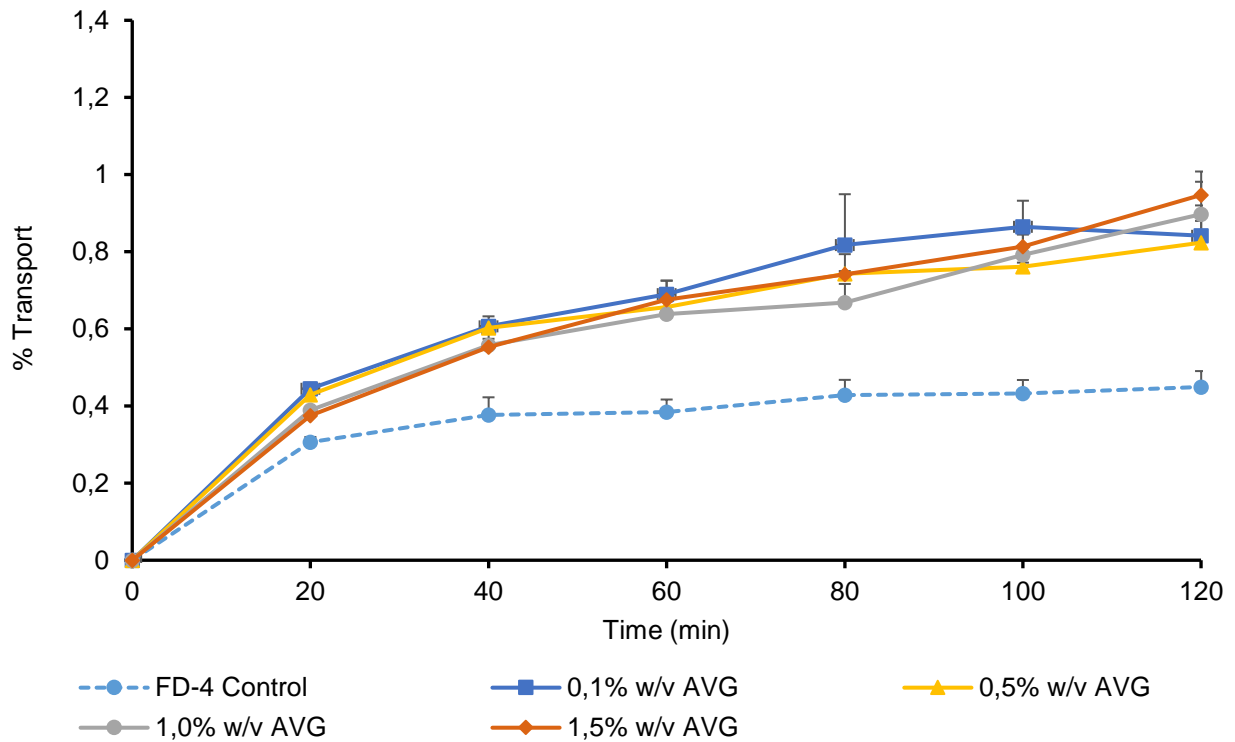


**Figure 4.6:** Percentage transport of FITC-dextran (MW = 4 000 Da) plotted as a function of time across Caco-2 cell monolayers in the presence of *Aloe vera* gel solutions with different concentrations (n = 3; error bars represent SD) (AVG = *Aloe vera* gel, FD-4 = FITC-dextran 4 000 Da, MW = molecular weight)

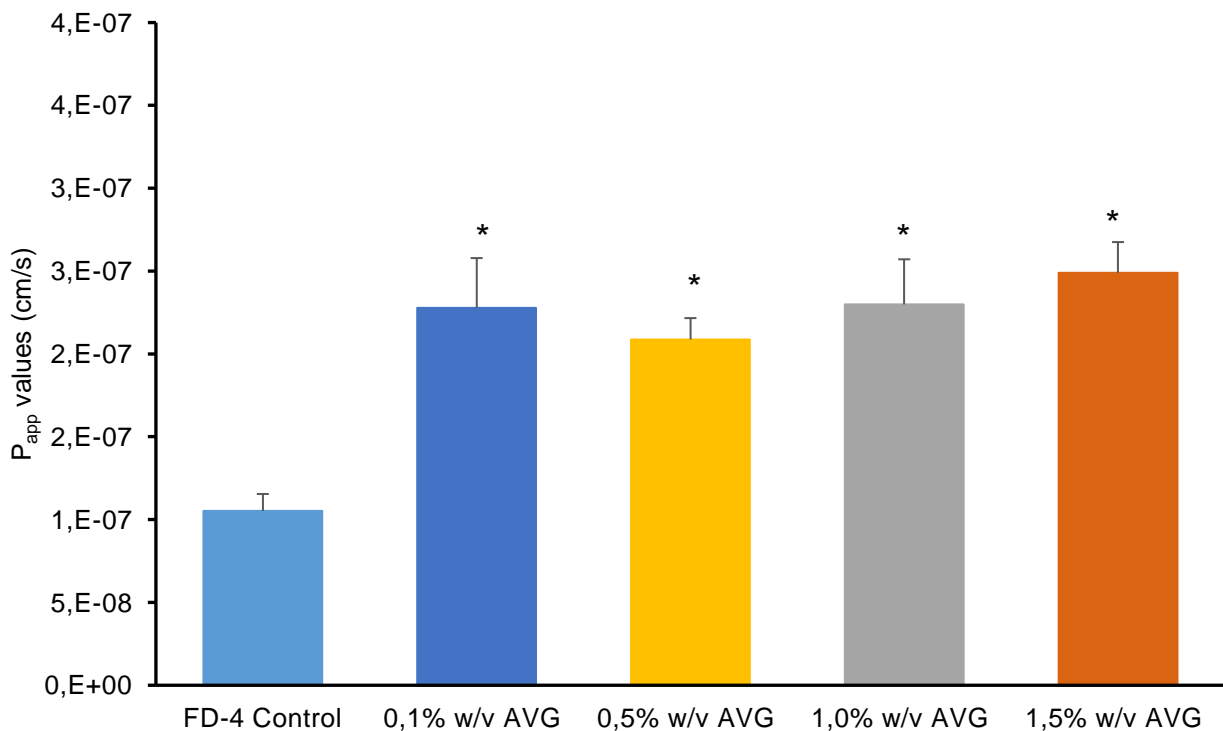


**Figure 4.7:** Apparent permeability coefficient ( $P_{app}$ ) values of FITC-dextran (4 000 Da) across Caco-2 cell monolayers when applied with *Aloe vera* gel solutions. Bars marked with an asterisk (\*) indicates statistical significant differences from the negative control group ( $p < 0.05$ ) (n = 3; error bars represent SD) (AVG = *Aloe vera* gel, FD-4 = FITC-dextran 4 000 Da)

From Figure 4.6, a clear increase in the percentage transport of FD-4 in relation to the negative control (FD-4 alone) can be seen for all concentrations of the *A. vera* gel solutions that were tested. The transport of FD-4 alone showed an initial increase until 20 min, where after it reached a plateau and stayed relatively stable over the rest of the 120 min transport period. From Figure 4.7, an approximate two-fold increase can be seen for the  $P_{app}$  values of FD-4 in the presence of the *A. vera* gel solutions in relation to the control group (FD-4 alone). This increase in transport occurred in a concentration dependent manner for the concentration range between 0.5% w/v to 1.5% w/v *A. vera* gel solutions. The lowest *A. vera* gel solution concentration (i.e. 0.1% w/v) gave a slightly higher transport enhancement effect than the 0.5% w/v and the 1.0% w/v *A. vera* gel solutions, but it was lower than that of the 1.5% w/v *A. vera* gel solution. The transport of FD-4 was statistically significantly higher ( $p < 0.05$ ) in the presence of all the *A. vera* gel solutions compared to the transport of the control group (FD-4 alone). The transport enhancement effects of the *A. vera* gel solutions across the Caco-2 cell monolayers corresponded with the TEER reduction results (Figure 4.2) and it can therefore be attributed to tight junction modulating activities. The tight junction modulating activities of *A. vera* gel were further investigated by immunofluorescent staining and confocal laser scanning microscopy (CLSM) as reported in section 4.6 (*Confocal laser scanning microscopy studies to determine the mechanism of drug absorption enhancement*) of this chapter.

#### **4.5.1.2 *Aloe vera* whole leaf extract**

The effect of *A. vera* whole leaf extract solutions (in different concentrations) on the percentage transport of FITC-dextran 4 000 Da across Caco-2 cell monolayers is shown in Figure 4.8 and the calculated apparent permeability coefficient ( $P_{app}$ ) values are given in Figure 4.9.

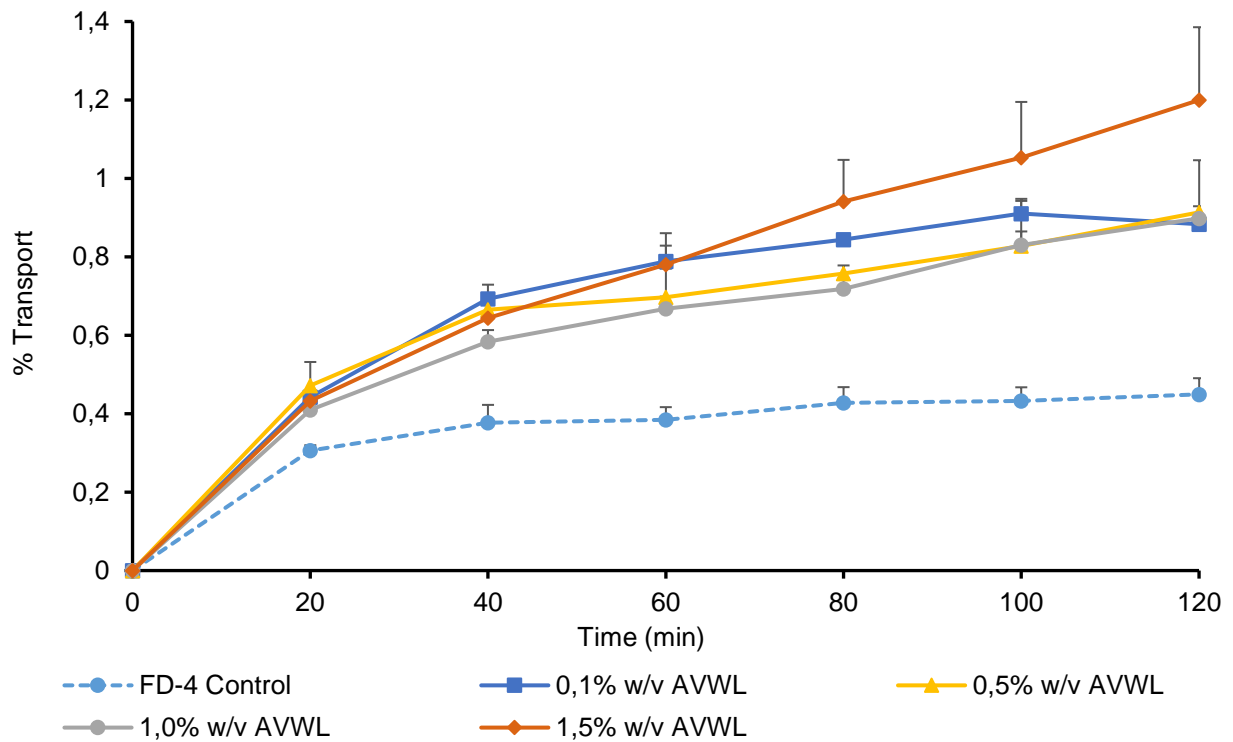


**Figure 4.8:** Percentage transport of FITC-dextran (MW = 4 000 Da) plotted as a function of time across Caco-2 cell monolayers in the presence of *Aloe vera* whole leaf extract solutions with different concentrations (n = 3; error bars represent SD) (AVWL = *Aloe vera* whole leaf extract, FD-4 = FITC-dextran 4 000 Da; MW = molecular weight)

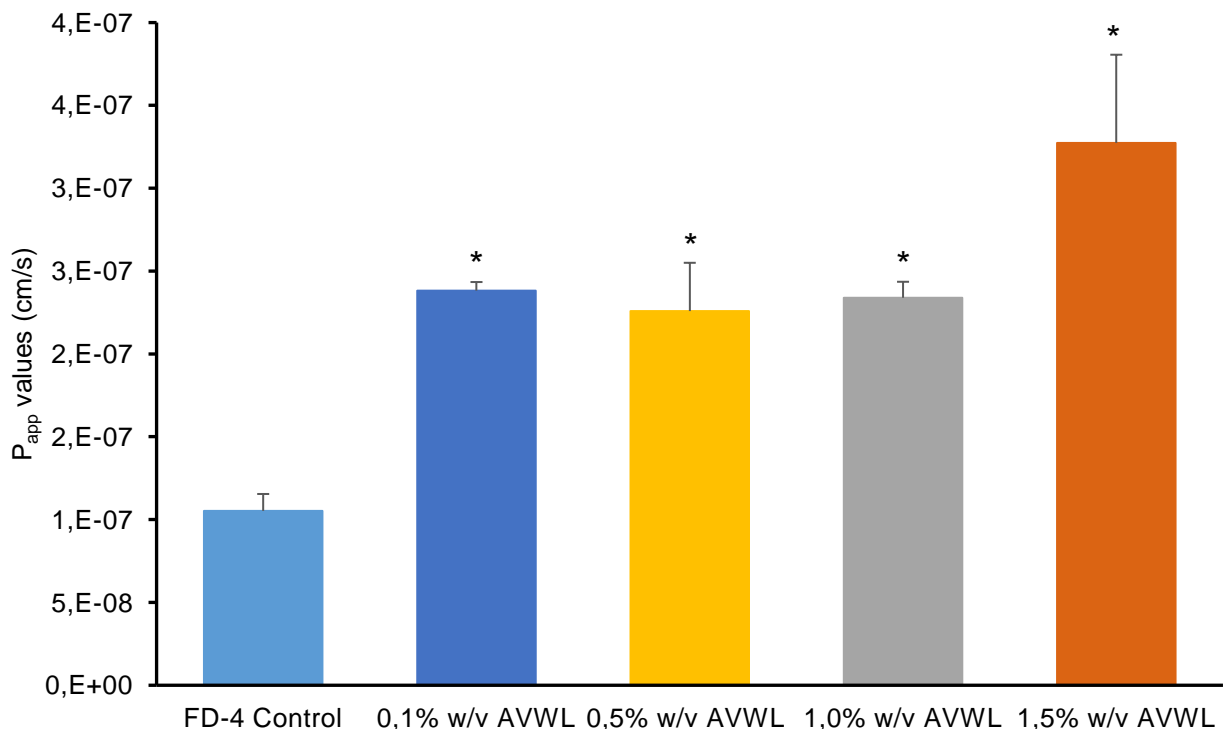


**Figure 4.9:** Apparent permeability coefficient ( $P_{app}$ ) of FITC-dextran (4 000 Da) across Caco-2 cell monolayers when applied with *Aloe vera* whole leaf extract solutions. Bars marked with an asterisk (\*) indicates statistical significant differences from the negative control group ( $p < 0,05$ ) (n = 3; error bars represent SD) (AVWL = *Aloe vera* whole leaf extract, FD-4 = FITC-dextran 4 000 Da)

In Figure 4.8, a distinct increase in FD-4 absorption can be seen for all the concentrations of *A. vera* whole leaf extract solutions tested when compared to the negative control (FD-4 alone). During the first 20 min of the experiment, the transport of FD-4 alone (negative control) reached a plateau after a relatively sharp increase, and stayed comparatively constant over the remainder of the transport period (120 min). The *A. vera* whole leaf extract solutions at concentrations of 0.1% w/v to 1.0% w/v increased the  $P_{app}$  values of FD-4 approximately two-fold and three-fold at the concentration of 1.5% w/v when compared to FD-4 alone (Figure 4.9). A concentration dependent increase in the transport can be seen for the concentration range between 0.5% w/v to 1.5% w/v of *A. vera* whole leaf extract solutions applied to the Caco-2 cell monolayers. The lowest concentration (i.e. 0.1% w/v) had a slightly higher transport enhancement effect than the 0.5% w/v and 1.0% w/v *A. vera* whole leaf extract solutions, but still lower than that of the 1.5% w/v *A. vera* whole leaf extract solution. The absorption enhancement effect of all concentrations *A. vera* whole leaf extracts were significantly higher than that of the control group (FD-4 alone) ( $p < 0.05$ ). The absorption enhancing effect of *A. vera* whole leaf extract was in agreement with the TEER reduction results (Figure 4.4) and can therefore be attributed to its tight junction modulating activities. Immunofluorescent staining and CLSM was done to further investigate the tight junction modulating activities of *A. vera* whole leaf extract and is reported in section 4.6 (*Confocal laser scanning microscopy studies to determine the mechanism of drug absorption enhancement*) of this chapter.

## **4.5.2 FITC-dextran 10 000 Da**

### **4.5.2.1 *Aloe vera* gel**

In Figure 4.10, the effect of *A. vera* gel solutions on the percentage transport of FITC-dextran 10 000 Da is plotted as a function of time and Figure 4.11 illustrates the calculated apparent permeability coefficient ( $P_{app}$ ) values.

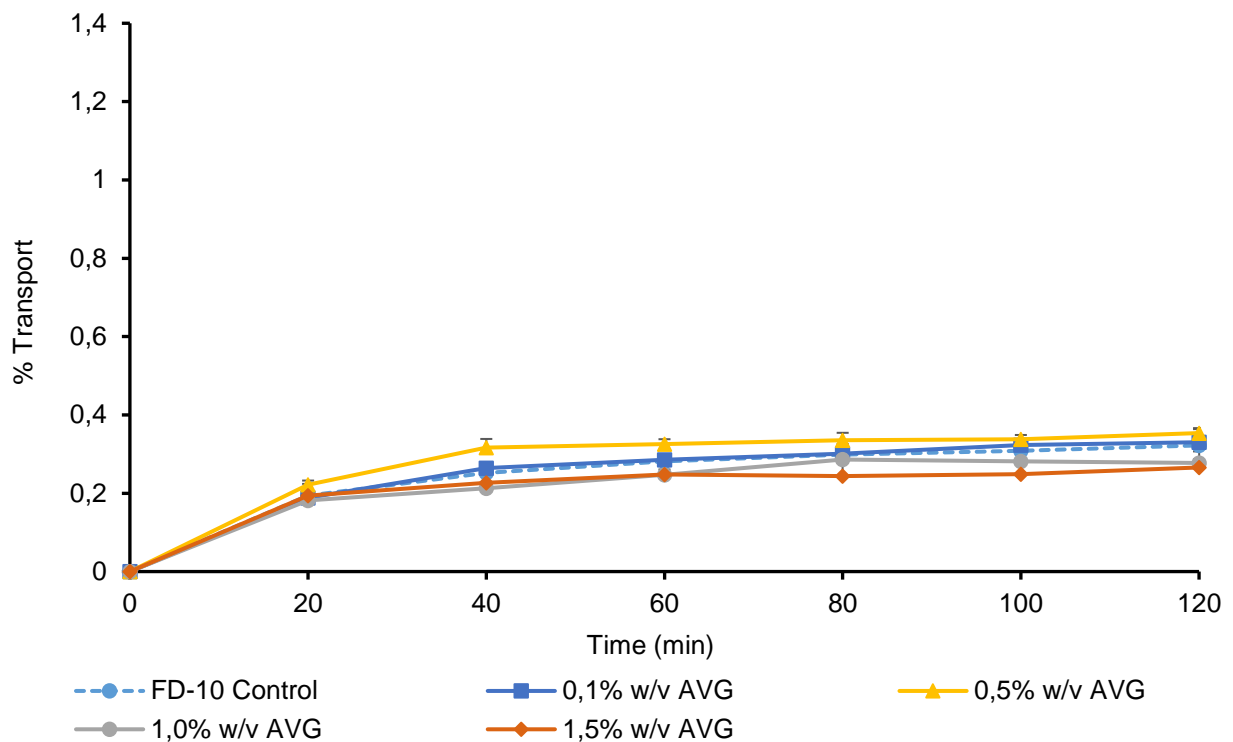


**Figure 4.10:** Percentage transport of FITC-dextran (MW = 10 000 Da) plotted as a function of time across Caco-2 cell monolayers in the presence of different concentrations *Aloe vera* gel (n = 3; error bars represent SD) (AVG = *Aloe vera* gel, FD-10 = FITC-dextran 10 000 Da, MW = molecular weight)

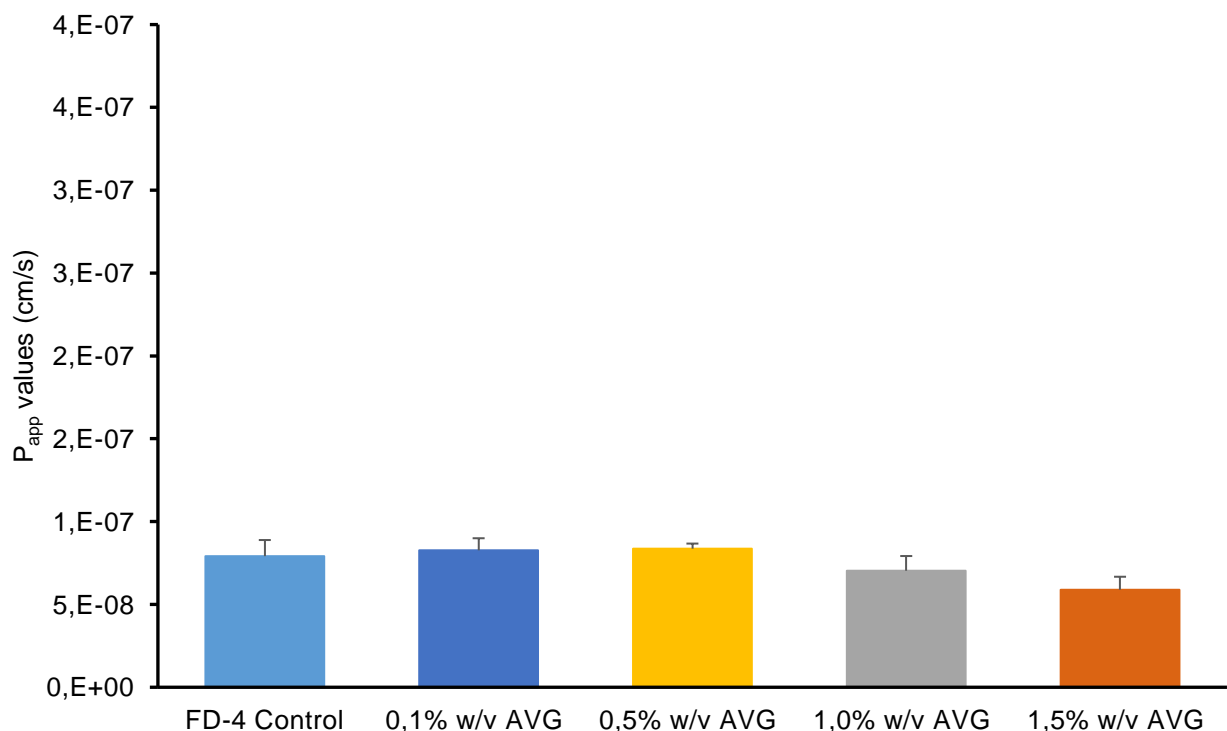


**Figure 4.11:** The effect of different concentrations *Aloe vera* gel on the transport ( $P_{app}$  values) of FITC-dextran (10 000 Da) across Caco-2 cell monolayers in the presence of different concentrations *Aloe vera* gel solutions. Bars marked with an asterisk (\*) indicates statistical significant differences from the negative control group (FD-10 alone) ( $p < 0.05$ ) (n = 3; error bars represent SD) (AVG = *Aloe vera* gel, FD-10 = FITC-dextran 10 000 Da, MW = molecular weight)

From Figure 4.10, it is evident that almost no change in the percentage transport of FD-10 is visible when applied with *A. vera* gel solutions compared to the negative control (FD-10 alone). This is true for all concentrations *A. vera* gel solutions tested. The transport of FD-10 reached a plateau at 20 min and stayed comparatively similar for all experimental groups for the duration of the transport period (120 min). From Figure 4.11, a decrease in the  $P_{app}$  value of FD-10 in the presence of 1.0% w/v and 1.5% w/v *A. vera* gel solutions is evident when compared with that of the control group. The effect of the *A. vera* gel on the transport of FD-10 was indirectly proportionate over the concentration range between 0.5% w/v to 1.5% w/v *A. vera* gel solutions. The decrease in the transport of FD-10 in the presence of 1.0% w/v and 1.5% w/v *A. vera* gel solutions can possibly be explained by the increase in viscosity of the higher concentration gel material (containing polysaccharides) in the solutions, which may contribute to slow diffusion of FD-10 molecules as well as potentially blocking the openings in the tight junctions. These transport results therefore did not correspond with the TEER reduction results observed for *A. vera* gel (Figure 4.2), indicating that the large molecular weight of FD-10 (10 000 Da) exceeded the absorption enhancing abilities of *A. vera* gel.

#### **4.5.2.2 *Aloe vera* whole leaf extract**

Figure 4.12 illustrates the effect of different concentrations of *A. vera* whole leaf extract solutions on the percentage transport of FITC-dextran 10 000 Da across Caco-2 cell monolayers. The calculated apparent permeability coefficient ( $P_{app}$ ) of FITC-dextran 10 000 Da applied with various concentrations *A. vera* whole leaf extract solutions are given in Figure 4.13.

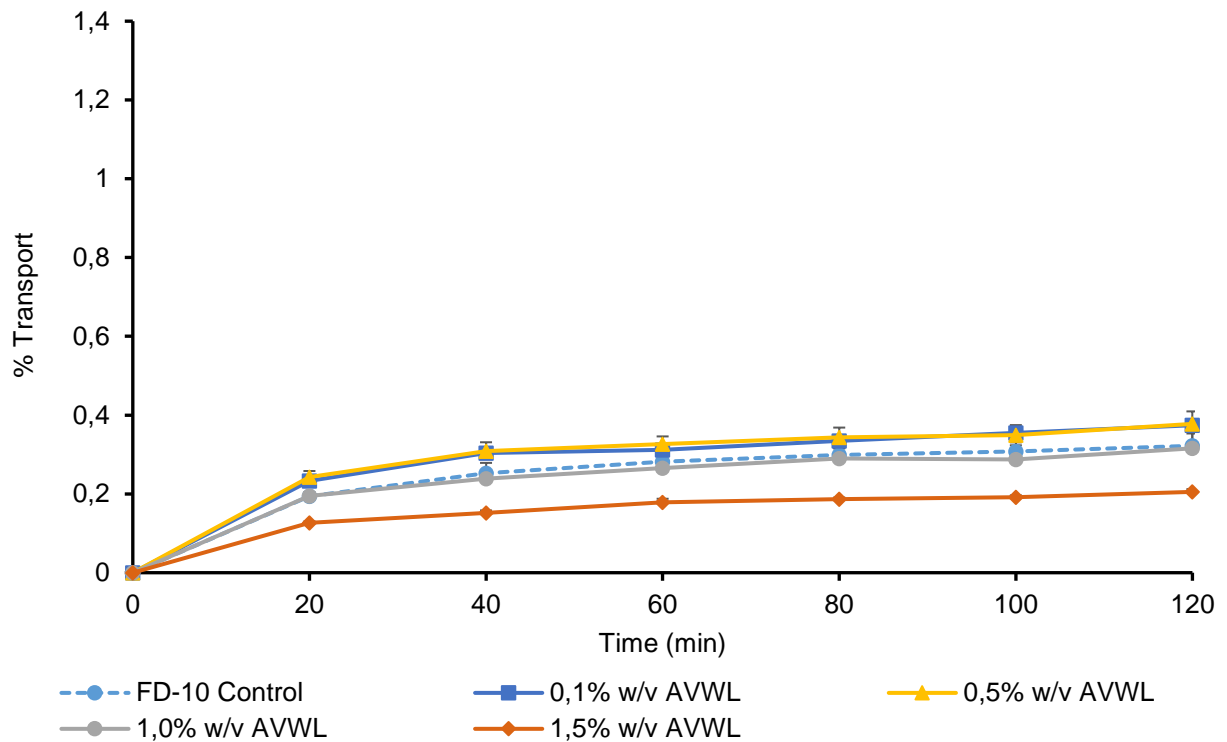


**Figure 4.12:** Percentage transport of FITC-dextran (MW = 10 000 Da) plotted as a function of time across Caco-2 cell monolayers in the presence of *Aloe vera* whole leaf extract solutions with different concentrations (n = 3; error bars represent SD) (AVWL = *Aloe vera* whole leaf extract, FD-10 = FITC-dextran 10 000 Da, MW = molecular weight)

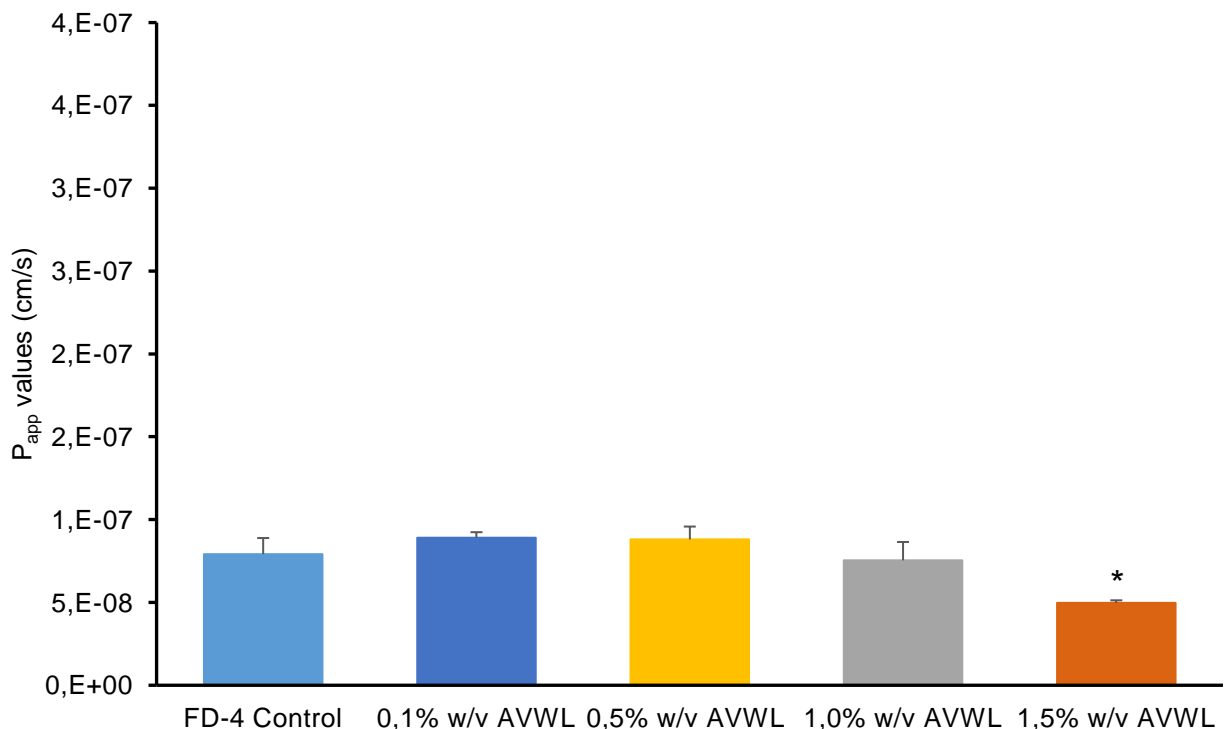


**Figure 4.13:** Apparent permeability coefficient ( $P_{app}$ ) values of FITC-dextran (10 000 Da) across Caco-2 cell monolayers in the presence of *Aloe vera* whole leaf extract solutions with different concentrations. Bars marked with an asterisk (\*) indicates statistical significant differences from the negative control group (FD-10 alone) ( $p < 0.05$ ) (n = 3; error bars represent SD) (AVWL = *Aloe vera* whole leaf extract, FD-10 = FITC-dextran 10 000 Da)

From Figure 4.12, a clear decrease in the percentage transport of FD-10 when compared to the negative control (FD-10 alone), can be seen for 1.5% w/v *A. vera* whole leaf extract solution. The percentage transport of FD-10 in all the experimental groups tested reached a plateau at 20 min and remained relatively constant for the 120 min transport period. The  $P_{app}$  values in Figure 4.13 showed a decrease in the FD-10  $P_{app}$  transport in the presence of the 1.0% w/v and 1.5% w/v *A. vera* whole leaf extract solutions when compared to FD-10 alone. The decrease in the absorption of FD-10 by the *A. vera* whole leaf extract solutions took place in an indirectly proportionate manner. The effect of the two lowest concentrations *A. vera* whole leaf extract solutions (i.e. 0.1% w/v and 0.5% w/v) did not lower the absorption, but their effect on FD-10 transport was not statistically significantly different from to the control. The 1.5% w/v *A. vera* whole leaf extract solution significantly decreased the absorption of FD-10 when compared to the control ( $p < 0.05$ ). The decreased absorption of FD-10 in the presence of the higher concentrations of *A. vera* whole leaf extract solutions (i.e. 1.0% w/v and 1.5% w/v) can probably be attributed to an increase in viscosity of the solution or potentially a restriction in the flow of molecules through the tight junction openings. The transport results seen in Figure 4.12 and Figure 4.13 did not agree with the TEER reduction abilities of *A. vera* whole leaf extract (Figure 4.4). This indicates that the molecular weight of FD-10 (10 000 Da) exceeded the size of the openings of the tight junctions after modulation by the *A. vera* whole leaf extract.

### **4.5.3 FITC-dextran 20 000 Da**

#### **4.5.3.1 *Aloe vera* gel**

In Figure 4.14, the effect of different concentrations *A. vera* gel solutions on the percentage transport of FITC-dextran 20 000 Da across Caco-2 cell monolayers is shown and the calculated apparent permeability coefficient ( $P_{app}$ ) values are given in Figure 4.15.

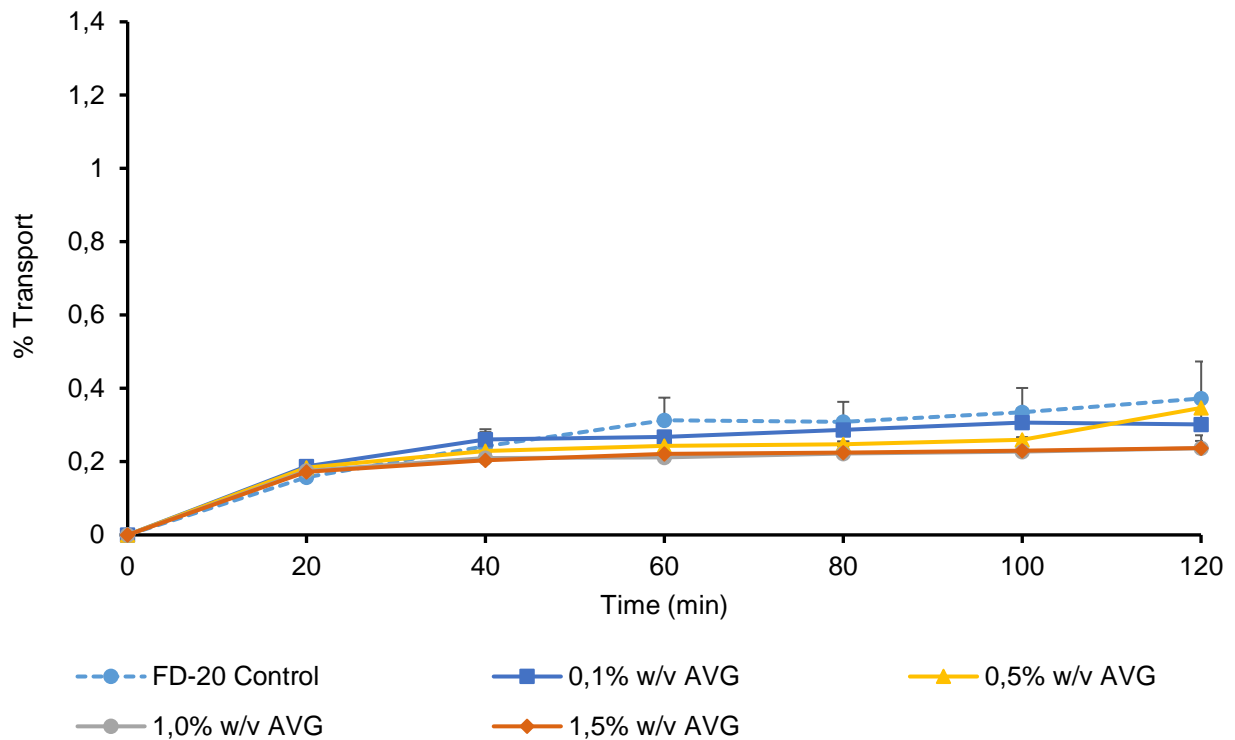


**Figure 4.14:** Percentage transport of FITC-dextran (MW = 20 000 Da) plotted as a function of time across Caco-2 cell monolayers in the presence of *Aloe vera* gel solutions in different concentrations (n = 3; error bars represent SD) (AVG = *Aloe vera* gel, FD-20 = FITC-dextran 20 000 Da, MW = molecular weight)

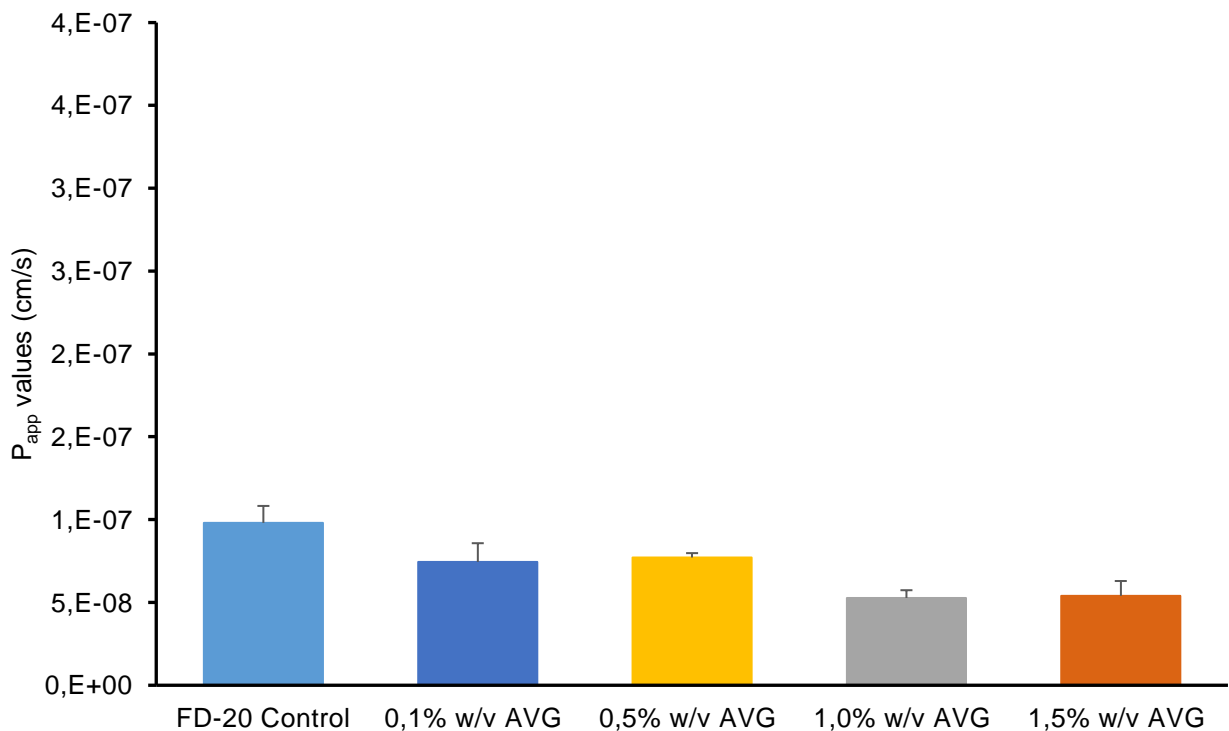


**Figure 4.15:** Apparent permeability coefficient ( $P_{app}$ ) values of FITC-dextran (20 000 Da) across Caco-2 cell monolayers in the presence of different concentrations *Aloe vera* gel solutions. Bars marked with an asterisk (\*) indicates statistical significant differences from the negative control group ( $p < 0.05$ ) (n = 3; error bars represent SD) (AVG = *Aloe vera* gel, FD-20 = FITC-dextran 20 000 Da)

In Figure 4.14, a clear decrease in the percentage transport of FD-20 is observed when compared to the negative control (FD-20 alone) for all the tested concentrations of *A. vera* gel solutions. The percentage transport of FD-20 was reached a constant level at 20 min for all the experimental groups for the duration of the experimental period (120 min). The  $P_{app}$  values shown in Figure 4.15, demonstrate a decrease in the transport of FD-20 in the presence of different concentrations of *A. vera* gel solutions compared to that of the negative control. The decrease in FD-20 transport was indirectly proportionate to the concentration *A. vera* gel solutions applied, with the lower concentrations *A. vera* gel solutions (i.e. 0.1% w/v and 0.5% w/v) decreasing the transport to a lesser degree than the higher concentrations (i.e. 1.0% w/v and 1.5% w/v). This can probably be attributed to an increase in the viscosity of the *A. vera* gel solutions or the increase in polysaccharides that may restrict the permeation of molecules across the Caco-2 cell monolayer through the opening of the tight junctions. These transport results of FD-20 do not correspond with the TEER reduction seen (Figure 4.2) showing that the large molecular weight of FD-20 (20 000 Da) exceeded the size of the tight junction opened by the modulation of *A. vera* gel.

#### 4.5.3.2 *Aloe vera* whole leaf extract

In Figure 4.16, the effect of different concentrations *A. vera* whole leaf extract solutions on the percentage transport of FITC-dextran 20 000 Da across Caco-2 cell monolayers is shown. The calculated apparent permeability coefficient ( $P_{app}$ ) values are given in Figure 4.17.

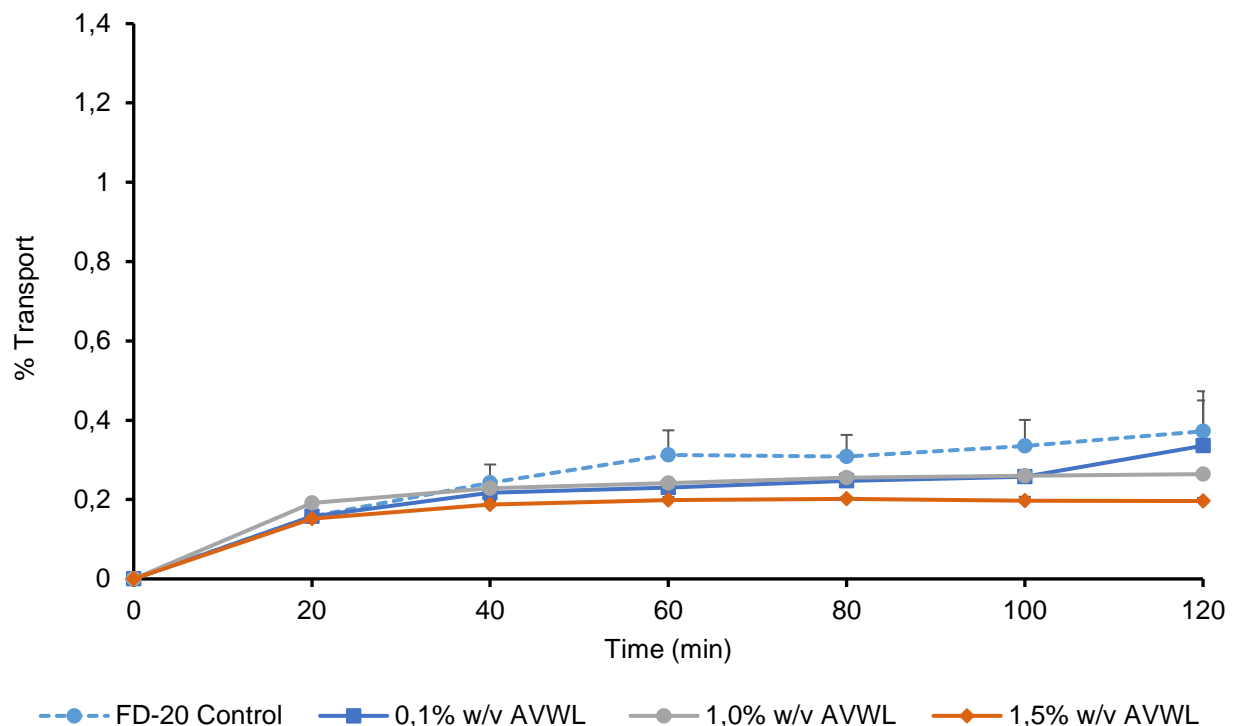


**Figure 4.16:** Percentage transport of FITC-dextran (MW = 20 000 Da) plotted as a function of time across Caco-2 cell monolayers in the presence of different concentrations *Aloe vera* whole leaf extract solutions (n = 3; error bars represent SD) (AVWL = *Aloe vera* whole leaf extract, FD-20 = FITC-dextran 20 000 Da, MW= molecular weight)

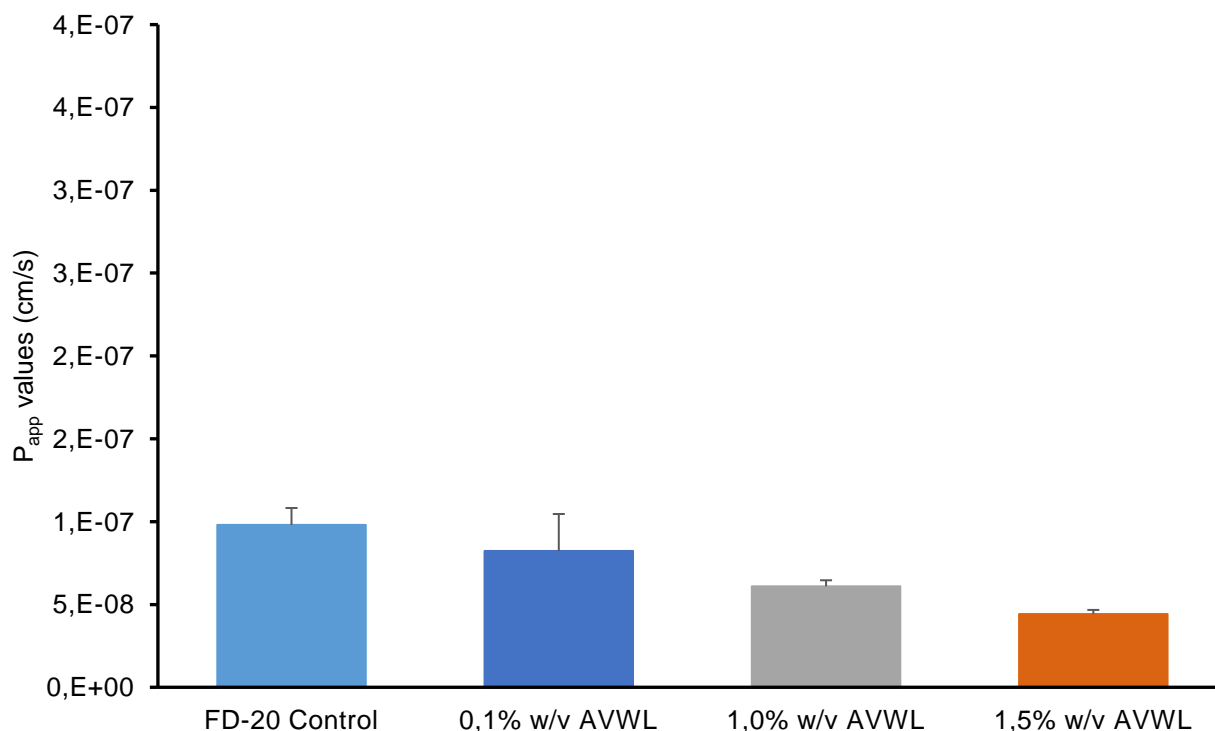


**Figure 4.17:** Apparent permeability coefficient ( $P_{app}$ ) values of FITC-dextran (20 000 Da) across Caco-2 cell monolayers in the presence of *Aloe vera* whole leaf extract solutions with different concentrations. Bars marked with an asterisk (\*) indicates statistical significant differences from the negative control group ( $p < 0.05$ ) ( $n = 3$ ; error bars represent SD) (AVWL = *Aloe vera* whole leaf extract, FD-20 = FITC-dextran 20 000 Da)

In Figure 4.16, a distinct decrease in the percentage transport of FD-20 when compared to the negative control (FD-20 alone) can be seen for the different concentrations *A. vera* whole leaf extract solutions (except for 0.5% w/v). The percentage transport of FD-20 stabilised at 20 min for the duration of the transport period (120 min). The  $P_{app}$  values shown in Figure 4.17, clearly demonstrate the decrease in FD-20 transport in the presence of *A. vera* whole leaf extract solutions (0.1% w/v, 1.0% w/v and 1.5% w/v) in relation to the negative control. The decrease in FD-20 transport occurred in an indirectly proportionate manner in relation to the concentration *A. vera* whole leaf extract solutions applied, with the highest degree of FD-20 transport reduction by the highest concentration *A. vera* whole leaf extract solution (i.e. 1.5% w/v). This can possibly be explained by an increase in the viscosity of the solutions or an increase in the concentration of polysaccharides present in the *A. vera* whole leaf extract solutions, thus potentially obstructing the flow of molecules through the opening of the tight junctions. These transport results of FD-20 do not correspond with the TEER reduction seen (Figure 4.4) by *A. vera* whole leaf extract; indicating that the large molecular weight of FD-20 exceeded the tight junction opening abilities of *A. vera* whole leaf extract.

#### 4.5.4 FITC-dextran 40 000 Da

##### 4.5.4.1 *Aloe vera* gel

In Figure 4.18, the effect of different concentrations *A. vera* gel solutions on the percentage transport of FITC-dextran 40 000 Da across Caco-2 cell monolayers is shown. In Figure 4.19 the apparent permeability coefficient ( $P_{app}$ ) values of FITC-dextran 40 000 Da (in the presence and absence of *A. vera* gel solutions) are given.

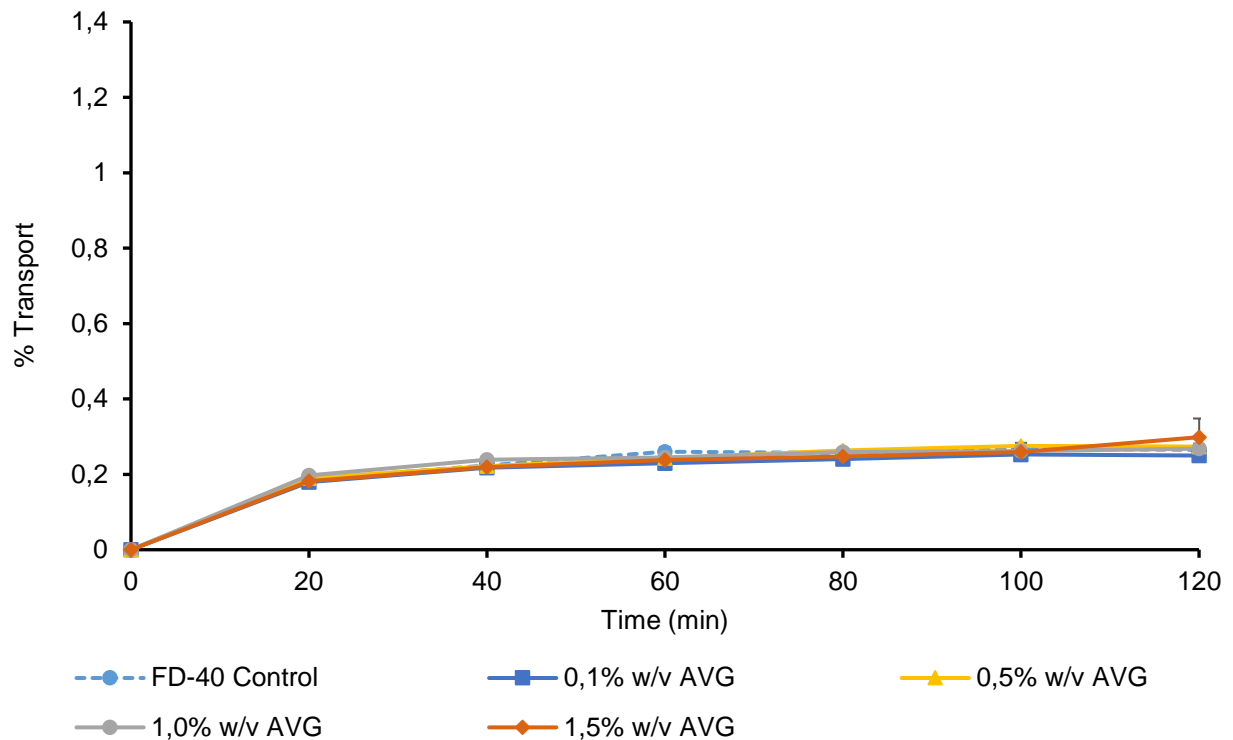


**Figure 4.18:** Percentage transport of FITC-dextran (MW = 40 000 Da) plotted as a function of time across Caco-2 cell monolayers in the presence of *Aloe vera* gel solutions with different concentrations (n = 3; error bars represent SD) (AVG = *Aloe vera* gel, FD-40 = FITC-dextran 40 000 Da, MW= molecular weight)

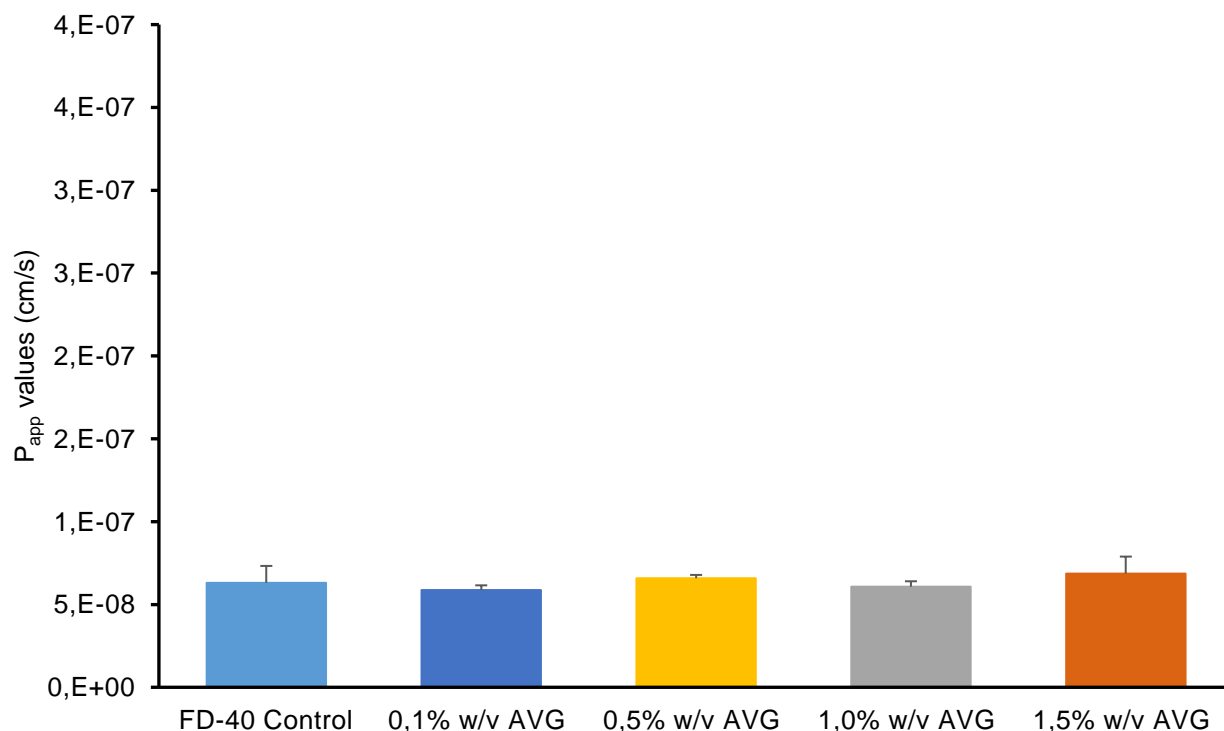


**Figure 4.19:** Apparent permeability coefficient ( $P_{app}$ ) values of FITC-dextran (40 000 Da) across Caco-2 cell monolayers in the presence of different concentrations *Aloe vera* gel solutions. Bars marked with an asterisk (\*) indicates statistical significant differences from the negative control group ( $p < 0.05$ ) ( $n = 3$ ; error bars represent SD) (AVG = *Aloe vera* gel, FD-40 = FITC-dextran 40 000 Da)

From Figure 4.18, no clear difference in the percentage transport of FD-40 can be seen for any of the *A. vera* whole leaf solutions tested compared to the negative control group (FD-40 alone). The percentage transport for all experimental groups reached a plateau and stayed constant for the duration of the transport experimental period (120 min). In Figure 4.19, it can be seen that the  $P_{app}$  values stays relatively the same over the whole concentration range *A. vera* gel solutions tested, indicating that there was no change in the absorption of FD-40 in the presence of *A. vera* gel solutions when compared to the negative control. These results do not correspond with the TEER reduction seen in Figure 4.2, indicating the absorption enhancing abilities of *A. vera* gel is exceeded by the large molecular weight of FD-40 (40 000 Da).

#### 4.5.4.2 *Aloe vera* whole leaf extract

The effect of *A. vera* whole leaf extract (in different concentrations) on the percentage transport of FITC-dextran 40 000 Da across Caco-2 cell monolayers is shown in Figure 4.20 and the calculated apparent permeability ( $P_{app}$ ) values are given in Figure 4.21.

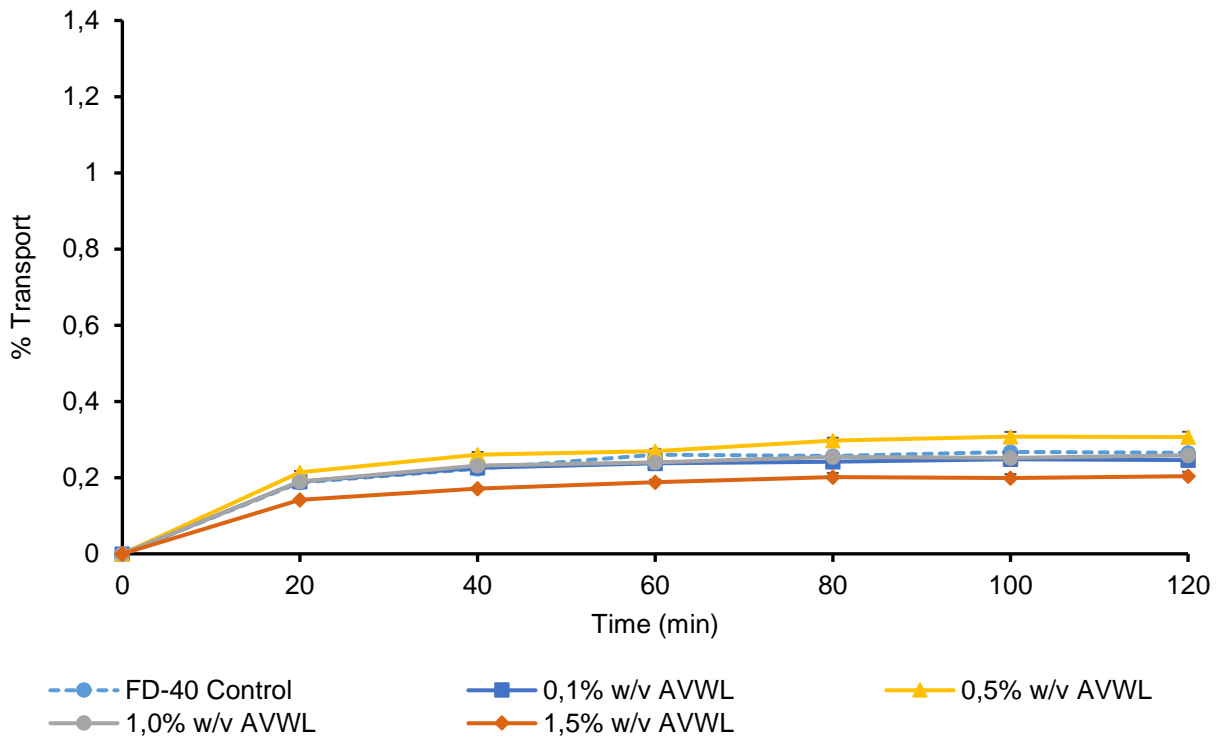


**Figure 4.20:** Percentage transport of FITC-dextran plotted (40 000 Da) as a function of time across Caco-2 cell monolayers in the presence of *Aloe vera* whole leaf extract solutions with different concentrations (n = 3; error bars represent SD) (AVWL = *Aloe vera* whole leaf extract, FD-40 = FITC-dextran 40 000 Da)

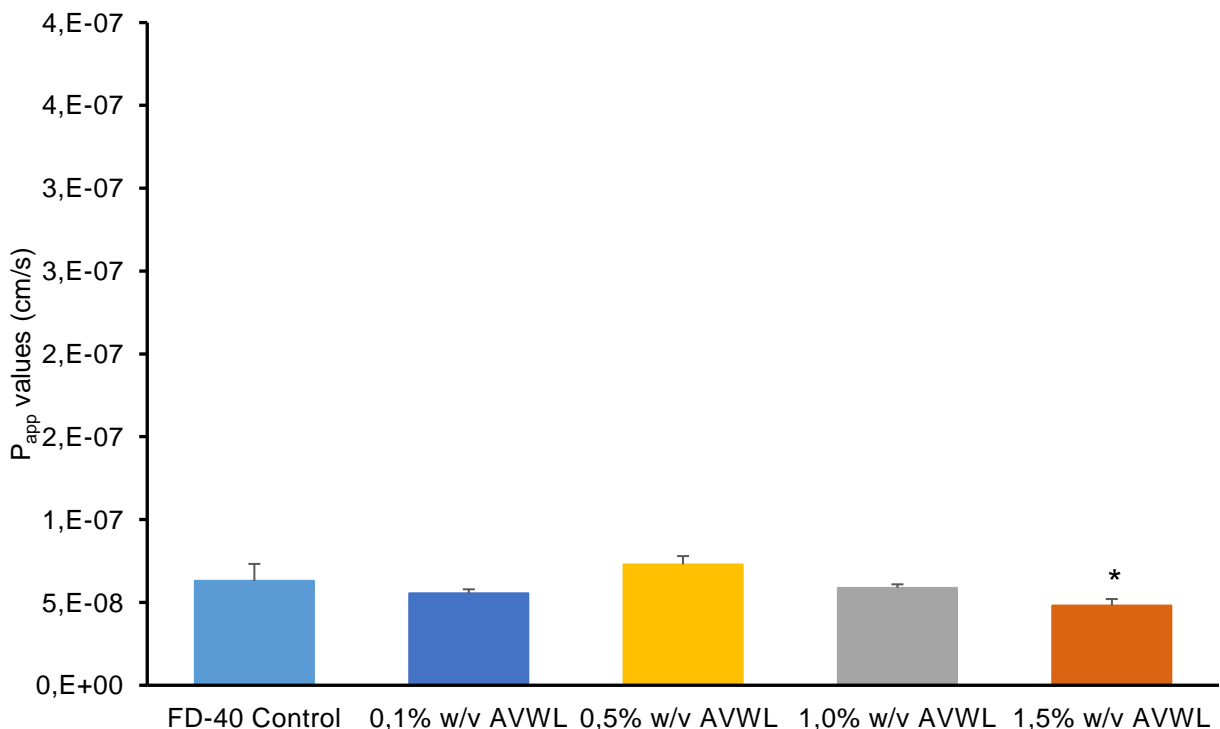


**Figure 4.21:** Apparent permeability coefficient ( $P_{app}$ ) values of FITC-dextran (40 000 Da) across Caco-2 cell monolayers in the presence of *Aloe vera* whole leaf extract solutions with different concentrations. Bars marked with an asterisk (\*) indicates statistical significant differences from the negative control group ( $p < 0.05$ ) (n = 3; error bars represent SD) (AVWL = *Aloe vera* whole leaf extract, FD-40 = FITC-dextran 40 000 Da)

In Figure 4.20, a decrease can be seen for the percentage transport of FD-40 in the presence of 1.5% w/v *A. vera* whole leaf extract solution, when compared to the negative control (FD-40 alone). The percentage transport of FD-40 (for all experimental groups) stabilized at 20 min and continued this trend until 120 min. From the  $P_{app}$  values shown in Figure 4.21 an indirectly proportional decrease in the transport of FD-40 can be noticed, for the concentration range 0.5% w/v to 1.5% w/v *A. vera* whole leaf extract solutions. The lowest concentration *A. vera* whole leaf extract (0.1% w/v) applied did not follow this trend, as the  $P_{app}$  value is lower than the  $P_{app}$  value of 0.5% w/v *A. vera* whole leaf extract. The  $P_{app}$  value of FD-40 in presence of 1.5% w/v *A. vera* whole leaf extract solution was statistically significantly lower when compared to the negative control ( $p > 0.05$ ). This can possibly be explained by an increase in the concentration polysaccharides present in the solution and/or an increase in the viscosity, thus obstructing the movement of large molecules through the tight junctions. These results do not agree with the TEER reduction results found (Figure 4.4), showing the tight junction opening abilities of *A. vera* whole leaf extract is exceeded by the large molecular weight of FD-40 (40 000 Da).

#### **4.5.5 Conclusions form *in vitro* permeation results**

The *in vitro* permeation study with different molecular weight FITC-dextran molecules provided further information on the efficacy of the absorption enhancement abilities of aloe leaf materials. Both *A. vera* gel and whole leaf extract (in all the tested concentrations) statistically significantly ( $p < 0.05$ ) increased the absorption of FITC-dextran 4 000 Da across Caco-2 cell monolayers. This corresponded with the TEER reduction by *A. vera* gel and whole leaf extract, seen in the previous section. For the larger molecular weight FITC-dextran (i.e. 10 000 Da, 20 000 Da and 40 000 Da) no absorption enhancement was seen. In contrast, statistically significant reduction in the absorption of 10 000 Da and 40 000 Da FITC-dextran was found in the presence of 1.5% w/v *A. vera* whole leaf extract. The mechanism of absorption enhancement seen with FD-40 in the presence of aloe leaf materials were further investigated with confocal laser scanning microscopy (CLSM).

#### **4.6 Confocal laser scanning microscopy (CLSM) studies to determine the mechanism of drug absorption enhancement of aloe leaf materials**

Confocal laser scanning microscopy (CLSM) was used to determine the mechanism of action of *A. vera* gel and whole leaf extract as drug absorption enhancers across intestinal epithelial cell monolayers. To confirm the paracellular drug absorption enhancement pathway, Caco-2 cell monolayers were incubated with FITC-dextran 4 000 Da (FD-4) in the presence of selected aloe leaf materials solutions (i.e. 1.0% w/v *A. vera* gel and whole leaf extract) and 0.5% w/v TMC (positive control), as well as in the absence of absorption enhancers (negative control). F-actin was immunofluorescently stained in order to visualize the F-actin re-arrangement effected by the tight junction modulation of the *A. vera* gel and whole leaf extract. All cell monolayers were co-stained with propidium iodide in order to visualize cell nuclei. All experiments were done in triplicate and representative micrograph images are shown.

##### **4.6.1 Visualization of transport pathway**

The top-view confocal micrograph images of Caco-2 cell monolayers in Figure 4.22 show the paracellular accumulation of FD-4 around Caco-2 cells in the presence of 1.0% w/v of *A. vera* gel and whole leaf extract solutions as well as 0.5% w/v TMC (positive control).

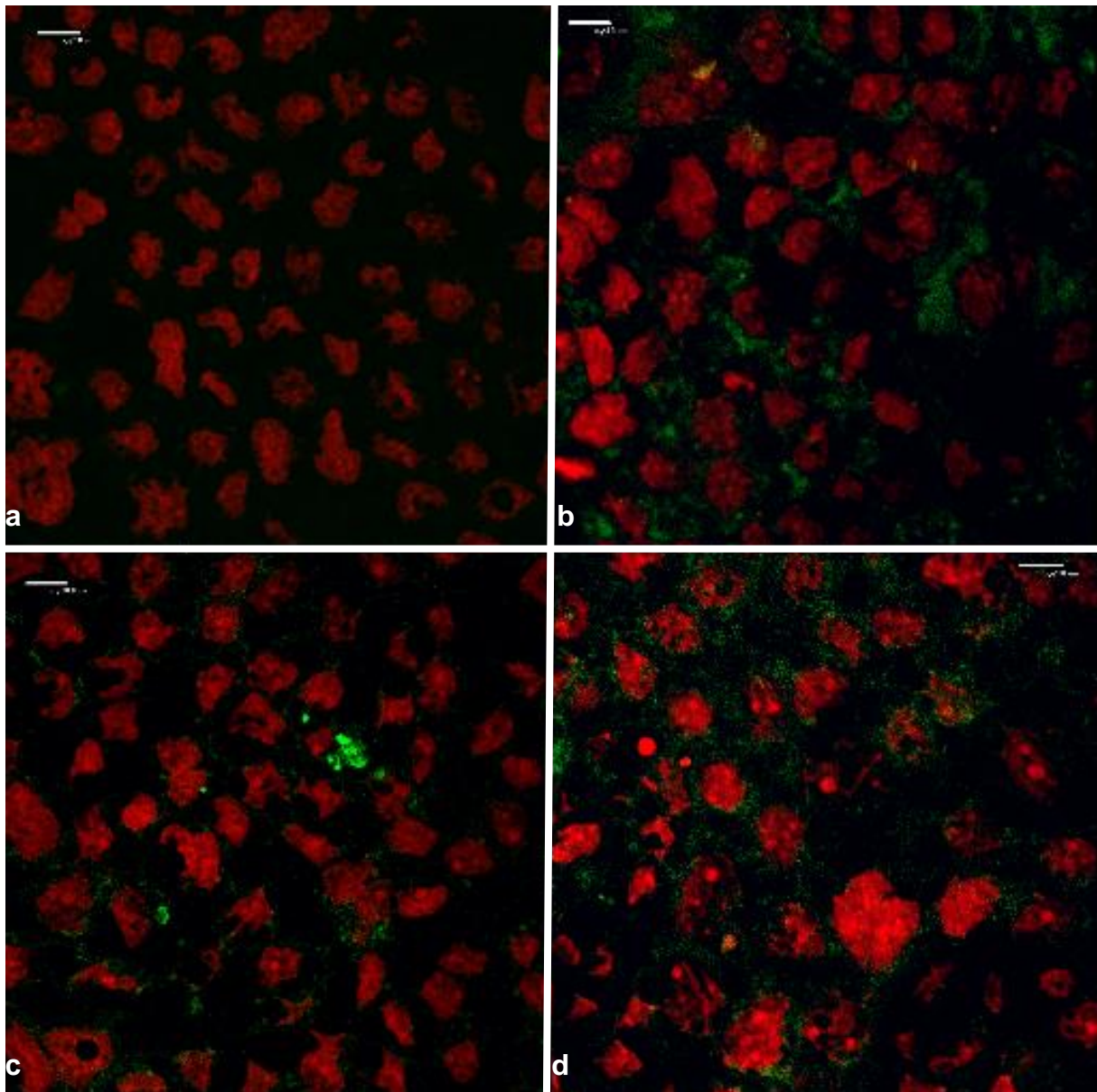


**Figure 4.22:** Top-view confocal micrograph images of Caco-2 cell monolayers on which FITC-dextran 4000 Da (FD-4) was applied (**green:** FITC-dextran 4000 Da and **red:** cell nuclei stained with propidium iodide). **a)** Negative control (FD-4 alone), **b)** positive control (0.5% w/v TMC), **c)** *A. vera* gel (1.0% w/v) and **d)** *A. vera* whole leaf extract (1.0% w/v) (Scale bars represents 10  $\mu$ m)

From the confocal micrograph images in Figure 4.22, a clear difference is visible in the intercellular accumulation of FITC-dextran (green) on the Caco-2 cell monolayers incubated with absorption enhancers (Figure 4.22 b, c & d) compared to the negative control (Figure 4.22 a). The FITC-dextran (green) is particularly visible between the cells (cell nuclei are stained red with propidium iodide), indicating that FITC-dextran accumulated around the cells in the intercellular spaces (indicating movement via the paracellular pathway). The increased intercellular accumulation of FITC-dextran (Figure 4.22 b) with the co-incubation of 0.5% w/v TMC (a known paracellular absorption enhancer) is in accordance to previous research done by Kotzé *et al.* (1997:1201) and Thanou *et al.* (2001:122). The lack of green fluorescence inside the cells, confirms that the incubation with TMC did not damage the cell membranes. The accumulation of

FITC-dextran in Figure 4.22 c and d is similar to that of the positive control and it can therefore be concluded that the absorption of FITC-dextran in the presence of both aloe leaf materials occurred via the same way as in the presence of TMC, which was previously shown to be paracellular permeation. As the tight junction is the main restriction for paracellular permeability of hydrophilic, large molecular weight molecules (Salama *et al.*, 2006:17), the increased paracellular accumulation and transport of FD-4 caused by *A. vera* gel and whole leaf extract is most probably the result of their ability to open/modulate tight junctions.

#### **4.6.2 Visualization of F-actin filaments in the cytoskeleton**

According to Ward *et al.* (2000:351), disruption in the actin cytoskeleton through modulation of the actin structure, caused an increase in paracellular permeability by opening of the tight junctions. The re-arrangement of filamentous actin (F-actin) in the cytoskeleton of the Caco-2 cells was visualized in order to determine the possible mechanism of action by which aloe leaf materials increase paracellular absorption. The confocal micrograph images in Figure 4.23 show the F-actin expression in a Caco-2 cell monolayer after incubation with 0.5% w/v TMC (positive control) and 1.0% w/v *A. vera* gel and whole leaf extract as well as without an absorption enhancer (negative control).

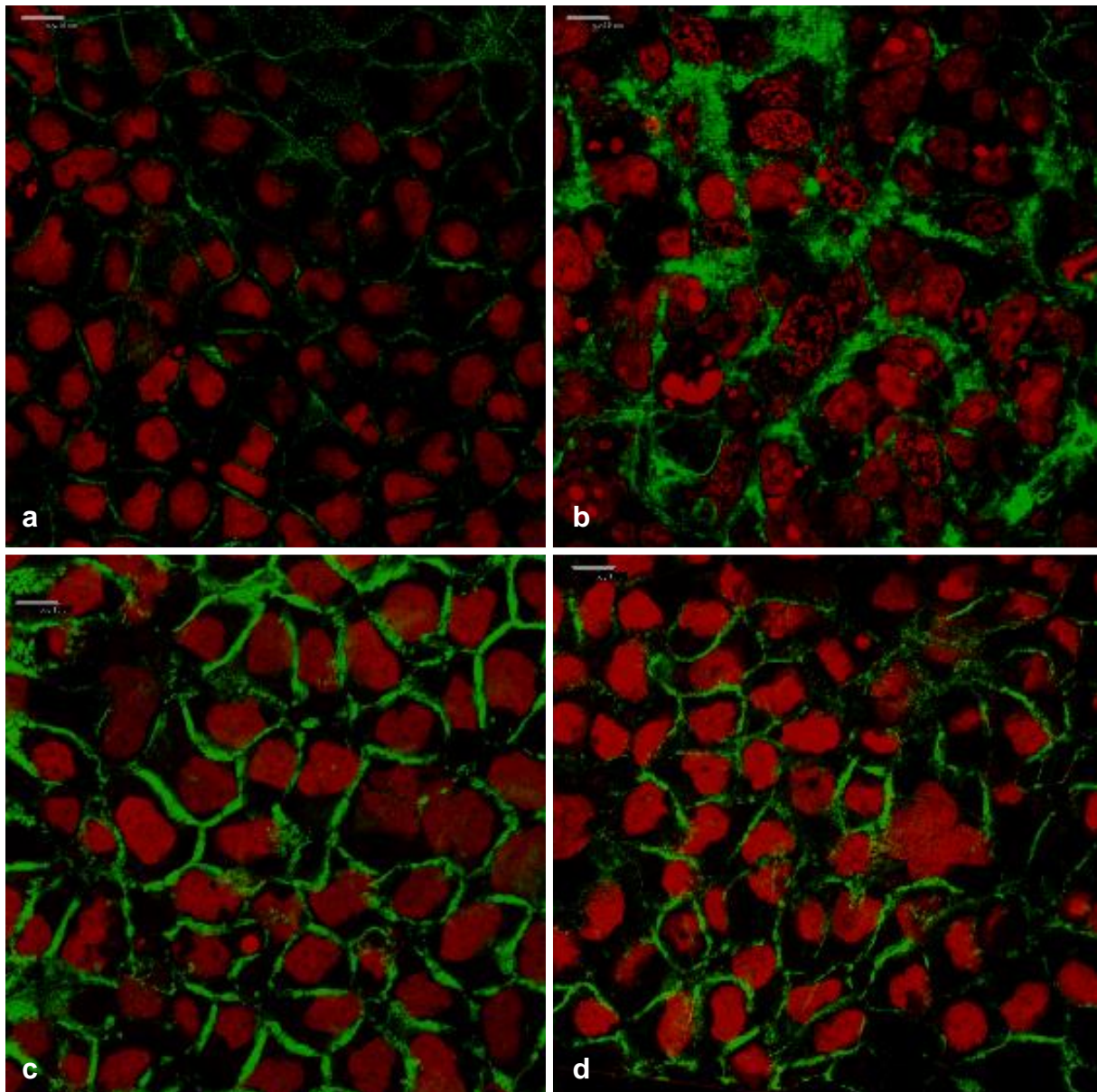


**Figure 4.23:** Confocal micrograph images of F-actin distribution in Caco-2 cell monolayers (**green:** F-actin stained with CytoPainter® Phalloidin iFluor 488 and **red:** cell nuclei stained with propidium iodide). **a)** Negative control (untreated Caco-2 cell monolayer), **b)** positive control (0.5% w/v TMC), **c)** 1.0% w/v *A. vera* gel and **d)** 1.0% w/v *A. vera* whole leaf extract (Scale bars represents 10 μm)

In the confocal micrograph images shown in Figure 4.23, differences can be seen in the appearance of F-actin when the Caco-2 cells were treated with *A. vera* gel and whole leaf extract and TMC when compared to the negative control (untreated cells). Figure 4.23 a presents a confocal micrograph image of an intact, untreated Caco-2 cell monolayer (negative control), which showed very little and irregular fluorescence (green) distribution of the F-actin along the cell borders. In contrast to this, the F-actin fluorescence (green) in all the other images are visibly different (Figure 4.23 b, c & d), which indicated a rearrangement of F-actin distribution. The rearranged F-actin fluorescence pattern seen in Figure 4.23 b is in congruence with previously published research on the effect of TMC (a chitosan derivative and known tight junction modulator) on the actin cytoskeleton of Caco-2 cells (Hsu *et al.*, 2013:792). The changed

fluorescence patterns of F-actin seen in the Caco-2 cells that were treated with *A. vera* gel (Figure 4.23 c) and *A. vera* whole leaf extract (Figure 4.23 d) were similar to that of TMC. The changed F-actin distribution therefore indicates that tight junction modulation occurred in the presence of *A. vera* gel and whole leaf extract.

#### **4.6.3 Conclusions from confocal laser scanning microscopy (CLSM) results**

From the paracellular accumulation of FITC-dextran (Figure 4.22 c & d) and the F-actin re-arrangement (Figure 4.23 c & d), it can be concluded that the increased absorption caused by *A. vera* gel and whole leaf extract is most likely due to its tight junction modulating activities. This is the first account (to the best of our knowledge) that the mechanism of action of *A. vera* absorption enhancement has been reported.

## CHAPTER 5: FINAL CONCLUSIONS AND FUTURE RECOMMENDATIONS

### 5.1 Final conclusions

The aim of this study was two-fold, namely to determine the capacity and the mechanism of action of drug absorption enhancement by *Aloe vera* gel and whole leaf extract. This was done by investigating the abilities of the *A. vera* gel and whole leaf extract to reduce TEER and to increase permeation of different molecular weight FITC-dextran marker molecules across Caco-2 cell monolayers. Furthermore, the mechanism of action of the drug absorption enhancement abilities of *A. vera* gel and whole leaf extract were investigated with the immunofluorescent staining of F-actin in the cytoskeleton of Caco-2 cell monolayers.

Both *A. vera* gel and whole leaf extract rapidly and markedly decreased the TEER when applied to Caco-2 cell monolayers, which was comparable to the TEER reduction seen in the positive control group (TMC; a known absorption enhancer). A reduction in TEER across a cell monolayer is an indication of the tight junction opening. After the test solutions were removed from the Caco-2 cell monolayers, the TEER of all the experimental groups returned towards the initial TEER value, indicating that the effect of the *A. vera* gel and whole leaf extract on the tight junctions were reversible.

The capacity of the drug absorption enhancing abilities of *A. vera* gel and whole leaf extract, was determined by the *in vitro* permeation of different molecular weight FITC-dextran molecules (i.e. 4 000 Da, 10 000 Da, 20 000 Da and 40 000 Da) in the presence of different concentrations *A. vera* gel and whole leaf extract. The presence of all concentrations *A. vera* gel and whole leaf extract statistically significantly increased the permeation of FITC-dextran 4 000 Da (FD-4) across Caco-2 cell monolayers when compared to the control (FD-4 alone). In contrast to this, almost no change in the permeation of FITC-dextran 10 000 Da, 20 000 Da or 40 000 Da (i.e. FD-10, FD-20 and FD-40, respectively) was seen when incubated with *A. vera* gel and whole leaf extract when compared to the control groups (i.e. FD-10, FD-20, or FD-40 alone). This indicated that these large molecular weight molecules exceeded the size of the openings in the tight junction after modulation by *A. vera* gel and whole leaf extract.

In order to confirm the pathway of transport as well as the mechanism of action of drug absorption enhancement by *A. vera* gel and whole leaf extract, Caco-2 cell monolayers were incubated with FD-4 and F-actin was immunofluorescently stained in the presence of the aloe leaf materials. As the intercellular accumulation of FD-4 when incubated with *A. vera* gel and whole leaf extract was similar to that seen when FD-4 was incubated with TMC (the positive control), it can be concluded that the increased permeation of FD-4 occurred via the paracellular pathway. Additionally, a

change in F-actin distribution indicated tight junction modulation. Incubation with TMC showed a rearrangement in the F-actin distribution when compared to that of the negative control (untreated Caco-2 cell monolayers). The F-actin distribution seen in Caco-2 cell monolayers treated with aloe leaf materials, was similar to the fluorescence pattern seen when cells were incubated with TMC, indicating the modulation of tight junctions as the most probable mechanism of action of the absorption enhancing effects of *A. vera* gel and whole leaf extract.

The abovementioned results all contributed to achieve the aim of this study. The increase in paracellular permeability via intercellular tight junction modulation was confirmed by the TEER, *in vitro* permeation, and CLSM studies. The capacity of the absorption enhancing abilities of *A. vera* gel and whole leaf extract were found to be limited between 4 000 Da and 10 000 Da. This agrees with a previous study which showed the increased transport of insulin (MW=5800 Da; Moroz *et al.*, 2016:116) in the presence of *A. vera* gel and whole leaf extract across Caco-2 cell monolayers (Chen *et al.*, 2009:589).

## 5.2 Recommendations for future studies

As a result of the various *in vitro* studies done, the following recommendations are made for future studies:

- Further *in vitro* studies should be conducted with a range of macromolecules between 4 000 Da and 10 000 Da to determine a more precise limit of the absorption enhancement capacity of *A. vera* gel and whole leaf extract.
- A detailed mechanism of tight junction modulation should be investigated for *A. vera* gel or whole leaf extract (i.e. the interaction of *A. vera* gel and/or whole leaf extract with specific tight junction proteins) on a molecular level.
- Characterization and isolation of the single active phytoconstituents that are responsible for absorption enhancing abilities of both *A. vera* gel and whole leaf extract.
- *In vivo* studies in appropriate animal models are needed to confirm the possible clinical relevance of the drug absorption enhancement effect of *A. vera* gel and whole leaf extract.
- Different formulations that include *A. vera* gel or whole leaf extract should be investigated for targeted delivery in the gastrointestinal tract to facilitate local delivery of the absorption enhancer, minimising possible side effects and increasing permeability of the included active pharmaceutical ingredient (API), as a result of the modulated tight junctions.
- Further *in vitro* permeation studies can be conducted with clinically relevant macromolecular drugs (i.e. insulin, human growth hormone, calcitonin and parathyroid hormone (PTH)) in the presence of *A. vera* gel or whole leaf extract.

## REFERENCES

- Abcam. 2017a. Protocol booklet: CytoPainter Phalloidin-iFluor 488 reagent: instructions for use for staining F-actin in adherent or suspension cells. [http://www.abcam.com/ps/products/176/ab176753/documents/ab176753%20CytoPainter%20Phalloidin-iFluor%20488%20Reagent%20protocol%20v3%20\(website\).pdf](http://www.abcam.com/ps/products/176/ab176753/documents/ab176753%20CytoPainter%20Phalloidin-iFluor%20488%20Reagent%20protocol%20v3%20(website).pdf) Date of access: 9 Nov. 2017.
- Abcam. 2017b. Product datasheet: Fluoroshield mounting medium with Propidium Iodide ab104129. <http://www.abcam.com/fluoroshield-mounting-medium-with-propidium-iodide-20ml-ab104129.html> Date of access: 9 Nov. 2017.
- Abcam. 2017c. Immunocytochemistry and immunofluorescence protocol: procedure for staining of cell cultures using immunofluorescence. <http://www.abcam.com/protocols/immunocytochemistry-immunofluorescence-protocol> Date of access: 9 Nov. 2017.
- Adachi, Y., Suzuki, H. & Sugiyama, Y. 2001. Comparative studies on *in vitro* methods for evaluating *in vivo* function of MDR1 P-glycoprotein. *Pharmaceutical research*, 18:1660–1668.
- Aguirre, T.A.S., Teijeiro-Osorio, D., Rosa, M., Coulter, I.S., Alonso, M.J. & Brayden, D.J. 2016. Current status of selected oral peptide technologies in advanced preclinical development and in clinical trials. *Advanced drug delivery reviews*, 106:223–241.
- Alqahtani, S., Mohamed, L.A. & Kaddoumi, A. 2013. Experimental models for predicting drug absorption and metabolism. *Expert opinion on drug metabolism and toxicology*, 9:1–14.
- Amin, L. 2013. P-glycoprotein inhibition for optimal drug delivery. *Drug target insights*, 7:27–34.
- Anilkumar, P., Badarinath, A.V., Naveen, N., Prasad, B., Reddy, B.R.S., Hyndhavi, M. & Nirosha, M. 2011. A rationalized description on study of intestinal barrier, drug permeability and permeation enhancers. *Journal of global trends in pharmaceutical sciences*, 2:431–449.
- Antunes, F., Andrade, F., Ferreira, D., Nielsen, H.M. & Sarmiento, B. 2013. Models to predict intestinal absorption of therapeutic peptides and proteins. *Current drug metabolism*, 14:4–20.
- Artursson, P. & Karlsson, J. 1991. Correlation between oral drug absorption in humans and apparent drug permeability coefficients in human intestinal epithelial (Caco-2) cells. *Biochemical and biophysical research communications*, 175:880–885.
- Artursson, P., Palm, K. & Luthman, K. 2012. Caco-2 monolayers in experimental and theoretical predictions of drug transport. *Advanced drug delivery reviews*, 64:280–289.

- Aungst, B. 2012. Absorption enhancers: applications and advances. *The American Association of Pharmaceutical Scientists journal*, 14:10–18.
- Beg, S., Swain, S., Rizwan, M., Irfanuddin, M. & Malini, D.S. 2011. Bioavailability enhancement strategies: basics, formulation approaches and regulatory considerations. *Current drug delivery*, 8:691–702.
- Beneke, C., Viljoen, A. & Hamman, J.H. 2012. *In vitro* drug absorption enhancement effects of *Aloe vera* and *Aloe ferox*. *Scientia pharmaceutica*, 80:475–486.
- Beneke, C., Viljoen, A. & Hamman, J.H. 2013. Modulation of drug efflux by aloe materials: an *in vitro* investigation across rat intestinal tissue. *Pharmacognosy magazine*, 9:44–48.
- Berben, P., Brouwers, J. & Augustijns, P. 2018. Assessment of passive permeability using an artificial membrane insert system. *Journal of pharmaceutical sciences*, 107:250–256.
- Bhushani, J.A., Karthik, P. & Anandharamakrishnan, C. 2016. Nanoemulsion based delivery system for improved bioaccessibility and Caco-2 cell monolayer permeability of green tea extract. *Food hydrocolloids*, 56:372–382.
- Borska, S., Sopel, M., Chmielewska, M., Zabel, M. & Dziegiel, P. 2010. Quercetin as a potential modulator of P-glycoprotein expression and function in cells of human pancreatic carcinoma line resistant to daunorubicin. *Molecules*, 15:857–870.
- Boudreau, M.D. & Beland, F.A. 2006. An evaluation of the biological and toxicological properties of *Aloe barbadensis* (Miller), *Aloe vera*. *Journal of environmental science and health. Part C*, 24:103–154.
- Cabrera-Pérez, M.A., Sanz, M.B., Sanjuan, V.M., González-Álvarez, M. & González-Álvarez, I. 2016. Importance and applications of cell- and tissue-based *in vitro* models for drug permeability screening in early stages of drug development. (In Sarmiento, B. ed. Concepts and models for drug permeability studies. Cambridge: Woodhead. p. 3–29).
- Cai, Y., Xu, C., Chen, P., Hu, J., Hu, R., Huang, M. & Bi, H. 2014. Development, validation and application of a novel 7-day Caco-2 cell culture system. *Journal of pharmacological and toxicological methods*, 70:175–181.
- Chen, W., Lu, Z., Viljoen, A. & Hamman, J. 2009. Intestinal drug transport enhancement by *Aloe vera*. *Planta medica*, 75:587–595.
- Choi, S. & Chung, M. 2003. A review on the relationship between *Aloe vera* components and their biologic effects. *Seminars in integrative medicine*, 1:53–62.

- Choonara, B.F., Choonara, Y.E., Kumar, P., Bijukumar, D., Du Toit, L.C. & Pillay, V. 2014. A review of advanced oral drug delivery technologies facilitating the protection and absorption of protein and peptide molecules. *Biotechnology advances*, 32:1269–1282.
- Cole, L. & Heard, C. 2007. Skin permeation enhancement potential of *Aloe vera* and a proposed mechanism of action based upon size exclusion and pull effect. *International journal of pharmaceuticals*, 333:10–16.
- Deferme, S., Annaert, P. & Augustijns, P. 2008. *In vitro* screening models to assess intestinal drug absorption and metabolism. (In Ehrhardt, C. & Kim, K., eds. Drug absorption studies: *in situ*, *in vitro* and *in silico* models. New York: Springer. p. 182–215).
- Du Plessis, L.H. & Hamman, J.H. 2014. *In vitro* evaluation of the cytotoxic and apoptogenic properties of aloe whole leaf and gel materials. *Drug and chemical toxicology*, 37:169–177.
- Djuv, A. & Nilsen, O.G. 2008. Caco-2 cell methodology and inhibition of the P-glycoprotein transport of digoxin by *Aloe vera* juice. *Phytotherapy research*, 22:1623–1628.
- Dorkoosh, F.A., Broekhuizen, C.A.N., Borchard, G., Rafiee-Tehrani, M., Verhoef, J.C. & Junginger, H.E. 2004. Transport of octreotide and evaluation of mechanism of action of opening the paracellular tight junction using superporous hydrogel polymers in Caco-2 cell monolayers. *Journal of pharmaceutical sciences*, 93:743–752.
- Du Toit, T., Malan, M.M., Lemmer, H.J.R., Gouws, C., Aucamp, M.E., Breytenbach, W.J. & Hamman, J.H. 2016. Combining chemical permeation enhancers for synergistic effects. *European journal of drug metabolism and pharmacokinetics*, 41:575–586.
- Eshun, K. & He, Q. 2004. *Aloe vera*: a valuable ingredient for the food, pharmaceutical and cosmetic industries – a review. *Critical reviews in food science and nutrition*, 44:91–96.
- Fasano, A. & Nataro, J.P. 2004. Intestinal epithelial tight junctions as targets for enteric bacteria-derived toxins. *Advanced drug delivery reviews*, 56:795–807.
- Femenia, A., Sánchez, E.S., Simal, S. & Rosselló, C. 1999. Compositional features of polysaccharides from *Aloe vera* (*Aloe barbadensis* Miller) plant tissues. *Carbohydrate polymers*, 39:109–117.
- Fox, L., Gerber, M., Du Preez, J.L., Du Plessis, J. & Hamman, J.H. 2014. Skin permeation enhancement effects of the gel and whole leaf materials of *Aloe vera*, *Aloe marlothii* and *Aloe ferox*. *Journal of pharmacy and pharmacology*, 67:96–106.

Gamboa, J.M. & Leong, K.W. 2013. *In vitro* and *in vivo* models for the oral delivery of nanoparticles. *Advanced drug delivery reviews*, 65:800–810.

Gouws, C. 2014. Reviving frozen cell stocks. Centre of Excellence for Pharmaceutical Sciences: mammalian cell cultures. SOP no: Pharmacen\_CTC\_SOP007\_v01\_Reviving cell stocks. Potchefstroom: NWU. p. 1–4.

Griffin, B.T., Guo, J., Presas, E., Donovan, M.D., Alonso, M.J. & O'Driscoll, C.M. 2016. Pharmacokinetic, pharmacodynamic and biodistribution following oral administration of nanocarriers containing peptide and protein drugs. *Advanced drug delivery reviews*, 106:367–380.

Hamman, J.H., Stander, M. & Kotzé, A.F. 2002. Effect of the degree of quaternisation of *N*-trimethyl chitosan chloride of absorption enhancement: *in vivo* evaluation in rat nasal epithelia. *International journal of pharmaceutics*, 232:235–242.

Hamman, J.H., Enslin, G.M. & Kotzé, A.F. 2005. Oral delivery of peptide drugs: barriers and developments. *Biodrugs*, 19:165–177.

Hamman, J.H. 2008. Composition and applications of *Aloe vera* leaf gel. *Molecules*, 13:1599–1616.

Hochman, J. & Artursson, P. 1994. Mechanisms of absorption enhancement and tight junction regulation. *Journal of controlled release*, 29:253–267

Hsu, L., Lee, P., Chen, C., Mi, F., Juang, J., Hwang, S., Ho, Y. & Sung, H. 2012. Elucidating the signalling mechanism of an epithelial tight junction opening by chitosan. *Biomaterials*, 33:6254–6263.

Hsu, L., Ho, Y., Chuang, E., Chen, C., Juang, J., Su, F., Hwang, S. & Sung, H. 2013. Effects of pH on molecular mechanisms of chitosan-integrin interactions and resulting tight-junction disruptions. *Biomaterials*, 34:784–793.

ICH (International Conference on Harmonisation of Technical Requirements for Registration of Pharmaceuticals for Human Use). 2005. Validation of analytical procedures: text and methodology Q2(R1). [http://www.ich.org/fileadmin/Public\\_Web\\_Site/ICH\\_Products/Guidelines/Quality/Q2\\_R1/Step4/Q2\\_R1\\_\\_Guideline.pdf](http://www.ich.org/fileadmin/Public_Web_Site/ICH_Products/Guidelines/Quality/Q2_R1/Step4/Q2_R1__Guideline.pdf) Date of access: 9 Nov. 2017.

Isoda, H., Han, J., Tominaga, M. & Maekawa, T. 2001. Effects of capsaicin on human intestinal cell line Caco-2. *Cytotechnology*, 36:155–161.

- Johnson, P.H., Frank, D. & Costantino., H.R. 2008. Discovery of tight junction modulators: significance for drug development and delivery. *Drug discovery today*, 13:261–267.
- Kang, M.J., Cho, J.Y., Shim, B.H., Kim, D.K. & Lee, J. 2009. Bioavailability enhancing activities of natural compounds from medicinal plants. *Journal of medicinal plants research*, 3:1204–1211.
- Kesarwani, K. & Gupta, R. 2013. Bioavailability enhancers of herbal origin: an overview. *Asian Pacific journal of tropical biomedicine*, 3:253–266.
- Khajuria, A., Thusu, N. & Zutshi, U. 2002. Piperine modulates permeability characteristics of intestine by inducing alterations in membrane dynamics: influence on brush border membrane fluidity, ultrastructure and enzyme kinetics. *Phytomedicine*, 9:224–231.
- Kotzé, A.F., Leußen, H.L., De Leeuw, B.J., De Boer, B.G., Verhoef, J.C. & Junginger, H.E. 1997. N-Trimethyl chitosan chloride as a potential absorption enhancer across mucosal surfaces: *in vitro* evaluation in intestinal epithelial cells (Caco-2). *Pharmaceutical research*, 14:1197–1202.
- Kotzé, A.F., Leußen, H.L., De Leeuw, B.J., De Boer, B.G., Verhoef, J.C. & Junginger, H.E. 1998. Comparison of the effect of different chitosan salts and N-trimethyl chitosan chloride on the permeability of intestinal epithelial cells (Caco-2). *Journal of controlled release*, 51:35–46.
- Krug, S.M., Fromm, M. & Günzel, D. 2009. Two-path impedance spectroscopy for measuring paracellular and transcellular epithelial resistance. *Biophysical journal*, 97:2202–2211.
- Le Ferrec, E., Chesne, C., Artursson, P., Brayden, D., Fabre, G., Gires, P., Guillou, F., Rousset, M., Rubas, W. & Scarino, M. 2001. *In vitro* models of the intestinal barrier. *European Centre for Validation of Alternative Methods*, 29:649–668.
- Lebitsa, T., Viljoen, A., Lu, Z. & Hamman, J. 2012. *In vitro* drug permeation enhancement potential of Aloe gel materials. *Current drug delivery*, 9:297–304.
- Lemmer, H.J.R. & Hamman, J.H. 2013. Paracellular drug absorption enhancement through tight junction modulation. *Expert opinion on drug delivery*, 10:103–114.
- Lennernäs, H., Ahrenstedt, O., Hällgren, R., Knutson, L., Ryde, M. & Paalzow, L.K. 1992. Regional jejunal perfusion, a new *in vivo* approach to study the oral absorption in man. *Pharmaceutical research*, 9:1243–1251.
- Li, Y., Duan, Z., Tian, Y., Liu, Z. & Wang, Q. 2013. A novel perspective and approach to intestinal octreotide absorption: sinomenine-mediated reversible tight junction opening and its molecular mechanism. *International journal of molecular sciences*, 14:12873–12892.

- Lin, Y., Chen, C., Liang, H., Kulkarni, A.R., Lee, P., Chen, C. & Sung, H. 2007. Novel nanoparticles for oral insulin delivery via the paracellular pathway. *Nanotechnology*, 18:1–11.
- Lundquist, P. & Artursson, P. 2016. Oral absorption of peptides and nonparticles across the human intestine: opportunities, limitations and studies in human tissues. *Advanced drug delivery reviews*, 106:256–276.
- Mahato, R.I., Narang, A.S., Thoma, L. & Miller, D.D. 2003. Emerging trends in oral delivery of peptide and protein drugs. *Critical reviews in therapeutic drug carrier systems*, 20:153–214.
- Maher, S. & Brayden, D.J. 2012. Overcoming poor permeability: translating permeation enhancers for oral peptide delivery. *Drug discovery today: technologies*, 9:e113–e119.
- Mascolo, N., Izzo, A.A., Borrelli, F., Capasso, R., Di Carlo, G., Sautebin, L. & Capasso, F. 2004. Healing powers of aloes. (*In Reynolds, T., ed. Aloes: the genus Aloe. Washington DC: CRC Press. p. 209–238*).
- Matter, K. & Balda, M.S. 2003. Functional analysis of tight junctions. *Methods*, 30:228–234.
- Moroz, E., Matoori, S. & Leroux, J. 2016. Oral delivery of macromolecular drugs: where we are after almost 100 years of attempts. *Advanced drug delivery reviews*, 101:108–121.
- Muheem, A., Shakeel, F., Jahangir, M.A., Anwar, M., Mallick, N., Jain, G.K., Warsi, M.H. & Ahmad, F.J. 2016. A review on the strategies for the oral delivery of proteins and peptides and their clinical perspectives. *Saudi pharmaceutical journal*, 24:413–428.
- Mukherjee, P.K., Nema, N.K., Maity, N., Mukherjee, K. & Harwansh, R.K. 2014. Phytochemical and therapeutic profile of *Aloe vera*. *Journal of natural remedies*, 14:1–26.
- Nagumo, Y., Han, J., Belila, A., Isoda, H. & Tanaka, T. 2008. Cofilin mediates tight-junction opening by redistributing actin and tight-junction proteins. *Biochemical and biophysical research communications*, 377:921–925.
- Natoli, M., Leoni, B.D., D'Agnano, I., Zucco, F. & Felsani, A. 2012. Good Caco-2 cell culture practices. *Toxicology in vitro*, 26:1243–1246.
- Nielsen, R., Birn, H., Moestrup, S.K., Nielsen, M., Verroust, P. & Christensen, E.I. 1998. Characterization of a kidney proximal tubule cell line, LLC-PK1, expressing endocytotic active megalin. *Journal of the American Society of Nephrology*, 9:1767–1776.

- Nunes, R., Silva, C. & Chaves, L. 2016. Tissue-based *in vitro* and *ex vivo* models for intestinal permeability studies. (In Sarmento, B. ed. Concepts and models for drug permeability studies. Cambridge: Woodhead. p. 203–236).
- Ojewole, E., Mackraj, I., Akhundov, K., Hamman, J., Viljoen, A., Olivier, E., Wesley-Smith, J. & Govender, T. 2012. Investigating the effect of *Aloe vera* gel on the buccal permeability of didanosine. *Planta medica*, 78:354–361.
- Palumbo, P., Picchini, U., Beck, B., van Gelder, J., Delbar, N. & DaGaetano, A. 2008. A general approach to the apparent permeability index. *Journal of pharmacokinetics and pharmacodynamics*, 35:235–248.
- Park, J.W., Kim, S.K., Al-Hilal, T.A., Jeon, O.C., Moon, H.T. & Byun, Y. 2010. Strategies for oral delivery of macromolecule drugs. *Biotechnology and bioprocess engineering*, 15:66–75.
- Park, K., Kwon, I.C. & Park, K. 2011. Oral protein delivery: current status and future prospect. *Reactive and functional polymers*, 71:280–287.
- Peng, L., He, Z., Chen, W., Holzman, I.R. & Lin, J. 2007. Effects of butyrate on intestinal barrier function in a Caco-2 cell monolayer model of intestinal barrier. *Pediatric research*, 61:37–41.
- Pereira, C., Costa, J., Sarmento, B. & Araújo, F. 2016. Cell-based *in vitro* models for intestinal permeability studies. (In Sarmento, B. ed. Concepts and models for drug permeability studies. Cambridge: Woodhead. p. 57–81).
- Pick, D., Degen, C., Leiterer, M., Jahreis, G. & Einax, J.W. 2013. Transport of selenium species in Caco-2 cells: analytical approach employing the Ussing chamber technique and HPLC-ICP-MS. *Microchemical journal*, 110:8–14.
- Renukuntla, J., Vadlapudi, A. D., Patel, A., Boddu, S.H.S. & Mitra, A.K. 2013. Approaches for enhancing oral bioavailability of peptides and proteins. *International journal of pharmaceutics*, 447:75–93.
- Rosenthal, R., Günzel, D., Finger, C., Krug, S.M., Richter, J.F., Schulzke, J., Fromm, M. & Amasheh, S. 2012a. The effect of chitosan on transcellular and paracellular mechanisms in the intestinal epithelial barrier. *Biomaterials*, 33:2791–2800.
- Rosenthal, R., Heydt, M.S., Amasheh, M., Stein, C., Fromm, M. & Amasheh, S. 2012b. Analysis of absorption enhancers in epithelial cell models. *Annals of the New York Academy of Sciences*, 1258:86–92.

Rubas, W., Cromwell, M.E.M., Shahrokh, Z., Villagran, J., Nguyen, T.N., Wellton, M., Nguyen, T.H. & Mrsny, R.J. 1996. Flux measurements across Caco-2 monolayers may predict transport in human large intestinal tissue. *Journal of pharmaceutical sciences*, 85:165–169.

Sahu, P.K., Giri, D.D., Singh, R., Pandey, P., Gupta, S., Shrivastava, A.K., Kumar, A. & Pandey, K.D. 2013. Therapeutic and medicinal uses of *Aloe vera*: a review. *Pharmacology and pharmacy*, 4:599–610.

Salama, N.N., Eddington, N.D. & Fasano, A. 2006. Tight junction modulation and its relationship to drug delivery. *Advanced drug delivery reviews*, 58:15–28.

Sambuy, Y., De Angelis, I., Ranaldi, G., Scarino, M.L., Stamatii, A. & Zucco, F. 2005. The Caco-2 cell line as a model of the intestinal barrier: influence of cell and culture-related factors on Caco-2 cell functional characteristics. *Cell biology and toxicology*, 21:1–26.

Sánchez-Machado, D.I., López-Cervantes, J., Sendón, R. & Sanches-Silva, A. 2017. *Aloe vera*: ancient knowledge with new frontiers. *Trends in food science and technology*, 61:94–102.

Sánchez-Navarro, M., Garcia, J., Giralt, E. & Teixidó, M. 2016. Using peptides to increase transport across the intestinal barrier. *Advanced drug delivery reviews*, 106:355–366.

Sarmento, B., Andrade, F., da Silva, S.B., Rodrigues, F., das Neves, J. & Ferreira, D. 2012. Cell-based *in vitro* models for predicting drug permeability. *Expert opinion on drug metabolism and toxicology*, 8:607–621.

Servier Medical Art. 2017. SMART: Servier Medical Art. Cellular biology. <http://smart.servier.com/> Date of access: 9 Nov. 2017.

Sharom, F.J. 2011. The P-glycoprotein multidrug transporter. *Essays in biochemistry*, 50:161–178.

Shrivastava, A. & Gupta, V.B. 2011. Methods for the determination of the limit of detection and limit of quantification of the analytical methods. *Chronicles of young scientists*, 2:21–25.

Sieval, A.B., Thanou, M., Kotzé, A.F., Verhoef, J.C., Brussee, J. & Junginger, H.E. 1998. Preparation and NMR characterization of highly substituted *N*-trimethyl chitosan chloride. *Carbohydrate polymers*, 36:157–165.

Sjögren, E., Abrahamsson, B., Augustijns, P., Becker, D., Bolger, M.B., Brewster, M., Brouwers, J., Flanagan, T., Harwood, M., Heinen, C., Holm, R., Juretschke, H., Kubbinga, M., Lindahl, A., Lukacova, V., Münster, U., Neuhoff, S., Nguyen, M.A., van Peer, A., Reppas, C., Hodjegan, A.R., Tannergren, C., Weitschies, W., Wilson, C., Zane, P., Lennernäs, H. & Langguth, P. 2014. *In*

*in vivo* methods for drug absorption: comparative physiologies, model selection, correlations with *in vitro* methods (IVIVC), and applications for formulation/API/excipient characterization including food effects. *European journal of pharmaceutical sciences*, 57:99–151.

Sun, H., Chow, E.C.Y., Liu, S., Du, Y. & Pang, K.S. 2008. The Caco-2 cell monolayer: usefulness and limitations. *Expert opinion on drug metabolism and toxicology*, 4:395–411.

Tatiraju, D.V., Bagade, V.B., Karambelkar, P.J., Jadhav, V.M. & Kadam, V. 2013. Natural bioenhancers: an overview. *Journal of pharmacognosy and phytochemistry*, 2:55–60.

Tavelin, S., Milovic, V., Ocklind, G., Olsson, S. & Artursson, P. 1999. A conditionally immortalized epithelial cell line for studies of intestinal drug transport. *The journal of pharmacology and experimental therapeutics*, 290:1212–1221.

Tavelin, S., Taipalensuu, J., Söderberg, L., Morrison, R., Chong, S. & Artursson, P. 2003. Prediction of oral absorption of low-permeability drugs using small intestine-like 2/4/A1 cell monolayers. *Pharmaceutical research*, 20:397–405.

Thanou, M., Verhoef, J.C. & Junginger, H.E. 2001. Oral drug absorption enhancement by chitosan and its derivatives. *Advanced drug delivery review*, 52:117–126.

Tscheik, C., Blasig, I.E. & Winkler, L. 2013. Trends in drug delivery through tissue barriers containing tight junctions. *Tissue barriers*, 1(e24565):1–8.

USP (United States Pharmacopeial Convention). 2017a. Fluorescence spectroscopy. <http://app.uspnf.com/uspnf/pub/index?usp=40&nf=35&s=1&officialOn=August%201,%202017> Date of access: 9 Nov. 2017.

USP (United States Pharmacopeial Convention). 2017b. Validation of compendial procedures. <http://app.uspnf.com/uspnf/pub/index?usp=40&nf=35&s=1&officialOn=August%201,%202017> Date of access: 9 Nov. 2017.

Vinson, J.A., Al Kharrat, H. & Andreoli, L. 2005. Effect of *Aloe vera* preparations on the human bioavailability of vitamins C and E. *Phytomedicine*, 12:760–765.

Wahlang, B., Pawar, Y.B. & Bansal, A.K. 2011. Identification of permeability-related hurdles in oral delivery of curcumin using the Caco-2 cell model. *European journal of pharmaceuticals and biopharmaceutics*, 77:275–282.

Wallis, L., Kleynhans, E., Du Toit, T., Gouws, C., Steyn, D., Steenekamp, J., Viljoen, J. & Hamman, J. 2014. Novel non-invasive protein and peptide drug delivery approaches. *Protein and peptide letters*, 21:1087–1101.

- Wallis, L., Malan, M., Gouws, C., Steyn, D., Ellis, S., Abay, E., Wiesner, L., Otto, D.P. & Hamman, J. 2016. Evaluation of isolated fractions of *Aloe vera* gel materials on Indinavir pharmacokinetics: *in vitro* and *in vivo* studies. *Current drug delivery*, 13:471–480.
- Ward, P.D., Tippin, T.K. & Thakker, D.R. 2000. Enhancing paracellular permeability by modulating epithelial tight junctions. *Pharmaceutical science and technology today*, 3:346–358.
- Weinheimer, M., Fricker, G., Burhenne, J., Mylius, P. & Schubert, R. 2017. The application of P-gp inhibiting phospholipids as novel oral bioavailability enhancers: an *in vitro* and *in vivo* comparison. *European journal of pharmaceutical sciences*, 106:13–22.
- Werle, M. & Bernkop-Schnürch, A. 2008. Thiolated chitosans: useful excipients for oral drug delivery. *Journal of pharmacy and pharmacology*, 60:273–281.
- Werle, M., Takeuchi, H. & Bernkop-Schnürch, A. 2009. Modified chitosans for oral drug delivery. *Journal of pharmaceutical sciences*, 98:1643–1656.
- Wu, S., Don, T., Lin, C. & Mi, F. 2014. Delivery of berberine using chitosan/fucoidan-aurine conjugate nanoparticles for treatment of defective intestinal epithelial tight junction barrier. *Marine drugs*, 12:5677–5697.
- Yang, Y., Zhao, Y., Yu, A., Sun, D. & Yu, L.X. 2017. Oral drug absorption: evaluation and prediction. (In Qiu, Y., Chen, Y., Zhang, G.G.Z., Yu, L. & Mantri, R.V., eds. *Developing solid oral dosage forms: pharmaceutical theory & practice*. Amsterdam: Elsevier. p. 331–354).
- Zhu, H., Li, B.V., Uppoor, R.S., Mehta, M. & Yu, L.X. 2017. Bioavailability and bioequivalence. (In Qiu, Y., Chen, Y., Zhang, G.G.Z., Yu, L. & Mantri, R.V., eds. *Developing solid oral dosage forms: pharmaceutical theory & practice*. Netherlands: Elsevier. p. 381–397).
- Zolnericks, J.K., Booth-Genthe, C.L., Gupta, A., Harris, J. & Unadkat, J.D. 2011. Substrate- and species-dependent inhibition of P-glycoprotein-mediated transport: implications for predicting *in vivo* drug interactions. *Journal of pharmaceutical sciences*, 100:3055–3061.

## **APPENDIX A**

### **CHARACTERIZATION OF ALOE LEAF MATERIALS AND N-TRIMETHYL CHITOSAN CHLORIDE (TMC)**

---

A.1 Characterization of *Aloe vera* gel and whole leaf extract

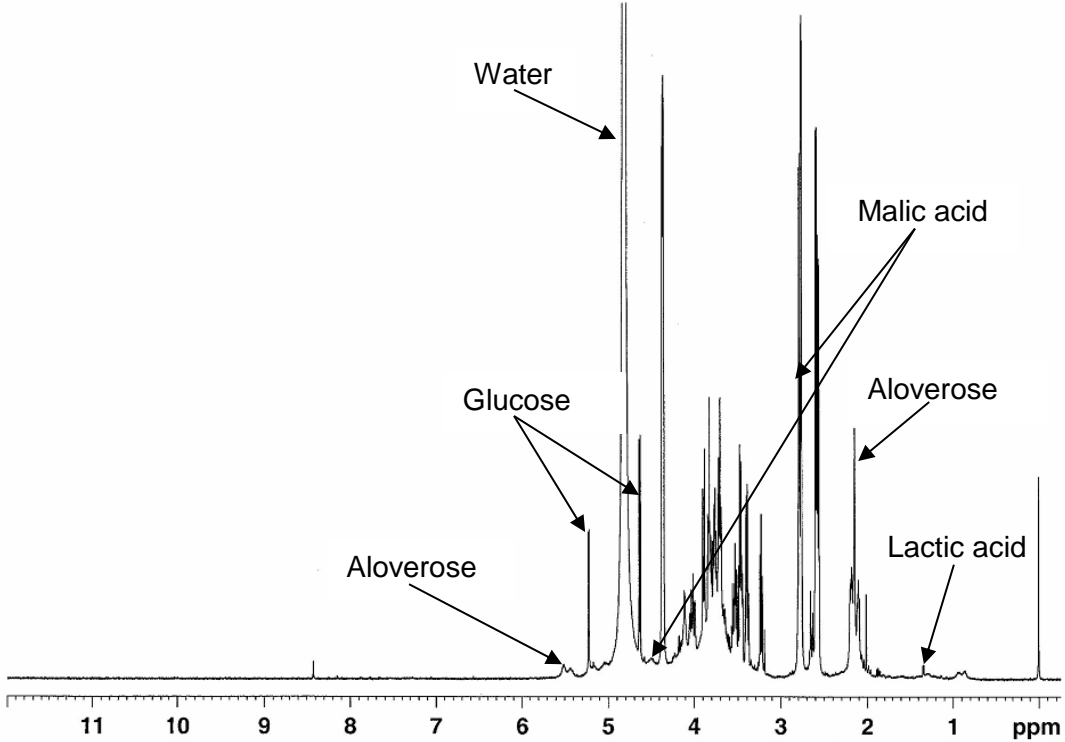


Figure A.1: 1H-NMR spectrum for *Aloe vera* gel

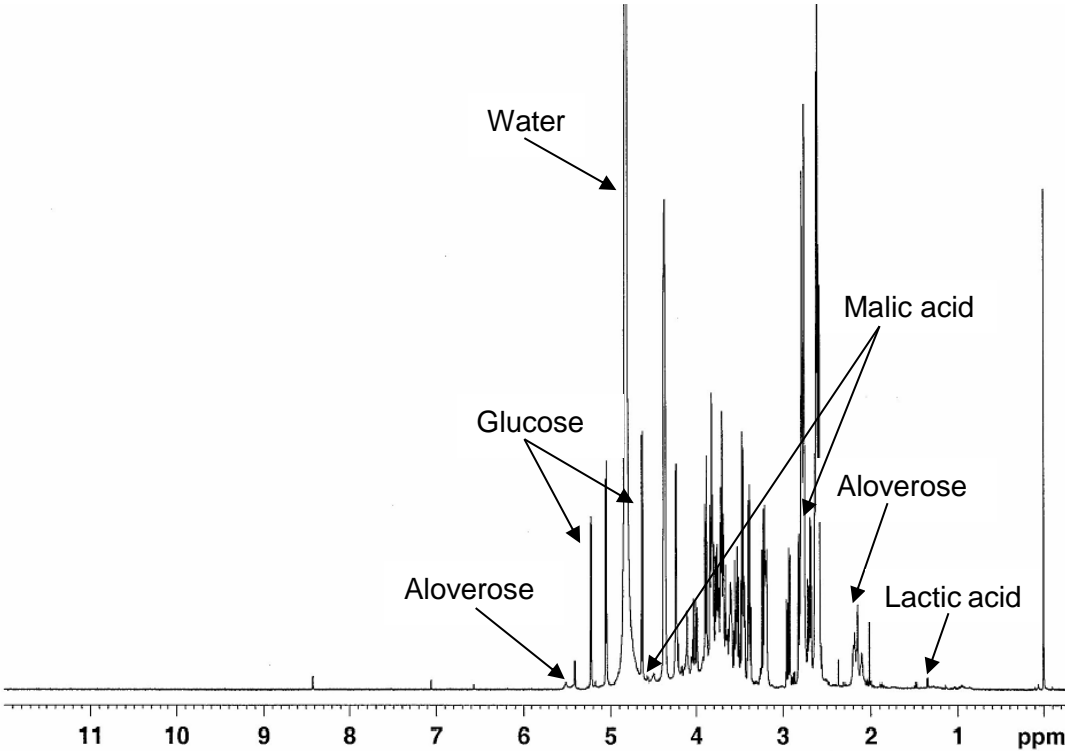
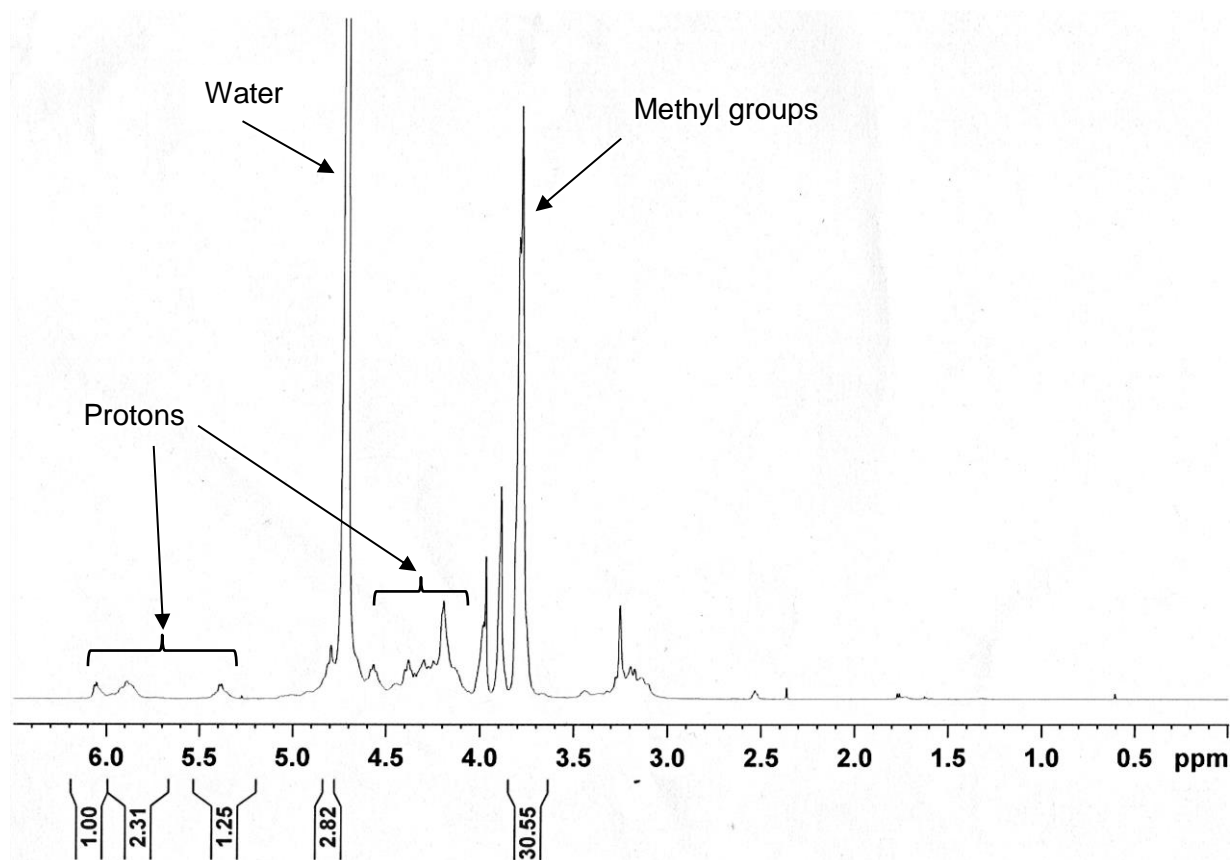


Figure A.2: 1H-NMR spectrum for *Aloe vera* whole leaf extract

## A.2 Characterization of *N*-trimethyl chitosan chloride



**Figure A.3:**  $^1\text{H}$ -NMR spectrum for *N*-trimethyl chitosan chloride

Degree of quaternisation was calculated from the  $^1\text{H}$ -NMR spectrum for *N*-trimethyl chitosan chloride in Figure A.3, with the following equation (Hamman *et al.*, 2002:237):

$$\text{DQ (\%)} = \left[ \left( \frac{\int^{\text{TM}}}{\int^{\text{H}}} \right) \times \frac{1}{9} \right] \times 100 \quad \text{Equation 8}$$

Where DQ (%) is the degree of quaternisation,  $\int^{\text{TM}}$  is the integral of the trimethyl amino group peak at 3.7–4.0 ppm, and  $\int^{\text{H}}$  is the integral of the  $^1\text{H}$  peaks from 4.7–6.2 ppm.

With Equation 8, the degree of quaternisation of the TMC used was calculated:

$$\text{DQ (\%)} = \left[ \left( \frac{30.55}{(1.00+2.31+1.25+2.82)} \right) \times \frac{1}{9} \right] \times 100$$

$$\text{DQ (\%)} = \left[ \left( \frac{30.55}{(7.38)} \right) \times \frac{1}{9} \right] \times 100$$

$$\text{DQ} = 45.995\%$$

## **APPENDIX B**

### **SUPPLEMENTARY DATA: VALIDATION OF FLUOROMETRIC ANALYTICAL METHOD ON THE SPECTRAMAX<sup>®</sup> PLATE READER**

---

**B.1 Fluorescence detection values measured for a specified concentration range and the resulting linear regression coefficient values**

**Table B.1:** Fluorescence detection and linear regression coefficient ( $R^2$ ) values of FITC-dextran (4 000 Da) standard/calibration solutions

<b>FITC-dextran 4 000Da concentration (<math>\mu\text{g/ml}</math>)</b>	<b>Fluorescence detection value</b>
125.00	635359968
62.50	335240832
13.89	82861176
7.81	45675588
4.63	28403168
3.90	23297372
1.54	10993882
0.51	5082752
<b><math>R^2</math></b>	<b>0.9991</b>
<b>Slope</b>	<b>5082165.06</b>

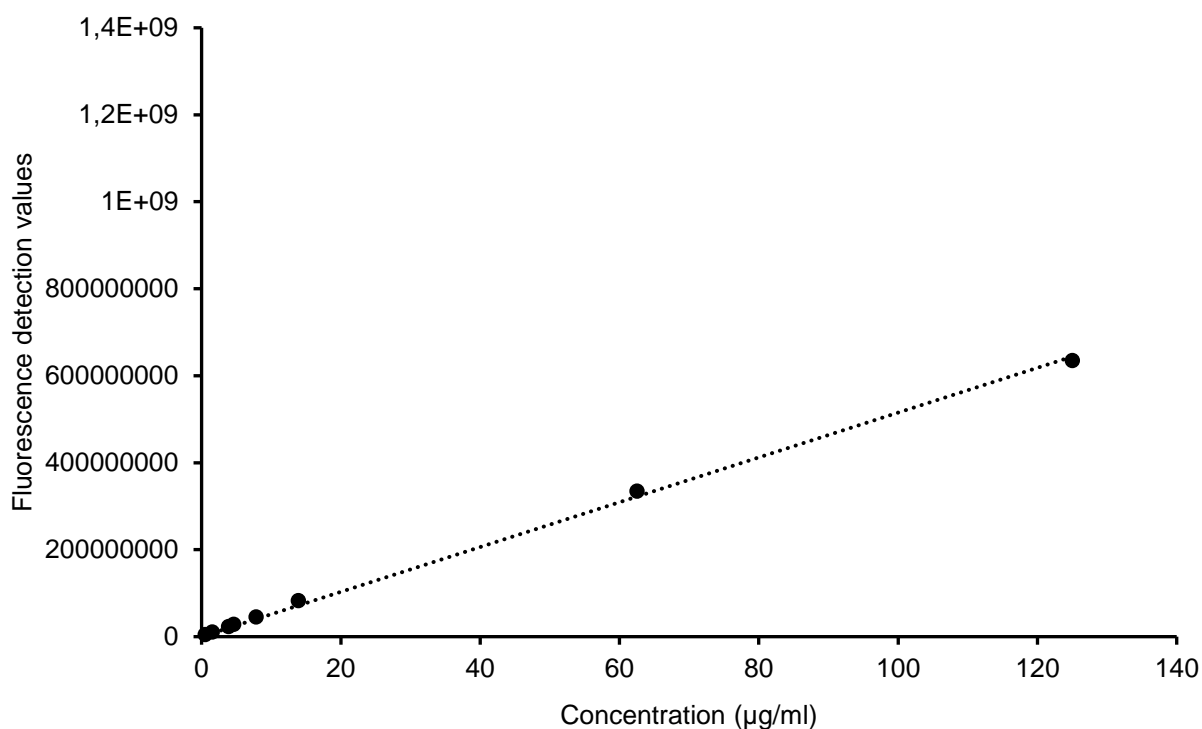


**Figure B.1:** Standard curve for FITC-dextran 4 000 Da

**Table B.2:** Fluorescence detection and linear regression coefficient ( $R^2$ ) values of FITC-dextran (10 000 Da) standard/calibration solutions

<b>FITC-dextran 10 000Da concentration (<math>\mu\text{g/ml}</math>)</b>	<b>Fluorescence detection value</b>
125.00	794315328
62.50	400489376
13.89	71014384
7.81	55212392
4.63	27686078
3.90	28271178
1.54	11619431
0.51	5867168
<b><math>R^2</math></b>	<b>0.9995</b>
<b>Slope</b>	<b>6360487.73</b>

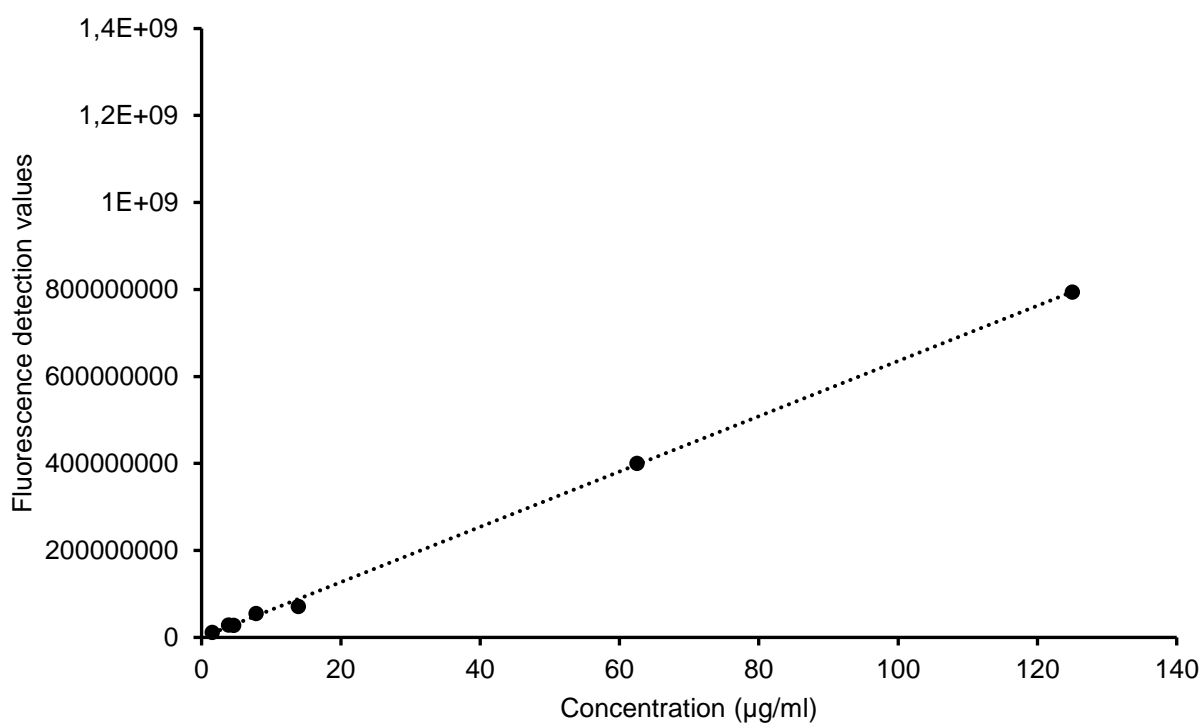


**Figure B.2:** Standard curve for FITC-dextran 10 000 Da

**Table B.3:** Fluorescence detection and linear regression coefficient ( $R^2$ ) values of FITC-dextran (20 000 Da) standard/calibration solutions

<b>FITC-dextran 20 000Da concentration (<math>\mu\text{g/ml}</math>)</b>	<b>Fluorescence detection value</b>
125.00	1331221376
62.50	739047872
13.89	191094896
7.81	106864464
4.63	72464128
3.90	52896012
1.54	16986200
0.51	6173769
<b><math>R^2</math></b>	<b>0.9971</b>
<b>Slope</b>	<b>10699908.63</b>

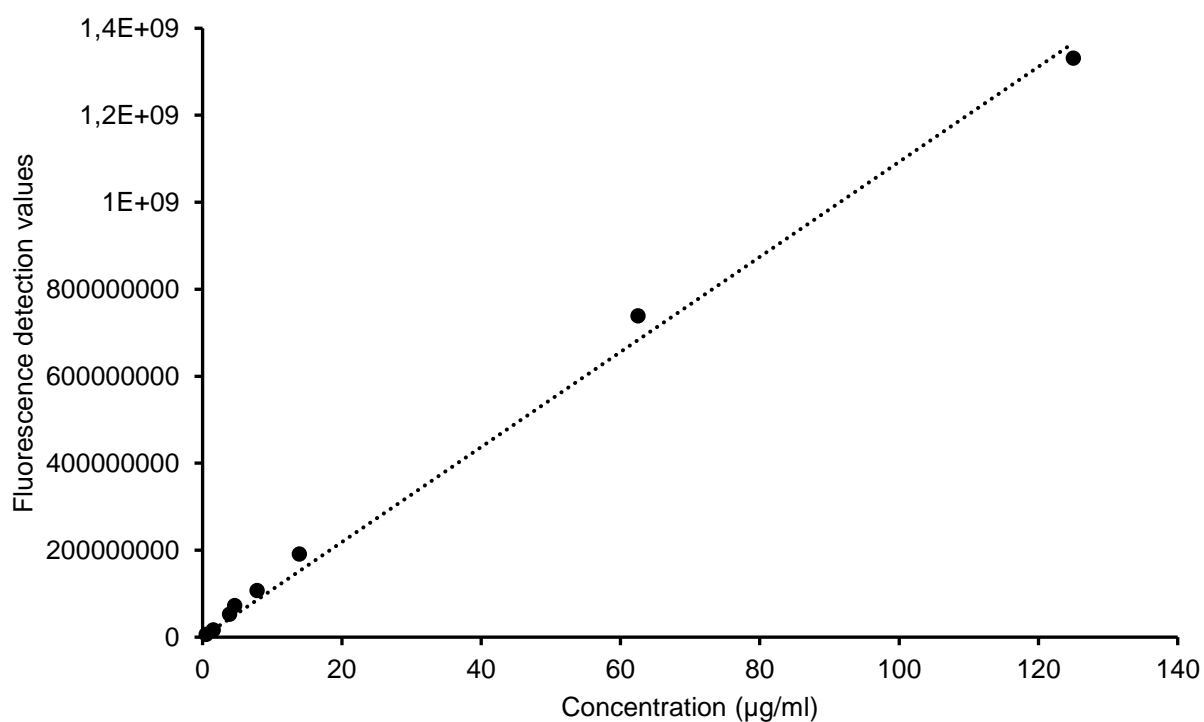


**Figure B.3:** Standard curve for FITC-dextran 20 000 Da

**Table B.4** Fluorescence detection and linear regression coefficient ( $R^2$ ) values of FITC-dextran (40 000 Da) standard/calibration solutions

FITC-dextran 40 000Da concentration ( $\mu\text{g/ml}$ )	Fluorescence detection value
125.00	1086409472
62.50	632352512
13.89	142240784
7.81	77659528
4.63	46359612
3.90	41795748
1.54	18085484
0.51	6847372
<b><math>R^2</math></b>	<b>0.9958</b>
<b>Slope</b>	<b>8845597.95</b>

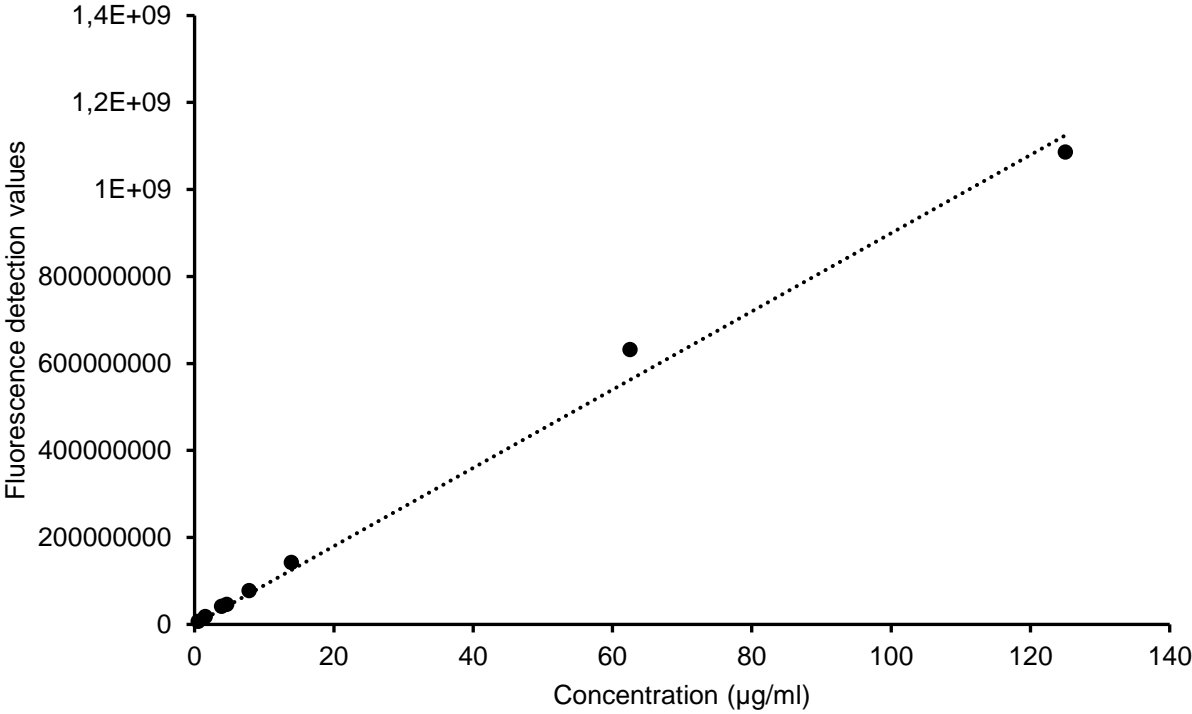


**Figure B.4:** Standard curve for FITC-dextran 40 000 Da

**Table B.5:** Fluorescence detection and linear regression coefficient ( $R^2$ ) values of Lucifer yellow standard/calibration solutions

Lucifer yellow concentration ( $\mu\text{g/ml}$ )	Fluorescence detection value
50.00	59067602
25.00	29490064
16.67	19107348
12.50	13946910
6.25	6852421
1.56	884150
0.78	649164
0.62	415429
<b><math>R^2</math></b>	<b>0.9996</b>
<b>Slope</b>	<b>1193233.27</b>

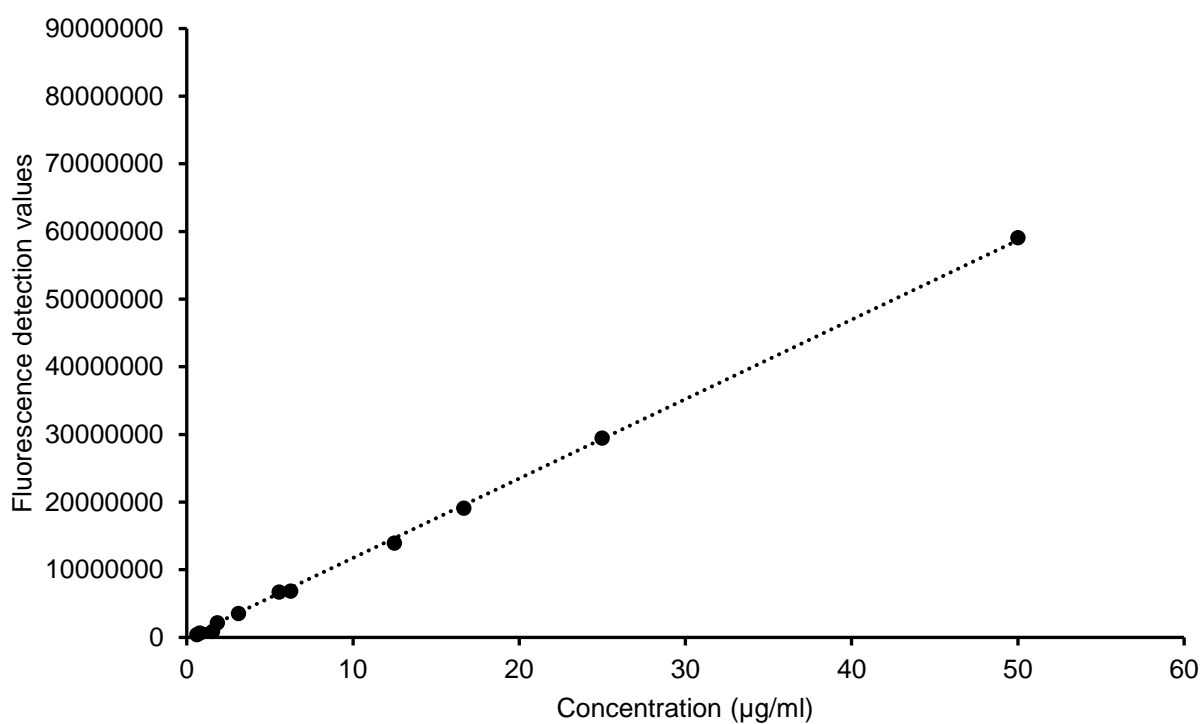


**Figure B.5:** Standard curve for Lucifer yellow

**B.2 Fluorescence detection values measured for specified concentrations used for determining the accuracy and precision of the fluorometric analytical method**

**Table B.6:** Fluorescence detection values and percentage recovery obtained from three different FITC-dextran concentrations to determine accuracy

<b>Theoretical concentration <math>\mu\text{g/ml}</math></b>	<b>Fluorescence detection value</b>	<b>Average fluorescence detection value</b>	<b>Actual concentration</b>	<b>% Recovery</b>
125.00	655269952 654054976 641501120	650275349	125.29	100.23
62.50	317763648 325289312 325767040	322940000	62.22	99.55
31.25	162484576 168231920 164388672	165035056	31.80	101.75

**Table B.7:** Fluorescence detection values and percentage recovery obtained from three different Lucifer yellow concentrations to determine accuracy

<b>Theoretical concentration <math>\mu\text{g/ml}</math></b>	<b>Fluorescence detection value</b>	<b>Average Fluorescence detection value</b>	<b>Actual concentration</b>	<b>% Recovery</b>
50.00	54675406 55729218 54603902	55002842	49.81	99.63
25.00	27854954 27850916 27378956	27694942	25.08	100.33
12.50	14055752 14210102 13886252	14050702	12.73	101.80

## **APPENDIX C**

### **TRANSEPITHELIAL ELECTRICAL RESISTANCE (TEER) ACROSS CACO-2 CELL MONOLAYERS**

---

**Table C.1:** TEER values measured across Caco-2 cell monolayers (as indication of intact monolayer formation,  $\geq 750 \Omega$ ; Du Toit *et al.*, 2016:578) before TEER study of the effect of *Aloe vera* gel and whole leaf extract solutions with different concentrations on Caco-2 cell monolayers

Groups	TEER value ( $\Omega$ )		
	Well 1	Well 2	Well 3
Negative Control	2240	2010	1896
0.5% w/v TMC (positive control)	3240	2880	2670
0.1% w/v <i>A. vera</i> gel	3340	4010	4340
0.5% w/v <i>A. vera</i> gel	4010	3790	4240
1.0% w/v <i>A. vera</i> gel	3450	3630	3480
1.5% w/v <i>A. vera</i> gel	3680	3450	3740
0.1% w/v <i>A. vera</i> whole leaf extract	3660	2380	2770
0.5% w/v <i>A. vera</i> whole leaf extract	4040	3400	4130
1.0% w/v <i>A. vera</i> whole leaf extract	3490	3860	3770
1.5% w/v <i>A. vera</i> whole leaf extract	3070	3700	2750

**Table C.2:** Percentage TEER normalised in regard to the initial TEER value ( $T_0$ ) for the negative control (DMEM alone)

Time (min)	TEER value ( $\Omega$ )			Normalised % TEER			Average	SD
	Well 1	Well 2	Well 3	Well 1	Well 2	Well 3		
<b>0</b>	1331	1255	1018	100.00	100.00	100.00	100.00	0.00
<b>20</b>	1600	1425	1248	120.21	113.55	122.59	118.78	3.83
<b>40</b>	1715	1528	1372	128.85	121.75	134.77	128.46	5.32
<b>60</b>	1825	1579	1430	137.11	125.82	140.47	134.47	6.27
<b>80</b>	1872	1620	1512	140.65	129.08	148.53	139.42	7.98
<b>100</b>	1933	1638	1548	145.23	130.52	152.06	142.60	8.99
<b>120</b>	1986	1694	1595	149.21	134.98	156.68	146.96	9.00

SD = standard deviation

**Table C.3:** Percentage TEER reduction by the negative control (DMEM alone) across Caco-2 cell monolayers

Time (min)	% TEER reduction			Average	SD
	Well 1	Well 2	Well 3		
<b>0</b>	0.00	0.00	0.00	0.00	0.00
<b>20</b>	-20.21	-13.55	-22.59	-18.78	3.83
<b>40</b>	-28.85	-21.75	-34.77	-28.46	5.32
<b>60</b>	-37.11	-25.82	-40.47	-34.47	6.27
<b>80</b>	-40.65	-29.08	-48.53	-39.42	7.98
<b>100</b>	-45.23	-30.52	-52.06	-42.60	8.99
<b>120</b>	-49.21	-34.98	-56.68	-46.96	9.00

SD = standard deviation

**Table C.4:** Percentage TEER normalised in regard to the initial TEER value ( $T_0$ ) in the presence of 0.5% w/v TMC (positive control)

Time (min)	TEER value ( $\Omega$ )			Normalised % TEER			Average	SD
	Well 1	Well 2	Well 3	Well 1	Well 2	Well 3		
<b>0</b>	3260	3060	2780	100.00	100.00	100.00	100.00	0.00
<b>20</b>	866	808	920	26.56	26.41	33.09	28.69	3.12
<b>40</b>	1133	1208	1063	34.75	39.48	38.24	37.49	2.00
<b>60</b>	1280	1446	1271	39.26	47.25	45.72	44.08	3.46
<b>80</b>	1420	1573	1366	43.56	51.41	49.14	48.03	3.30
<b>100</b>	1466	1699	1476	44.97	55.52	53.09	51.20	4.51
<b>120</b>	1498	1755	1517	45.95	57.35	54.57	52.62	4.85

SD = standard deviation

**Table C.5:** Percentage TEER reduction by 0.5% w/v TMC (positive control) across Caco-2 cell monolayers

Time (min)	% TEER reduction			Average	SD
	Well 1	Well 2	Well 3		
<b>0</b>	0.00	0.00	0.00	0.00	0.00
<b>20</b>	73.44	73.59	66.91	71.31	3.12
<b>40</b>	65.25	60.52	61.76	62.51	2.00
<b>60</b>	60.74	52.75	54.28	55.92	3.46
<b>80</b>	56.44	48.59	50.86	51.97	3.30
<b>100</b>	55.03	44.48	46.91	48.80	4.51
<b>120</b>	54.05	42.65	45.43	47.38	4.85

SD = standard deviation

**Table C.6:** Percentage TEER recovery after 0.5% w/v TMC solutions (positive control) were removed (percentage is normalised in regard to the initial TEER value,  $T_0$ )

Time (min) after removal of test solution	Time (hr) after removal of test solution	TEER value ( $\Omega$ )			Normalised %			Average	SD
		Well 1	Well 2	Well 3	Well 1	Well 2	Well 3		
<b>0</b>	<b>0.00</b>	3260	3060	2780	100.00	100.00	100.00	100.00	0.00
<b>20</b>	<b>0.33</b>	1112	749	561	34.11	24.48	20.18	26.26	5.82
<b>40</b>	<b>0.67</b>	1298	813	647	39.82	26.57	23.27	29.89	7.15
<b>60</b>	<b>1.00</b>	1488	977	762	45.64	31.93	27.41	34.99	7.75
<b>80</b>	<b>1.33</b>	1639	1204	896	50.28	39.35	32.23	40.62	7.42
<b>100</b>	<b>1.67</b>	1746	1398	1025	53.56	45.69	36.87	45.37	6.82
<b>120</b>	<b>2.00</b>	1868	1638	1156	57.30	53.53	41.58	50.80	6.70
<b>180</b>	<b>3.00</b>	2120	2140	1598	65.03	69.93	57.48	64.15	5.12
<b>240</b>	<b>4.00</b>	2320	2460	1894	71.17	80.39	68.13	73.23	5.21
<b>360</b>	<b>6.00</b>	2740	2920	2320	84.05	95.42	83.45	87.64	5.51
<b>720</b>	<b>12.00</b>	3490	3660	2750	107.06	119.61	98.92	108.53	8.51
<b>1440</b>	<b>24.00</b>	3580	3770	2830	109.82	123.20	101.80	111.61	8.83
<b>2880</b>	<b>48.00</b>	4140	4120	3390	126.99	134.64	121.94	127.86	5.22
<b>4320</b>	<b>72.00</b>	4860	4310	3730	149.08	140.85	134.17	141.37	6.10

SD = standard deviation

**Table C.7:** Percentage TEER normalised in regard to the initial TEER value ( $T_0$ ) in the presence of 0.1% w/v *Aloe vera* gel solutions

Time (min)	TEER value ( $\Omega$ )			Normalised % TEER			Average	SD
	Well 1	Well 2	Well 3	Well 1	Well 2	Well 3		
<b>0</b>	3570	4200	4660	100.00	100.00	100.00	100.00	0.00
<b>20</b>	640	869	694	17.93	20.69	14.89	17.84	2.37
<b>40</b>	896	1297	1046	25.10	30.88	22.45	26.14	3.52
<b>60</b>	1045	1655	1402	29.27	39.40	30.09	32.92	4.60
<b>80</b>	1138	1883	1678	31.88	44.83	36.01	37.57	5.40
<b>100</b>	1266	2190	2070	35.46	52.14	44.42	44.01	6.82
<b>120</b>	1399	2450	2400	39.19	58.33	51.50	49.67	7.92

SD = standard deviation

**Table C.8:** Percentage TEER reduction by 0.1% w/v *Aloe vera* gel solution across Caco-2 cell monolayers

Time (min)	% TEER reduction			Average	SD
	Well 1	Well 2	Well 3		
<b>0</b>	0.00	0.00	0.00	0.00	0.00
<b>20</b>	82.07	79.31	85.11	82.16	2.37
<b>40</b>	74.90	69.12	77.55	73.86	3.52
<b>60</b>	70.73	60.60	69.91	67.08	4.60
<b>80</b>	68.12	55.17	63.99	62.43	5.40
<b>100</b>	64.54	47.86	55.58	55.99	6.82
<b>120</b>	60.81	41.67	48.50	50.33	7.92

SD = standard deviation

**Table C.9:** Percentage TEER recovery after 0.1% w/v *Aloe vera* gel solutions were removed (percentage is normalised in regard to the initial TEER value,  $T_0$ )

Time (min) after removal of test solution	Time (hr) after removal of test solution	TEER value ( $\Omega$ )			Normalised %			Average	SD
		Well 1	Well 2	Well 3	Well 1	Well 2	Well 3		
<b>0</b>	<b>0.00</b>	3570	4200	4660	100.00	100.00	100.00	100.00	0.00
<b>20</b>	<b>0.33</b>	334	314	254	9.36	7.48	5.45	7.43	1.59
<b>40</b>	<b>0.67</b>	369	370	257	10.34	8.81	5.52	8.22	2.01
<b>60</b>	<b>1.00</b>	407	453	283	11.40	10.79	6.07	9.42	2.38
<b>80</b>	<b>1.33</b>	448	540	299	12.55	12.86	6.42	10.61	2.97
<b>100</b>	<b>1.67</b>	505	627	303	14.15	14.93	6.50	11.86	3.80
<b>120</b>	<b>2.00</b>	513	718	322	14.37	17.10	6.91	12.79	4.31
<b>180</b>	<b>3.00</b>	617	1070	364	17.28	25.48	7.81	16.86	7.22
<b>240</b>	<b>4.00</b>	712	1349	406	19.94	32.12	8.71	20.26	9.56
<b>360</b>	<b>6.00</b>	899	1647	484	25.18	39.21	10.39	24.93	11.77
<b>720</b>	<b>12.00</b>	1188	2380	621	33.28	56.67	13.33	34.42	17.71
<b>1440</b>	<b>24.00</b>	1577	3130	828	44.17	74.52	17.77	45.49	23.19
<b>2880</b>	<b>48.00</b>	2780	5760	1822	77.87	137.14	39.10	84.70	40.32
<b>4320</b>	<b>72.00</b>	4720	5800	4970	132.21	138.10	106.65	125.65	13.65

SD = standard deviation

**Table C.10:** Percentage TEER normalised in regard to the initial TEER value ( $T_0$ ) in the presence of 0.5% w/v *Aloe vera* gel solutions

Time (min)	TEER value ( $\Omega$ )			Normalised % TEER			Average	SD
	Well 1	Well 2	Well 3	Well 1	Well 2	Well 3		
<b>0</b>	4160	3240	4320	100.00	100.00	100.00	100.00	0.00
<b>20</b>	1144	803	811	27.50	24.78	18.77	23.69	3.65
<b>40</b>	1765	1210	1187	42.43	37.35	27.48	35.75	6.21
<b>60</b>	2200	1521	1602	52.88	46.94	37.08	45.64	6.52
<b>80</b>	2430	1692	1875	58.41	52.22	43.40	51.35	6.16
<b>100</b>	2740	1912	2260	65.87	59.01	52.31	59.06	5.53
<b>120</b>	2920	2050	2530	70.19	63.27	58.56	64.01	4.78

SD = standard deviation

**Table C.11:** Percentage TEER reduction by 0.5% w/v *Aloe vera* gel solutions across Caco-2 cell monolayers

Time (min)	% TEER reduction			Average	SD
	Well 1	Well 2	Well 3		
<b>0</b>	0.00	0.00	0.00	0.00	0.00
<b>20</b>	72.50	75.22	81.23	76.31	3.65
<b>40</b>	57.57	62.65	72.52	64.25	6.21
<b>60</b>	47.12	53.06	62.92	54.36	6.52
<b>80</b>	41.59	47.78	56.60	48.65	6.16
<b>100</b>	34.13	40.99	47.69	40.94	5.53
<b>120</b>	29.81	36.73	41.44	35.99	4.78

SD = standard deviation

**Table C.12:** Percentage TEER recovery after 0.5% w/v *Aloe vera* gel solutions were removed (percentage is normalised in regard to the initial TEER value,  $T_0$ )

Time (min) after removal of test solution	Time (hr) after removal of test solution	TEER value ( $\Omega$ )			Normalised %			Average	SD
		Well 1	Well 2	Well 3	Well 1	Well 2	Well 3		
<b>0</b>	<b>0.00</b>	4160	3240	4320	100.00	100.00	100.00	100.00	0.00
<b>20</b>	<b>0.33</b>	473	347	459	11.37	10.71	10.63	10.90	0.33
<b>40</b>	<b>0.67</b>	565	373	569	13.58	11.51	13.17	12.76	0.89
<b>60</b>	<b>1.00</b>	662	413	709	15.91	12.75	16.41	15.02	1.62
<b>80</b>	<b>1.33</b>	764	441	844	18.37	13.61	19.54	17.17	2.56
<b>100</b>	<b>1.67</b>	883	480	985	21.23	14.81	22.80	19.61	3.45
<b>120</b>	<b>2.00</b>	1016	525	1147	24.42	16.20	26.55	22.39	4.46
<b>180</b>	<b>3.00</b>	1357	682	1645	32.62	21.05	38.08	30.58	7.10
<b>240</b>	<b>4.00</b>	1703	842	1958	40.94	25.99	45.32	37.42	8.28
<b>360</b>	<b>6.00</b>	2220	1032	2490	53.37	31.85	57.64	47.62	11.28
<b>720</b>	<b>12.00</b>	3260	1276	3500	78.37	39.38	81.02	66.26	19.03
<b>1440</b>	<b>24.00</b>	5040	1524	4280	121.15	47.04	99.07	89.09	31.07
<b>2880</b>	<b>48.00</b>	5100	4360	5440	122.60	134.57	125.93	127.70	5.05
<b>4320</b>	<b>72.00</b>	5410	4550	5510	130.05	140.43	127.55	132.68	5.58

SD = standard deviation

**Table C.13:** Percentage TEER normalised in regard to the initial TEER value ( $T_0$ ) in the presence of 1.0% w/v *Aloe vera* gel solutions

Time (min)	TEER value ( $\Omega$ )			Normalised % TEER			Average	SD
	Well 1	Well 2	Well 3	Well 1	Well 2	Well 3		
<b>0</b>	3480	3580	4650	100.00	100.00	100.00	100.00	0.00
<b>20</b>	966	754	642	27.76	21.06	13.81	20.88	5.70
<b>40</b>	1558	1152	958	44.77	32.18	20.60	32.52	9.87
<b>60</b>	1968	1448	1270	56.55	40.45	27.31	41.44	11.96
<b>80</b>	2260	1712	1490	64.94	47.82	32.04	48.27	13.43
<b>100</b>	2430	1879	1695	69.83	52.49	36.45	52.92	13.63
<b>120</b>	2570	2050	1940	73.85	57.26	41.72	57.61	13.12

SD = standard deviation

**Table C.14:** Percentage TEER reduction by 1.0% w/v *Aloe vera* gel solutions across Caco-2 cell monolayers

Time (min)	% TEER reduction			Average	SD
	Well 1	Well 2	Well 3		
<b>0</b>	0.00	0.00	0.00	0.00	0.00
<b>20</b>	72.24	78.94	86.19	79.12	5.70
<b>40</b>	55.23	67.82	79.40	67.48	9.87
<b>60</b>	43.45	59.55	72.69	58.56	11.96
<b>80</b>	35.06	52.18	67.96	51.73	13.43
<b>100</b>	30.17	47.51	63.55	47.08	13.63
<b>120</b>	26.15	42.74	58.28	42.39	13.12

SD = standard deviation

**Table C.15:** Percentage TEER recovery after 1.0% w/v *Aloe vera* gel solutions were removed (percentage is normalised in regard to the initial TEER value,  $T_0$ )

Time (min) after removal of test solution	Time (hr) after removal of test solution	TEER value ( $\Omega$ )			Normalised %			Average	SD
		Well 1	Well 2	Well 3	Well 1	Well 2	Well 3		
<b>0</b>	<b>0.00</b>	3480	3580	4650	100.00	100.00	100.00	100.00	0.00
<b>20</b>	<b>0.33</b>	380	396	518	10.92	11.06	11.14	11.04	0.09
<b>40</b>	<b>0.67</b>	429	428	567	12.33	11.96	12.19	12.16	0.15
<b>60</b>	<b>1.00</b>	498	467	662	14.31	13.04	14.24	13.86	0.58
<b>80</b>	<b>1.33</b>	555	496	770	15.95	13.85	16.56	15.45	1.16
<b>100</b>	<b>1.67</b>	621	526	906	17.84	14.69	19.48	17.34	1.99
<b>120</b>	<b>2.00</b>	686	563	1028	19.71	15.73	22.11	19.18	2.63
<b>180</b>	<b>3.00</b>	862	646	1430	24.77	18.04	30.75	24.52	5.19
<b>240</b>	<b>4.00</b>	1029	741	1875	29.57	20.70	40.32	30.20	8.02
<b>360</b>	<b>6.00</b>	1204	923	2780	34.60	25.78	59.78	40.05	14.41
<b>720</b>	<b>12.00</b>	1685	1479	3590	48.42	41.31	77.20	55.65	15.52
<b>1440</b>	<b>24.00</b>	2190	2540	5080	62.93	70.95	109.25	81.04	20.21
<b>2880</b>	<b>48.00</b>	4420	3620	5140	127.01	101.12	110.54	112.89	10.70
<b>4320</b>	<b>72.00</b>	5100	5050	5520	146.55	141.06	118.71	135.44	12.04

SD = standard deviation

**Table C.16:** Percentage TEER normalised in regard to the initial TEER value ( $T_0$ ) in the presence of 1.5% w/v *Aloe vera* gel solutions

Time (min)	TEER value ( $\Omega$ )			Normalised % TEER			Average	SD
	Well 1	Well 2	Well 3	Well 1	Well 2	Well 3		
0	3790	3620	3850	100.00	100.00	100.00	100.00	0.00
20	1248	1075	1027	32.93	29.70	26.68	29.77	2.55
40	2200	1602	1656	58.05	44.25	43.01	48.44	6.81
60	2610	1980	2140	68.87	54.70	55.58	59.72	6.48
80	2680	2150	2460	70.71	59.39	63.90	64.67	4.65
100	2820	2380	2760	74.41	65.75	71.69	70.61	3.62
120	2900	2520	2880	76.52	69.61	74.81	73.65	2.94

SD = standard deviation

**Table C.17:** Percentage TEER reduction by 1.5% w/v *Aloe vera* gel solutions across Caco-2 cell monolayers

Time (min)	% TEER reduction			Average	SD
	Well 1	Well 2	Well 3		
0	0.00	0.00	0.00	0.00	0.00
20	67.07	70.30	73.32	70.23	2.55
40	41.95	55.75	56.99	51.56	6.81
60	31.13	45.30	44.42	40.28	6.48
80	29.29	40.61	36.10	35.33	4.65
100	25.59	34.25	28.31	29.39	3.62
120	23.48	30.39	25.19	26.35	2.94

SD = standard deviation

**Table C.18:** Percentage TEER recovery after 1.5% w/v *Aloe vera* gel solutions were removed (percentage is normalised in regard to the initial TEER value,  $T_0$ )

Time (min) after removal of test solution	Time (hr) after removal of test solution	TEER value ( $\Omega$ )			Normalised %			Average	SD
		Well 1	Well 2	Well 3	Well 1	Well 2	Well 3		
<b>0</b>	<b>0.00</b>	3790	3620	3850	100.00	100.00	100.00	100.00	0.00
<b>20</b>	<b>0.33</b>	577	446	619	15.22	12.32	16.08	14.54	1.61
<b>40</b>	<b>0.67</b>	800	529	711	21.11	14.61	18.47	18.06	2.67
<b>60</b>	<b>1.00</b>	1037	646	898	27.36	17.85	23.32	22.84	3.90
<b>80</b>	<b>1.33</b>	1196	760	1026	31.56	20.99	26.65	26.40	4.32
<b>100</b>	<b>1.67</b>	1386	900	1202	36.57	24.86	31.22	30.88	4.79
<b>120</b>	<b>2.00</b>	1608	1020	1372	42.43	28.18	35.64	35.41	5.82
<b>180</b>	<b>3.00</b>	2290	1444	1972	60.42	39.89	51.22	50.51	8.40
<b>240</b>	<b>4.00</b>	2780	1688	2270	73.35	46.63	58.96	59.65	10.92
<b>360</b>	<b>6.00</b>	3270	2190	2620	86.28	60.50	68.05	71.61	10.82
<b>720</b>	<b>12.00</b>	4060	3610	3160	107.12	99.72	82.08	96.31	10.51
<b>1440</b>	<b>24.00</b>	4520	4020	3500	119.26	111.05	90.91	107.07	11.91
<b>2880</b>	<b>48.00</b>	4890	4500	4040	129.02	124.31	104.94	119.42	10.42
<b>4320</b>	<b>72.00</b>	4660	4660	4220	122.96	128.73	109.61	120.43	8.01

SD = standard deviation

**Table C.19:** Percentage TEER normalised in regard to the initial TEER value ( $T_0$ ) in the presence of 0.1% w/v *Aloe vera* whole leaf extract solutions

Time (min)	TEER value ( $\Omega$ )			Normalised % TEER			Average	SD
	Well 1	Well 2	Well 3	Well 1	Well 2	Well 3		
0	4250	2720	3190	100.00	100.00	100.00	100.00	0.00
20	1062	1136	1508	24.99	41.76	47.27	38.01	9.48
40	1528	1583	1698	35.95	58.20	53.23	49.13	9.53
60	2030	1702	1849	47.76	62.57	57.96	56.10	6.19
80	2320	1751	1982	54.59	64.38	62.13	60.36	4.19
100	2810	1957	2370	66.12	71.95	74.29	70.79	3.44
120	3040	2020	2380	71.53	74.26	74.61	73.47	1.38

SD = standard deviation

**Table C.20:** Percentage TEER reduction by 0.1% w/v *Aloe vera* whole leaf extract solutions across Caco-2 cell monolayers

Time (min)	% TEER reduction			Average	SD
	Well 1	Well 2	Well 3		
0	0.00	0.00	0.00	0.00	0.00
20	75.01	58.24	52.73	61.99	9.48
40	64.05	41.80	46.77	50.87	9.53
60	52.24	37.43	42.04	43.90	6.19
80	45.41	35.63	37.87	39.64	4.19
100	33.88	28.05	25.71	29.21	3.44
120	28.47	25.74	25.39	26.53	1.38

SD = standard deviation

**Table C.21:** Percentage TEER recovery after 0.1% w/v *Aloe vera* whole leaf extract solutions were removed (percentage is normalised in regard to the initial TEER value,  $T_0$ )

Time (min) after removal of test solution	Time (hr) after removal of test solution	TEER value ( $\Omega$ )			Normalised %			Average	SD
		Well 1	Well 2	Well 3	Well 1	Well 2	Well 3		
<b>0</b>	<b>0.00</b>	4250	2720	3190	100.00	100.00	100.00	100.00	0.00
<b>20</b>	<b>0.33</b>	258	324	329	6.07	11.91	10.31	9.43	2.46
<b>40</b>	<b>0.67</b>	309	375	396	7.27	13.79	12.41	11.16	2.80
<b>60</b>	<b>1.00</b>	340	422	470	8.00	15.51	14.73	12.75	3.37
<b>80</b>	<b>1.33</b>	389	465	558	9.15	17.10	17.49	14.58	3.84
<b>100</b>	<b>1.67</b>	424	508	625	9.98	18.68	19.59	16.08	4.33
<b>120</b>	<b>2.00</b>	459	520	715	10.80	19.12	22.41	17.44	4.89
<b>180</b>	<b>3.00</b>	575	626	975	13.53	23.01	30.56	22.37	6.97
<b>240</b>	<b>4.00</b>	670	707	1237	15.76	25.99	38.78	26.84	9.41
<b>360</b>	<b>6.00</b>	842	870	1708	19.81	31.99	53.54	35.11	13.95
<b>720</b>	<b>12.00</b>	962	1069	2530	22.64	39.30	79.31	47.08	23.78
<b>1440</b>	<b>24.00</b>	1651	1418	3880	38.85	52.13	121.63	70.87	36.30
<b>2880</b>	<b>48.00</b>	4780	2800	3920	112.47	102.94	122.88	112.77	8.14
<b>4320</b>	<b>72.00</b>	5500	3230	4000	129.41	118.75	125.39	124.52	4.40

SD = standard deviation

**Table C.22:** Percentage TEER normalised in regard to the initial TEER value ( $T_0$ ) in the presence of 0.5% w/v *Aloe vera* whole leaf extract solutions

Time (min)	TEER value ( $\Omega$ )			Normalised % TEER			Average	SD
	Well 1	Well 2	Well 3	Well 1	Well 2	Well 3		
<b>0</b>	4410	3770	4600	100.00	100.00	100.00	100.00	0.00
<b>20</b>	1133	738	1012	25.69	19.58	22.00	22.42	2.51
<b>40</b>	1398	899	1147	31.70	23.85	24.93	26.83	3.47
<b>60</b>	1648	1138	1374	37.37	30.19	29.87	32.47	3.46
<b>80</b>	1755	1303	1515	39.80	34.56	32.93	35.76	2.93
<b>100</b>	1995	1653	1912	45.24	43.85	41.57	43.55	1.51
<b>120</b>	2030	1842	2070	46.03	48.86	45.00	46.63	1.63

SD = standard deviation

**Table C.23:** Percentage TEER reduction by 0.5% w/v *Aloe vera* whole leaf extract solutions across Caco-2 cell monolayers

Time (min)	% TEER reduction			Average	SD
	Well 1	Well 2	Well 3		
<b>0</b>	0.00	0.00	0.00	0.00	0.00
<b>20</b>	74.31	80.42	78.00	77.58	2.51
<b>40</b>	68.30	76.15	75.07	73.17	3.47
<b>60</b>	62.63	69.81	70.13	67.53	3.46
<b>80</b>	60.20	65.44	67.07	64.24	2.93
<b>100</b>	54.76	56.15	58.43	56.45	1.51
<b>120</b>	53.97	51.14	55.00	53.37	1.63

SD = standard deviation

**Table C.24:** Percentage TEER recovery after 0.5% w/v *Aloe vera* whole leaf extract solutions were removed (percentage is normalised in regard to the initial TEER value,  $T_0$ )

Time (min) after removal of test solution	Time (hr) after removal of test solution	TEER value ( $\Omega$ )			Normalised %			Average	SD
		Well 1	Well 2	Well 3	Well 1	Well 2	Well 3		
<b>0</b>	<b>0.00</b>	4410	3770	4600	100.00	100.00	100.00	100.00	0.00
<b>20</b>	<b>0.33</b>	808	307	310	18.32	8.14	6.74	11.07	5.16
<b>40</b>	<b>0.67</b>	1036	364	355	23.49	9.66	7.72	13.62	7.02
<b>60</b>	<b>1.00</b>	1218	421	446	27.62	11.17	9.70	16.16	8.12
<b>80</b>	<b>1.33</b>	1341	485	541	30.41	12.86	11.76	18.34	8.54
<b>100</b>	<b>1.67</b>	1469	558	657	33.31	14.80	14.28	20.80	8.85
<b>120</b>	<b>2.00</b>	1572	636	782	35.65	16.87	17.00	23.17	8.82
<b>180</b>	<b>3.00</b>	1844	933	1195	41.81	24.75	25.98	30.85	7.77
<b>240</b>	<b>4.00</b>	2080	1217	1568	47.17	32.28	34.09	37.84	6.63
<b>360</b>	<b>6.00</b>	2460	1724	2170	55.78	45.73	47.17	49.56	4.44
<b>720</b>	<b>12.00</b>	4310	3130	3160	97.73	83.02	68.70	83.15	11.85
<b>1440</b>	<b>24.00</b>	5140	4420	4310	116.55	117.24	93.70	109.16	10.94
<b>2880</b>	<b>48.00</b>	4460	4590	4620	101.13	121.75	100.43	107.77	9.89
<b>4320</b>	<b>72.00</b>	5220	4520	4910	118.37	119.89	106.74	115.00	5.87

SD = standard deviation

**Table C.25:** Percentage TEER normalised in regard to the initial TEER value ( $T_0$ ) in the presence of 1.0% w/v *Aloe vera* whole leaf extract solutions

Time (min)	TEER value ( $\Omega$ )			Normalised % TEER			Average	SD
	Well 1	Well 2	Well 3	Well 1	Well 2	Well 3		
<b>0</b>	3480	3980	3930	100.00	100.00	100.00	100.00	0.00
<b>20</b>	970	1234	1366	27.87	31.01	34.76	31.21	2.81
<b>40</b>	1359	1513	1844	39.05	38.02	46.92	41.33	3.98
<b>60</b>	1687	1979	2420	48.48	49.72	61.58	53.26	5.90
<b>80</b>	1836	2130	2460	52.76	53.52	62.60	56.29	4.47
<b>100</b>	1980	2360	2720	56.90	59.30	69.21	61.80	5.33
<b>120</b>	2090	2540	2840	60.06	63.82	72.26	65.38	5.10

SD = standard deviation

**Table C.26:** Percentage TEER reduction by 1.0% w/v *Aloe vera* whole leaf extract solutions across Caco-2 cell monolayers

Time (min)	% TEER reduction			Average	SD
	Well 1	Well 2	Well 3		
<b>0</b>	0.00	0.00	0.00	0.00	0.00
<b>20</b>	72.13	68.99	65.24	68.79	2.81
<b>40</b>	60.95	61.98	53.08	58.67	3.98
<b>60</b>	51.52	50.28	38.42	46.74	5.90
<b>80</b>	47.24	46.48	37.40	43.71	4.47
<b>100</b>	43.10	40.70	30.79	38.20	5.33
<b>120</b>	39.94	36.18	27.74	34.62	5.10

SD = standard deviation

**Table C.27:** Percentage TEER recovery after 1.0% w/v *Aloe vera* whole leaf extract solutions were removed (percentage is normalised in regard to the initial TEER value,  $T_0$ )

Time (min) after removal of test solution	Time (hr) after removal of test solution	TEER value ( $\Omega$ )			Normalised %			Average	SD
		Well 1	Well 2	Well 3	Well 1	Well 2	Well 3		
<b>0</b>	<b>0.00</b>	3480	3980	3930	100.00	100.00	100.00	100.00	0.00
<b>20</b>	<b>0.33</b>	722	1089	940	20.75	27.36	23.92	24.01	2.70
<b>40</b>	<b>0.67</b>	864	1497	1232	24.83	37.61	31.35	31.26	5.22
<b>60</b>	<b>1.00</b>	1044	1989	1735	30.00	49.97	44.15	41.37	8.39
<b>80</b>	<b>1.33</b>	1126	2290	1966	32.36	57.54	50.03	46.64	10.56
<b>100</b>	<b>1.67</b>	1258	2620	2380	36.15	65.83	60.56	54.18	12.93
<b>120</b>	<b>2.00</b>	1360	2750	2510	39.08	69.10	63.87	57.35	13.09
<b>180</b>	<b>3.00</b>	1591	2980	2900	45.72	74.87	73.79	64.79	13.50
<b>240</b>	<b>4.00</b>	1728	3190	3260	49.66	80.15	82.95	70.92	15.08
<b>360</b>	<b>6.00</b>	1979	3430	3630	56.87	86.18	92.37	78.47	15.48
<b>720</b>	<b>12.00</b>	2290	3960	3770	65.80	99.50	95.93	87.08	15.11
<b>1440</b>	<b>24.00</b>	2800	4530	4480	80.46	113.82	113.99	102.76	15.77
<b>2880</b>	<b>48.00</b>	3270	4580	4370	93.97	115.08	111.20	106.75	9.17
<b>4320</b>	<b>72.00</b>	5020	5500	5580	144.25	138.19	141.98	141.48	2.50

SD = standard deviation

**Table C.28:** Percentage TEER normalised in regard to the initial TEER value ( $T_0$ ) in the presence of 1.5% w/v *Aloe vera* whole leaf extract solutions

Time (min)	TEER value ( $\Omega$ )			Normalised % TEER			Average	SD
	Well 1	Well 2	Well 3	Well 1	Well 2	Well 3		
0	3380	4070	2950	100.00	100.00	100.00	100.00	0.00
20	715	750	767	21.15	18.43	26.00	21.86	3.13
40	1045	1072	1061	30.92	26.34	35.97	31.07	3.93
60	1402	1393	1350	41.48	34.23	45.76	40.49	4.76
80	1639	1617	1536	48.49	39.73	52.07	46.76	5.18
100	1822	1812	1727	53.91	44.52	58.54	52.32	5.83
120	1943	1930	1848	57.49	47.42	62.64	55.85	6.32

SD = standard deviation

**Table C.29:** Percentage TEER reduction by 1.5% w/v *Aloe vera* whole leaf extract solutions across Caco-2 cell monolayers

Time (min)	% TEER reduction			Average	SD
	Well 1	Well 2	Well 3		
0	0.00	0.00	0.00	0.00	0.00
20	78.85	81.57	74.00	78.14	3.13
40	69.08	73.66	64.03	68.93	3.93
60	58.52	65.77	54.24	59.51	4.76
80	51.51	60.27	47.93	53.24	5.18
100	46.09	55.48	41.46	47.68	5.83
120	42.51	52.58	37.36	44.15	6.32

SD = standard deviation

**Table C.30:** Percentage TEER recovery after 1.5% w/v *Aloe vera* whole leaf extract solutions were removed (percentage is normalised in regard to the initial TEER value,  $T_0$ )

Time (min) after removal of test solution	Time (hr) after removal of test solution	TEER value ( $\Omega$ )			Normalised %			Average	SD
		Well 1	Well 2	Well 3	Well 1	Well 2	Well 3		
<b>0</b>	<b>0.00</b>	3380	4070	2950	100.00	100.00	100.00	100.00	0.00
<b>20</b>	<b>0.33</b>	490	380	413	14.50	9.34	14.00	12.61	2.32
<b>40</b>	<b>0.67</b>	634	473	529	18.76	11.62	17.93	16.10	3.19
<b>60</b>	<b>1.00</b>	840	589	638	24.85	14.47	21.63	20.32	4.34
<b>80</b>	<b>1.33</b>	1056	698	750	31.24	17.15	25.42	24.61	5.78
<b>100</b>	<b>1.67</b>	1212	805	844	35.86	19.78	28.61	28.08	6.57
<b>120</b>	<b>2.00</b>	1380	908	950	40.83	22.31	32.20	31.78	7.57
<b>180</b>	<b>3.00</b>	1668	1205	1219	49.35	29.61	41.32	40.09	8.11
<b>240</b>	<b>4.00</b>	1760	1342	1318	52.07	32.97	44.68	43.24	7.86
<b>360</b>	<b>6.00</b>	2080	1644	1518	61.54	40.39	51.46	51.13	8.64
<b>720</b>	<b>12.00</b>	2460	2580	1820	72.78	63.39	61.69	65.96	4.88
<b>1440</b>	<b>24.00</b>	3230	3220	2680	95.56	79.12	90.85	88.51	6.92
<b>2880</b>	<b>48.00</b>	3980	3930	3040	117.75	96.56	103.05	105.79	8.87
<b>4320</b>	<b>72.00</b>	4250	4640	3170	125.74	114.00	107.46	115.73	7.56

SD = standard deviation

**Table C.31:** Average percentage TEER reduction at 20 min across Caco-2 cell monolayers for different concentrations *Aloe vera* gel and 0.5% w/v TMC solutions

Groups	Percentage TEER reduction			Average	SD
	Well 1	Well 2	Well 3		
<b>0.5% w/v TMC (Positive Control)</b>	73,44	73,59	66,91	71,31	3,12
<b>0,1% w/v <i>Aloe vera</i> gel</b>	82.07	79.31	85.11	82.16	2.37
<b>0,5% w/v <i>Aloe vera</i> gel</b>	72.50	75.22	81.23	76.31	3.65
<b>1,0% w/v <i>Aloe vera</i> gel</b>	72.24	78.94	86.19	79.12	5.70
<b>1,5% w/v <i>Aloe vera</i> gel</b>	67.07	70.30	73.32	70.23	2.55

SD = standard deviation

**Table C.32:** Average percentage TEER reduction at 20 min across Caco-2 cell monolayers for different concentrations *Aloe vera* whole leaf extract and 0.5% w/v TMC solutions

Groups	Percentage TEER reduction			Average	SD
	Well 1	Well 2	Well 3		
<b>0.5% w/v TMC (Positive Control)</b>	73,44	73,59	66,91	71,31	3,12
<b>0,1% w/v <i>Aloe vera</i> whole leaf extract</b>	75.01	58.24	52.73	61.99	9.48
<b>0,5% w/v <i>Aloe vera</i> whole leaf extract</b>	74.31	80.42	78.00	77.58	2.51
<b>1,0% w/v <i>Aloe vera</i> whole leaf extract</b>	72.13	68.99	65.24	68.79	2.81
<b>1,5% w/v <i>Aloe vera</i> whole leaf extract</b>	78.85	81.57	74.00	78.14	3.13

SD = standard deviation

## APPENDIX D

### ***IN VITRO* PERMEATION OF DIFFERENT MOLECULAR WEIGHT FITC- DEXTRANS ACROSS CACO-2 CELL MONOLAYERS**

---

**Table D.1:** TEER values before *in vitro* permeation study (as measure of intact Caco-2 cell monolayer,  $\geq 150 \Omega$ ; Alqahtani *et al.*, 2013:2)

Time (min)	TEER value ( $\Omega$ )		
	Well 1	Well 2	Well 3
Before ( $T_0$ )	380	377	382

**Table D.2:** Percentage cumulative transport of Lucifer yellow across Caco-2 cell monolayers and the calculated apparent permeability coefficient ( $P_{app}$ ) values

Time (min)	Percentage cumulative transport			Average	SD
	Well 1	Well 2	Well 3		
0	0,00	0,00	0,00	0,00	0,0000
20	0,99	1,16	1,10	1,08	0,0675
40	1,22	1,22	1,04	1,16	0,0864
60	1,21	1,28	1,30	1,27	0,0364
80	1,35	1,34	1,46	1,38	0,0526
100	1,47	1,48	1,43	1,46	0,0200
120	1,41	1,57	1,48	1,48	0,0653
<b>Slope</b>	0,009471	0,009756	0,009852	0,009693161	0,0001616
<b>1/A.60.C0</b>	$3,56888 \times 10^{-5}$				
<b><math>P_{app}</math></b>	$3,38 \times 10^{-7}$	$3,48 \times 10^{-7}$	$3,52 \times 10^{-7}$	$3,459 \times 10^{-7}$	$5,76809 \times 10^{-9}$

$P_{app}$  = Apparent permeability coefficient, SD = Standard deviation

**Table D.3:** TEER values (as indication of intact Caco-2 cell monolayer,  $\geq 150 \Omega$ ; Alqahtani *et al.*, 2013:2) before *in vitro* permeation study with FITC-dextran 4 000 Da in the presence of *Aloe vera* gel and whole leaf extract solutions with different concentrations

Groups	TEER value ( $\Omega$ )		
	Well 1	Well 2	Well 3
FD-4 Control	321	318	319
0.1% w/v <i>A. vera</i> gel	362	328	309
0.5% w/v <i>A. vera</i> gel	346	337	332
1.0% w/v <i>A. vera</i> gel	352	343	334
1.5% w/v <i>A. vera</i> gel	367	319	321
0.1% w/v <i>A. vera</i> whole leaf extract	344	348	342
0.5% w/v <i>A. vera</i> whole leaf extract	366	336	318
1.0% w/v <i>A. vera</i> whole leaf extract	353	327	315
1.5% w/v <i>A. vera</i> whole leaf extract	358	340	339

**Table D.4:** Percentage cumulative transport of FITC-dextran 4 000 Da without a permeation enhancer across Caco-2 cell monolayers (negative control)

Time (min)	Percentage cumulative transport			Average	SD
	Well 1	Well 2	Well 3		
0	0.00	0.00	0.00	0.00	0.0000
20	0.29	0.32	0.31	0.31	0.0135
40	0.33	0.44	0.36	0.38	0.0456
60	0.35	0.38	0.43	0.38	0.0323
80	0.38	0.42	0.48	0.43	0.0399
100	0.39	0.48	0.43	0.43	0.0349
120	0.39	0.47	0.49	0.45	0.0412

SD = Standard deviation

**Table D.5:** Percentage cumulative transport of FITC-dextran 4 000 Da in the presence of 0.1% w/v *Aloe vera* gel solutions

Time (min)	Percentage cumulative transport			Average	SD
	Well 1	Well 2	Well 3		
0	0.00	0.00	0.00	0.00	0.0000
20	0.45	0.42	0.46	0.44	0.0157
40	0.61	0.58	0.64	0.61	0.0260
60	0.69	0.65	0.73	0.69	0.0350
80	0.99	0.68	0.78	0.82	0.1319
100	0.95	0.78	0.87	0.86	0.0676
120	0.94	0.75	0.83	0.84	0.0787

SD = Standard deviation

**Table D.6:** Percentage cumulative transport of FITC-dextran 4 000 Da in the presence of 0.5% w/v *Aloe vera* gel solutions

Time (min)	Percentage cumulative transport			Average	SD
	Well 1	Well 2	Well 3		
0	0.00	0.00	0.00	0.00	0.0000
20	0.43	0.44	0.41	0.43	0.0124
40	0.58	0.61	0.61	0.60	0.0136
60	0.65	0.64	0.68	0.66	0.0141
80	0.75	0.73	0.74	0.74	0.0067
100	0.75	0.76	0.77	0.76	0.0104
120	0.86	0.74	0.87	0.82	0.0564

SD = Standard deviation

**Table D.7:** Percentage cumulative transport of FITC-dextran 4 000 Da in the presence of 1.0% w/v *Aloe vera* gel solutions

Time (min)	Percentage cumulative transport			Average	SD
	Well 1	Well 2	Well 3		
0	0.00	0.00	0.00	0.00	0.0000
20	0.40	0.38	0.39	0.39	0.0062
40	0.57	0.57	0.54	0.56	0.0162
60	0.60	0.60	0.71	0.64	0.0540
80	0.63	0.64	0.74	0.67	0.0482
100	0.73	0.78	0.86	0.79	0.0527
120	0.81	0.87	1.01	0.90	0.0842

SD = Standard deviation

**Table D.8:** Percentage cumulative transport of FITC-dextran 4 000 Da in the presence of 1.5% w/v *Aloe vera* gel solutions

Time (min)	Percentage cumulative transport			Average	SD
	Well 1	Well 2	Well 3		
0	0.00	0.00	0.00	0.00	0.0000
20	0.40	0.36	0.36	0.37	0.0195
40	0.62	0.51	0.52	0.55	0.0486
60	0.74	0.62	0.66	0.68	0.0491
80	0.80	0.67	0.75	0.74	0.0527
100	0.88	0.73	0.83	0.81	0.0591
120	1.00	0.86	0.98	0.95	0.0608

SD = Standard deviation

**Table D.9:** Apparent permeability coefficient ( $P_{app}$ ) values of FITC-dextran (4 000 Da) applied with different concentrations *Aloe vera* gel solutions

Groups	$P_{app}$ values			Average	SD	p-value
	Well 1	Well 2	Well 3			
<b>FD-4 Control</b>	$9.14 \times 10^{-8}$	$1.09 \times 10^{-7}$	$1.16 \times 10^{-7}$	$1.05 \times 10^{-7}$	$1.02 \times 10^{-8}$	-
<b>0.1% w/v <i>A. vera</i> gel</b>	$2.68 \times 10^{-7}$	$1.96 \times 10^{-7}$	$2.20 \times 10^{-7}$	$2.28 \times 10^{-7}$	$3.00 \times 10^{-8}$	<b>0.001176*</b>
<b>0.5% w/v <i>A. vera</i> gel</b>	$2.16 \times 10^{-7}$	$1.91 \times 10^{-7}$	$2.20 \times 10^{-7}$	$2.09 \times 10^{-7}$	$1.29 \times 10^{-8}$	<b>0.005582*</b>
<b>1.0% w/v <i>A. vera</i> gel</b>	$2.02 \times 10^{-7}$	$2.21 \times 10^{-7}$	$2.67 \times 10^{-7}$	$2.30 \times 10^{-7}$	$2.72 \times 10^{-8}$	<b>0.000995*</b>
<b>1.5% w/v <i>A. vera</i> gel</b>	$2.63 \times 10^{-7}$	$2.23 \times 10^{-7}$	$2.61 \times 10^{-7}$	$2.49 \times 10^{-7}$	$1.86 \times 10^{-8}$	<b>0.000239*</b>

$P_{app}$  = Apparent permeability coefficient, SD = Standard deviation

Asterisk (\*) indicates statistical significant difference when compared to the negative control ( $p \leq 0.05$ )

**Table D.10:** Percentage cumulative transport of FITC-dextran 4 000 Da in the presence of 0.1% w/v *Aloe vera* whole leaf extract solutions

Time (min)	Percentage cumulative transport			Average	SD
	Well 1	Well 2	Well 3		
0	0.00	0.00	0.00	0.00	0.0000
20	0.45	0.45	0.43	0.44	0.0110
40	0.70	0.67	0.70	0.69	0.0140
60	0.85	0.76	0.76	0.79	0.0403
80	0.86	0.85	0.83	0.84	0.0112
100	0.95	0.88	0.90	0.91	0.0321
120	0.89	0.90	0.86	0.88	0.0194

SD = Standard deviation

**Table D.11:** Percentage cumulative transport of FITC-dextran 4 000 Da in the presence of 0.5% w/v *Aloe vera* whole leaf extract solutions

Time (min)	Percentage cumulative transport			Average	SD
	Well 1	Well 2	Well 3		
0	0.00	0.00	0.00	0.00	0.0000
20	0.44	0.56	0.42	0.47	0.0599
40	0.64	0.75	0.61	0.66	0.0641
60	0.66	0.80	0.63	0.70	0.0728
80	0.78	0.76	0.73	0.76	0.0207
100	0.75	1.00	0.73	0.83	0.1201
120	0.86	1.10	0.78	0.91	0.1330

SD = Standard deviation

**Table D.12:** Percentage cumulative transport of FITC-dextran 4 000 Da in the presence of 1.0% w/v *Aloe vera* whole leaf extract solutions

Time (min)	Percentage cumulative transport			Average	SD
	Well 1	Well 2	Well 3		
0	0.00	0.00	0.00	0.00	0.0000
20	0.43	0.40	0.40	0.41	0.0158
40	0.63	0.56	0.56	0.58	0.0296
60	0.71	0.65	0.64	0.67	0.0309
80	0.75	0.69	0.72	0.72	0.0270
100	0.85	0.78	0.85	0.83	0.0348
120	0.93	0.86	0.91	0.90	0.0309

SD = Standard deviation

**Table D.13:** Percentage cumulative transport of FITC-dextran 4 000 Da in the presence of 1.5% w/v *Aloe vera* whole leaf extract solutions

Time (min)	Percentage cumulative transport			Average	SD
	Well 1	Well 2	Well 3		
0	0.00	0.00	0.00	0.00	0.0000
20	0.45	0.39	0.45	0.43	0.0276
40	0.70	0.57	0.67	0.64	0.0539
60	0.84	0.67	0.83	0.78	0.0804
80	1.03	0.79	1.01	0.94	0.1060
100	1.18	0.86	1.12	1.05	0.1417
120	1.40	0.95	1.25	1.20	0.1858

SD = Standard deviation

**Table D.14:** Apparent permeability coefficient ( $P_{app}$ ) values of FITC-dextran (4 000 Da) applied with different concentrations *Aloe vera* whole leaf extract solutions

Groups	$P_{app}$ values			Average	SD	p-value
	Well 1	Well 2	Well 3			
<b>FD-4 Control</b>	$9.14 \times 10^{-8}$	$1.09 \times 10^{-7}$	$1.16 \times 10^{-7}$	$1.05 \times 10^{-7}$	$1.02 \times 10^{-8}$	-
<b>0.1% w/v <i>A. vera</i> whole leaf extract</b>	$2.45 \times 10^{-7}$	$2.38 \times 10^{-7}$	$2.32 \times 10^{-7}$	$2.38 \times 10^{-7}$	$5.20 \times 10^{-9}$	0.000522*
<b>0.5% w/v <i>A. vera</i> whole leaf extract</b>	$2.13 \times 10^{-7}$	$2.66 \times 10^{-7}$	$1.98 \times 10^{-7}$	$2.26 \times 10^{-7}$	$2.92 \times 10^{-8}$	0.001375*
<b>1.0% w/v <i>A. vera</i> whole leaf extract</b>	$2.39 \times 10^{-7}$	$2.20 \times 10^{-7}$	$2.42 \times 10^{-7}$	$2.34 \times 10^{-7}$	$9.66 \times 10^{-9}$	0.000727*
<b>1.5% w/v <i>A. vera</i> whole leaf extract</b>	$3.81 \times 10^{-7}$	$2.55 \times 10^{-7}$	$3.46 \times 10^{-7}$	$3.27 \times 10^{-7}$	$5.32 \times 10^{-8}$	0.000035*

$P_{app}$  = Apparent permeability coefficient, SD = Standard deviation

Asterisk (\*) indicates statistically significant difference when compared to the negative control ( $p \leq 0.05$ )

**Table D.15:** TEER values (as indication of intact Caco-2 cell monolayer,  $\geq 150 \Omega$ ; Alqahtani *et al.*, 2013:2) before *in vitro* permeation study with FITC-dextran 10 000 Da in the presence of *Aloe vera* gel and whole leaf extract solutions with different concentrations

Groups	TEER value ( $\Omega$ )		
	Well 1	Well 2	Well 3
FD-10 Control	305	306	288
0.1% w/v <i>A. vera</i> gel	378	370	362
0.5% w/v <i>A. vera</i> gel	381	343	374
1.0% w/v <i>A. vera</i> gel	315	348	323
1.5% w/v <i>A. vera</i> gel	307	303	300
0.1% w/v <i>A. vera</i> whole leaf extract	368	352	348
0.5% w/v <i>A. vera</i> whole leaf extract	370	377	363
1.0% w/v <i>A. vera</i> whole leaf extract	296	303	311
1.5% w/v <i>A. vera</i> whole leaf extract	313	300	295

**Table D.16:** Percentage cumulative transport of FITC-dextran 10 000 Da without a permeation enhancer across Caco-2 cell monolayers (negative control)

Time (min)	Percentage cumulative transport			Average	SD
	Well 1	Well 2	Well 3		
0	0.00	0.00	0.00	0.00	0.0000
20	0.19	0.20	0.20	0.19	0.0062
40	0.22	0.25	0.29	0.25	0.0264
60	0.29	0.28	0.28	0.28	0.0060
80	0.28	0.30	0.32	0.30	0.0164
100	0.28	0.31	0.33	0.31	0.0228
120	0.27	0.38	0.32	0.32	0.0442

SD = Standard deviation

**Table D.17:** Percentage cumulative transport of FITC-dextran 10 000 Da in the presence of 0.1% w/v *Aloe vera* gel solutions

Time (min)	Percentage cumulative transport			Average	SD
	Well 1	Well 2	Well 3		
0	0.00	0.00	0.00	0.00	0.0000
20	0.21	0.18	0.18	0.19	0.0180
40	0.27	0.26	0.26	0.26	0.0061
60	0.28	0.29	0.28	0.29	0.0050
80	0.30	0.30	0.30	0.30	0.0043
100	0.31	0.34	0.32	0.32	0.0125
120	0.31	0.35	0.33	0.33	0.0155

SD = Standard deviation

**Table D.18:** Percentage cumulative transport of FITC-dextran 10 000 Da in the presence of 0.5% w/v *Aloe vera* gel solutions

Time (min)	Percentage cumulative transport			Average	SD
	Well 1	Well 2	Well 3		
0	0.00	0.00	0.00	0.00	0.0000
20	0.22	0.22	0.22	0.22	0.0025
40	0.30	0.30	0.35	0.32	0.0218
60	0.31	0.32	0.34	0.33	0.0121
80	0.32	0.33	0.36	0.34	0.0187
100	0.33	0.33	0.35	0.34	0.0110
120	0.34	0.35	0.37	0.35	0.0101

SD = Standard deviation

**Table D.19:** Percentage cumulative transport of FITC-dextran 10 000 Da in the presence of 1.0% w/v *Aloe vera* gel solutions

Time (min)	Percentage cumulative transport			Average	SD
	Well 1	Well 2	Well 3		
0	0.00	0.00	0.00	0.00	0.0000
20	0.19	0.18	0.18	0.18	0.0079
40	0.21	0.22	0.21	0.21	0.0042
60	0.26	0.25	0.23	0.25	0.0132
80	0.27	0.34	0.25	0.29	0.0398
100	0.27	0.33	0.25	0.28	0.0357
120	0.28	0.29	0.26	0.28	0.0102

SD = Standard deviation

**Table D.20:** Percentage cumulative transport of FITC-dextran 10 000 Da in the presence of 1.5% w/v *Aloe vera* gel solutions

Time (min)	Percentage cumulative transport			Average	SD
	Well 1	Well 2	Well 3		
0	0.00	0.00	0.00	0.00	0.0000
20	0.25	0.16	0.17	0.19	0.0382
40	0.29	0.19	0.20	0.23	0.0470
60	0.31	0.20	0.23	0.25	0.0467
80	0.30	0.20	0.23	0.24	0.0414
100	0.30	0.21	0.24	0.25	0.0377
120	0.32	0.22	0.26	0.27	0.0410

SD = Standard deviation

**Table D.21:** Apparent permeability coefficient ( $P_{app}$ ) values of FITC-dextran (10 000 Da) applied with different concentrations *Aloe vera* gel solutions

Groups	$P_{app}$ values			Average	SD	p-value
	Well 1	Well 2	Well 3			
<b>FD-10 Control</b>	$6.66 \times 10^{-8}$	$9.03 \times 10^{-8}$	$8.05 \times 10^{-8}$	$7.91 \times 10^{-8}$	$9.74 \times 10^{-9}$	-
<b>0.1% w/v <i>A. vera</i> gel</b>	$7.27 \times 10^{-8}$	$8.99 \times 10^{-8}$	$8.54 \times 10^{-8}$	$8.27 \times 10^{-8}$	$7.27 \times 10^{-9}$	0.99785
<b>0.5% w/v <i>A. vera</i> gel</b>	$7.97 \times 10^{-8}$	$8.40 \times 10^{-8}$	$8.73 \times 10^{-8}$	$8.37 \times 10^{-8}$	$3.08 \times 10^{-9}$	0.98993
<b>1.0% w/v <i>A. vera</i> gel</b>	$6.64 \times 10^{-8}$	$8.26 \times 10^{-8}$	$6.20 \times 10^{-8}$	$7.03 \times 10^{-8}$	$8.86 \times 10^{-9}$	0.77157
<b>1.5% w/v <i>A. vera</i> gel</b>	$6.82 \times 10^{-8}$	$4.89 \times 10^{-8}$	$5.95 \times 10^{-8}$	$5.88 \times 10^{-8}$	$7.87 \times 10^{-9}$	0.07384

$P_{app}$  = Apparent permeability coefficient, SD = Standard deviation

Asterisk (\*) indicates statistical significant difference when compared to the negative control ( $p \leq 0.05$ )

**Table D.22:** Percentage cumulative transport of FITC-dextran 10 000 Da in the presence of 0.1% w/v *Aloe vera* whole leaf extract solutions

Time (min)	Percentage cumulative transport			Average	SD
	Well 1	Well 2	Well 3		
0	0.00	0.00	0.00	0.00	0.0000
20	0.24	0.22	0.24	0.23	0.0083
40	0.32	0.29	0.30	0.30	0.0115
60	0.32	0.31	0.31	0.31	0.0076
80	0.35	0.32	0.34	0.33	0.0107
100	0.37	0.34	0.36	0.35	0.0098
120	0.39	0.36	0.37	0.37	0.0150

SD = Standard deviation

**Table D.23:** Percentage cumulative transport of FITC-dextran 10 000 Da in the presence of 0.5% w/v *Aloe vera* whole leaf extract solutions

Time (min)	Percentage cumulative transport			Average	SD
	Well 1	Well 2	Well 3		
0	0.00	0.00	0.00	0.00	0.0000
20	0.25	0.25	0.22	0.24	0.0154
40	0.32	0.33	0.28	0.31	0.0227
60	0.33	0.35	0.30	0.33	0.0194
80	0.34	0.37	0.31	0.34	0.0249
100	0.36	0.38	0.32	0.35	0.0254
120	0.38	0.41	0.34	0.38	0.0317

SD = Standard deviation

**Table D.24:** Percentage cumulative transport of FITC-dextran 10 000 Da in the presence of 1.0% w/v *Aloe vera* whole leaf extract solutions

Time (min)	Percentage cumulative transport			Average	SD
	Well 1	Well 2	Well 3		
0	0.00	0.00	0.00	0.00	0.0000
20	0.21	0.20	0.18	0.19	0.0097
40	0.26	0.24	0.21	0.24	0.0210
60	0.28	0.27	0.25	0.27	0.0090
80	0.30	0.31	0.25	0.29	0.0265
100	0.32	0.31	0.24	0.29	0.0362
120	0.35	0.33	0.26	0.32	0.0377

SD = Standard deviation

**Table D.25:** Percentage cumulative transport of FITC-dextran 10 000 Da in the presence of 1.5% w/v *Aloe vera* whole leaf extract solutions

Time (min)	Percentage cumulative transport			Average	SD
	Well 1	Well 2	Well 3		
0	0.00	0.00	0.00	0.00	0.0000
20	0.13	0.13	0.12	0.13	0.0034
40	0.16	0.16	0.14	0.15	0.0061
60	0.17	0.19	0.18	0.18	0.0091
80	0.18	0.19	0.18	0.19	0.0039
100	0.19	0.19	0.20	0.19	0.0045
120	0.21	0.20	0.20	0.21	0.0070

SD = Standard deviation

**Table D.26:** Apparent permeability coefficient ( $P_{app}$ ) values of FITC-dextran (10 000 Da) applied with different concentrations *Aloe vera* whole leaf extract solutions

Groups	$P_{app}$ values			Average	SD	p-value
	Well 1	Well 2	Well 3			
<b>FD-10 Control</b>	$6.66 \times 10^{-8}$	$9.03 \times 10^{-8}$	$8.05 \times 10^{-8}$	$7.91 \times 10^{-8}$	$9.74 \times 10^{-9}$	
<b>0.1% w/v <i>A. vera</i> whole leaf extract</b>	$9.37 \times 10^{-8}$	$8.58 \times 10^{-8}$	$8.76 \times 10^{-8}$	$8.90 \times 10^{-8}$	$3.35 \times 10^{-9}$	0.66819
<b>0.5% w/v <i>A. vera</i> whole leaf extract</b>	$8.78 \times 10^{-8}$	$9.77 \times 10^{-8}$	$7.87 \times 10^{-8}$	$8.81 \times 10^{-8}$	$7.74 \times 10^{-9}$	0.75815
<b>1.0% w/v <i>A. vera</i> whole leaf extract</b>	$8.36 \times 10^{-8}$	$8.29 \times 10^{-8}$	$5.98 \times 10^{-8}$	$7.54 \times 10^{-8}$	$1.11 \times 10^{-9}$	0.99717
<b>1.5% w/v <i>A. vera</i> whole leaf extract</b>	$5.03 \times 10^{-8}$	$4.77 \times 10^{-8}$	$5.13 \times 10^{-8}$	$4.97 \times 10^{-8}$	$1.53 \times 10^{-9}$	<b>0.00578*</b>

$P_{app}$  = Apparent permeability coefficient, SD = Standard deviation

Asterisk (\*) indicates statistical significant difference when compared to the negative control ( $p \leq 0.05$ )

**Table D.27:** TEER values (as indication of intact Caco-2 cell monolayer,  $\geq 150 \Omega$ ; Alqahtani *et al.*, 2013:2) before *in vitro* permeation study with FITC-dextran 20 000 Da in the presence of *Aloe vera* gel and whole leaf extract solutions with different concentrations

Groups	TEER value ( $\Omega$ )		
	Well 1	Well 2	Well 3
<b>FD-20 Control</b>	337	328	332
<b>0.1% w/v <i>A. vera</i> gel</b>	414	405	457
<b>0.5% w/v <i>A. vera</i> gel</b>	400	383	438
<b>1.0% w/v <i>A. vera</i> gel</b>	359	347	378
<b>1.5% w/v <i>A. vera</i> gel</b>	361	315	346
<b>0.1% w/v <i>A. vera</i> whole leaf extract</b>	408	379	402
<b>1.0% w/v <i>A. vera</i> whole leaf extract</b>	373	350	352
<b>1.5% w/v <i>A. vera</i> whole leaf extract</b>	375	338	351

**Table D.28:** Percentage cumulative transport of FITC-dextran 20 000 Da without a permeation enhancer across Caco-2 cell monolayers (negative control)

Time (min)	Percentage cumulative transport			Average	SD
	Well 1	Well 2	Well 3		
0	0.00	0.00	0.00	0.00	0.0000
20	0.15	0.16	0.16	0.16	0.0077
40	0.19	0.30	0.23	0.24	0.0463
60	0.24	0.39	0.31	0.31	0.0620
80	0.26	0.38	0.28	0.31	0.0548
100	0.28	0.43	0.30	0.34	0.0659
120	0.28	0.51	0.32	0.37	0.1010

SD = Standard deviation

**Table D.29:** Percentage cumulative transport of FITC-dextran 20 000 Da in the presence of 0.1% w/v *Aloe vera* gel solutions

Time (min)	Percentage cumulative transport			Average	SD
	Well 1	Well 2	Well 3		
0	0.00	0.00	0.00	0.00	0.0000
20	0.19	0.18	0.19	0.19	0.0054
40	0.27	0.27	0.23	0.26	0.0198
60	0.28	0.28	0.24	0.27	0.0169
80	0.30	0.31	0.25	0.29	0.0251
100	0.32	0.34	0.25	0.31	0.0380
120	0.34	0.31	0.26	0.30	0.0327

SD = Standard deviation

**Table D.30:** Percentage cumulative transport of FITC-dextran 20 000 Da in the presence of 0.5% w/v *Aloe vera* gel solutions

Time (min)	Percentage cumulative transport			Average	SD
	Well 1	Well 2	Well 3		
0	0.00	0.00	0.00	0.00	0.0000
20	0.18	0.17	0.20	0.18	0.0107
40	0.22	0.22	0.24	0.23	0.0079
60	0.24	0.23	0.25	0.24	0.0070
80	0.25	0.24	0.25	0.25	0.0067
100	0.27	0.26	0.25	0.26	0.0072
120	0.32	0.36	0.36	0.35	0.0195

SD = Standard deviation

**Table D.31:** Percentage cumulative transport of FITC-dextran 20 000 Da in the presence of 1.0% w/v *Aloe vera* gel solutions

Time (min)	Percentage cumulative transport			Average	SD
	Well 1	Well 2	Well 3		
0	0.00	0.00	0.00	0.00	0.0000
20	0.15	0.18	0.19	0.17	0.0160
40	0.19	0.21	0.22	0.21	0.0135
60	0.19	0.22	0.23	0.21	0.0183
80	0.19	0.24	0.24	0.22	0.0210
100	0.20	0.24	0.24	0.23	0.0187
120	0.21	0.25	0.26	0.24	0.0199

SD = Standard deviation

**Table D.32:** Percentage cumulative transport of FITC-dextran 20 000 Da in the presence of 1.5% w/v *Aloe vera* gel solutions

Time (min)	Percentage cumulative transport			Average	SD
	Well 1	Well 2	Well 3		
0	0.00	0.00	0.00	0.00	0.0000
20	0.14	0.19	0.18	0.17	0.0221
40	0.17	0.22	0.22	0.20	0.0236
60	0.18	0.25	0.23	0.22	0.0293
80	0.18	0.26	0.23	0.22	0.0305
100	0.19	0.27	0.24	0.23	0.0344
120	0.19	0.28	0.24	0.24	0.0348

SD = Standard deviation

**Table D.33:** Apparent permeability coefficient ( $P_{app}$ ) values of FITC-dextran (20 000 Da) applied with different concentrations *Aloe vera* gel solutions

Groups	$P_{app}$ values			Average	SD	p-value
	Well 1	Well 2	Well 3			
<b>FD-20 Control</b>	$7.53 \times 10^{-8}$	$1.37 \times 10^{-7}$	$8.13 \times 10^{-8}$	$9.80 \times 10^{-8}$	$2.79 \times 10^{-8}$	-
<b>0.1% w/v <i>A. vera</i> gel</b>	$8.27 \times 10^{-8}$	$8.21 \times 10^{-8}$	$5.84 \times 10^{-8}$	$7.44 \times 10^{-8}$	$1.13 \times 10^{-8}$	0.89679
<b>0.5% w/v <i>A. vera</i> gel</b>	$7.40 \times 10^{-8}$	$8.04 \times 10^{-8}$	$7.69 \times 10^{-8}$	$7.71 \times 10^{-8}$	$2.64 \times 10^{-9}$	0.94003
<b>1.0% w/v <i>A. vera</i> gel</b>	$4.61 \times 10^{-8}$	$5.57 \times 10^{-8}$	$5.63 \times 10^{-8}$	$5.27 \times 10^{-8}$	$4.69 \times 10^{-9}$	0.35057
<b>1.5% w/v <i>A. vera</i> gel</b>	$4.35 \times 10^{-8}$	$6.54 \times 10^{-8}$	$5.30 \times 10^{-8}$	$5.39 \times 10^{-8}$	$8.97 \times 10^{-9}$	0.37853

$P_{app}$  = Apparent permeability coefficient, SD = Standard deviation

Asterisk (\*) indicates statistical significant difference when compared to the negative control ( $p \leq 0.05$ )

**Table D.34:** Percentage cumulative transport of FITC-dextran 20 000 Da in the presence of 0.1% w/v *Aloe vera* whole leaf extract solutions

Time (min)	Percentage cumulative transport			Average	SD
	Well 1	Well 2	Well 3		
0	0,00	0,00	0,00	0,00	0,0000
20	0,15	0,18	0,19	0,17	0,0174
40	0,21	0,23	0,26	0,23	0,0202
60	0,22	0,25	0,27	0,25	0,0212
80	0,24	0,27	0,29	0,26	0,0209
100	0,25	0,28	0,29	0,27	0,0186
120	0,26	0,29	0,51	0,35	0,1155

SD = Standard deviation

**Table D.35:** Percentage cumulative transport of FITC-dextran 20 000 Da in the presence of 1.0% w/v *Aloe vera* whole leaf extract solutions

Time (min)	Percentage cumulative transport			Average	SD
	Well 1	Well 2	Well 3		
0	0.00	0.00	0.00	0.00	0.0000
20	0.19	0.19	0.19	0.19	0.0018
40	0.22	0.23	0.23	0.23	0.0028
60	0.24	0.24	0.24	0.24	0.0043
80	0.24	0.26	0.26	0.25	0.0079
100	0.24	0.26	0.27	0.26	0.0128
120	0.25	0.27	0.27	0.26	0.0092

SD = Standard deviation

**Table D.36:** Percentage cumulative transport of FITC-dextran 20 000 Da in the presence of 1.5% w/v *Aloe vera* whole leaf extract solutions

Time (min)	Percentage cumulative transport			Average	SD
	Well 1	Well 2	Well 3		
0	0.00	0.00	0.00	0.00	0.0000
20	0.16	0.15	0.15	0.15	0.0037
40	0.20	0.18	0.18	0.19	0.0087
60	0.20	0.21	0.19	0.20	0.0074
80	0.20	0.21	0.20	0.20	0.0051
100	0.20	0.21	0.18	0.20	0.0099
120	0.19	0.21	0.19	0.20	0.0077

SD = Standard deviation

**Table D.37:** Apparent permeability coefficient ( $P_{app}$ ) values of FITC-dextran (20 000 Da) applied with different concentrations *Aloe vera* whole leaf extract solutions

Groups	$P_{app}$ values			Average	SD	p-value
	Well 1	Well 2	Well 3			
<b>FD-20 Control</b>	$7.53 \times 10^{-8}$	$1.37 \times 10^{-7}$	$8.13 \times 10^{-8}$	$9.80 \times 10^{-8}$	$2.79 \times 10^{-8}$	-
<b>0.1% w/v <i>A. vera</i> whole leaf extract</b>	$6.37 \times 10^{-8}$	$6.95 \times 10^{-8}$	$1.14 \times 10^{-8}$	$8.23 \times 10^{-8}$	$2.23 \times 10^{-8}$	0.98685
<b>1.0% w/v <i>A. vera</i> whole leaf extract</b>	$5.59 \times 10^{-8}$	$6.26 \times 10^{-8}$	$6.44 \times 10^{-8}$	$6.09 \times 10^{-8}$	$3.66 \times 10^{-9}$	0.55296
<b>1.5% w/v <i>A. vera</i> whole leaf extract</b>	$4.30 \times 10^{-8}$	$4.77 \times 10^{-8}$	$4.19 \times 10^{-8}$	$4.42 \times 10^{-8}$	$2.51 \times 10^{-9}$	0.20117

$P_{app}$  = Apparent permeability coefficient, SD = Standard deviation

Asterisk (\*) indicates statistically significant difference when compared to the negative control ( $p \leq 0.05$ )

**Table D.38:** TEER values (as indication of intact Caco-2 cell monolayer,  $\geq 150 \Omega$ ; Alqahtani *et al.*, 2013:2) before *in vitro* permeation study with FITC-dextran 40 000 Da in the presence of *Aloe vera* gel and whole leaf extract solutions with different concentrations

Groups	TEER value ( $\Omega$ )		
	Well 1	Well 2	Well 3
<b>FD-40 Control</b>	355	338	334
<b>0.1% w/v <i>A. vera</i> gel</b>	427	405	426
<b>0.5% w/v <i>A. vera</i> gel</b>	373	355	381
<b>1.0% w/v <i>A. vera</i> gel</b>	416	423	430
<b>1.5% w/v <i>A. vera</i> gel</b>	406	368	423
<b>0.1% w/v <i>A. vera</i> whole leaf extract</b>	416	426	421
<b>0.5% w/v <i>A. vera</i> whole leaf extract</b>	381	379	382
<b>1.0% w/v <i>A. vera</i> whole leaf extract</b>	427	378	429
<b>1.5% w/v <i>A. vera</i> whole leaf extract</b>	422	404	421

**Table D.39:** Percentage cumulative transport of FITC-dextran 40 000 Da without a permeation enhancer across Caco-2 cell monolayers (negative control)

Time (min)	Percentage cumulative transport			Average	SD
	Well 1	Well 2	Well 3		
0	0.00	0.00	0.00	0.00	0.0000
20	0.18	0.19	0.18	0.19	0.0054
40	0.23	0.21	0.24	0.22	0.0120
60	0.24	0.26	0.27	0.26	0.0117
80	0.24	0.26	0.26	0.26	0.0096
100	0.25	0.28	0.27	0.27	0.0099
120	0.26	0.27	0.26	0.27	0.0068

SD = Standard deviation

**Table D.40:** Percentage cumulative transport of FITC-dextran 40 000 Da in the presence of 0.1% w/v *Aloe vera* gel solutions

Time (min)	Percentage cumulative transport			Average	SD
	Well 1	Well 2	Well 3		
0	0,00	0,00	0,00	0,00	0,0000
20	0,17	0,18	0,19	0,18	0,0099
40	0,21	0,22	0,22	0,22	0,0039
60	0,23	0,23	0,23	0,23	0,0030
80	0,24	0,24	0,23	0,24	0,0044
100	0,25	0,26	0,24	0,25	0,0092
120	0,25	0,25	0,25	0,25	0,0034

SD = Standard deviation

**Table D.41:** Percentage cumulative transport of FITC-dextran 40 000 Da in the presence of 0.5% w/v *Aloe vera* gel solutions

Time (min)	Percentage cumulative transport			Average	SD
	Well 1	Well 2	Well 3		
0	0.00	0.00	0.00	0.00	0.0000
20	0.19	0.19	0.19	0.19	0.0017
40	0.23	0.21	0.23	0.22	0.0109
60	0.24	0.25	0.24	0.24	0.0056
80	0.27	0.27	0.26	0.26	0.0039
100	0.29	0.27	0.27	0.28	0.0080
120	0.28	0.28	0.27	0.27	0.0045

SD = Standard deviation

**Table D.42:** Percentage cumulative transport of FITC-dextran 40 000 Da in the presence of 1.0% w/v *Aloe vera* gel solutions

Time (min)	Percentage cumulative transport			Average	SD
	Well 1	Well 2	Well 3		
0	0.00	0.00	0.00	0.00	0.0000
20	0.21	0.20	0.19	0.20	0.0076
40	0.25	0.24	0.23	0.24	0.0088
60	0.25	0.25	0.23	0.24	0.0079
80	0.27	0.26	0.25	0.26	0.0094
100	0.27	0.27	0.24	0.26	0.0125
120	0.28	0.27	0.25	0.27	0.0130

SD = Standard deviation

**Table D.43:** Percentage cumulative transport of FITC-dextran 40 000 Da in the presence of 1.5% w/v *Aloe vera* gel solutions

Time (min)	Percentage cumulative transport			Average	SD
	Well 1	Well 2	Well 3		
0	0.00	0.00	0.00	0.00	0.0000
20	0.19	0.18	0.18	0.18	0.0053
40	0.23	0.22	0.21	0.22	0.0049
60	0.24	0.25	0.23	0.24	0.0059
80	0.24	0.26	0.23	0.25	0.0121
100	0.26	0.28	0.24	0.26	0.0181
120	0.36	0.30	0.24	0.30	0.0495

SD = Standard deviation

**Table D.44:** Apparent permeability coefficient ( $P_{app}$ ) values of FITC-dextran (40 000 Da) applied with different concentrations *Aloe vera* gel solutions

Groups	$P_{app}$ values			Average	SD	p-value
	Well 1	Well 2	Well 3			
<b>FD-40 Control</b>	$5.93 \times 10^{-8}$	$6.66 \times 10^{-8}$	$6.32 \times 10^{-8}$	$6.30 \times 10^{-8}$	$3.02 \times 10^{-9}$	-
<b>0.1% w/v <i>A. vera</i> gel</b>	$6.15 \times 10^{-8}$	$5.98 \times 10^{-8}$	$5.48 \times 10^{-8}$	$5.87 \times 10^{-8}$	$2.86 \times 10^{-9}$	0.90153
<b>0.5% w/v <i>A. vera</i> gel</b>	$6.79 \times 10^{-8}$	$6.64 \times 10^{-8}$	$6.31 \times 10^{-8}$	$6.58 \times 10^{-8}$	$2.02 \times 10^{-9}$	0.99065
<b>1.0% w/v <i>A. vera</i> gel</b>	$6.25 \times 10^{-8}$	$6.36 \times 10^{-8}$	$5.61 \times 10^{-8}$	$6.07 \times 10^{-8}$	$3.28 \times 10^{-9}$	0.99695
<b>1.5% w/v <i>A. vera</i> gel</b>	$7.86 \times 10^{-8}$	$7.28 \times 10^{-8}$	$5.45 \times 10^{-8}$	$6.86 \times 10^{-8}$	$1.03 \times 10^{-8}$	0.75162

$P_{app}$  = Apparent permeability coefficient, SD = Standard deviation

Asterisk (\*) indicates statistically significant difference when compared to the negative control ( $p \leq 0.05$ )

**Table D.45:** Percentage cumulative transport of FITC-dextran 40 000 Da in the presence of 0.1% w/v *Aloe vera* whole leaf extract solutions

Time (min)	Percentage cumulative transport			Average	SD
	Well 1	Well 2	Well 3		
0	0.00	0.00	0.00	0.00	0.0000
20	0.19	0.19	0.19	0.19	0.0033
40	0.24	0.22	0.22	0.23	0.0084
60	0.25	0.24	0.23	0.24	0.0062
80	0.24	0.21	0.27	0.24	0.0215
100	0.26	0.24	0.25	0.25	0.0062
120	0.25	0.24	0.24	0.25	0.0053

SD = Standard deviation

**Table D.46:** Percentage cumulative transport of FITC-dextran 40 000 Da in the presence of 0.5% w/v *Aloe vera* whole leaf extract solutions

Time (min)	Percentage cumulative transport			Average	SD
	Well 1	Well 2	Well 3		
0	0.00	0.00	0.00	0.00	0.0000
20	0.22	0.21	0.21	0.21	0.0035
40	0.26	0.27	0.25	0.26	0.0074
60	0.28	0.27	0.26	0.27	0.0056
80	0.29	0.31	0.30	0.30	0.0076
100	0.29	0.31	0.32	0.31	0.0123
120	0.29	0.31	0.32	0.31	0.0139

SD = Standard deviation

**Table D.47:** Percentage cumulative transport of FITC-dextran 40 000 Da in the presence of 1.0% w/v *Aloe vera* whole leaf extract solutions

Time (min)	Percentage cumulative transport			Average	SD
	Well 1	Well 2	Well 3		
0	0.00	0.00	0.00	0.00	0.0000
20	0.19	0.20	0.19	0.19	0.0046
40	0.23	0.24	0.23	0.23	0.0025
60	0.24	0.24	0.23	0.24	0.0035
80	0.25	0.26	0.25	0.25	0.0069
100	0.25	0.26	0.24	0.25	0.0080
120	0.26	0.27	0.25	0.26	0.0074

SD = Standard deviation

**Table D.48:** Percentage cumulative transport of FITC-dextran 40 000 Da in the presence of 1.5% w/v *Aloe vera* whole leaf extract solutions

Time (min)	Percentage cumulative transport			Average	SD
	Well 1	Well 2	Well 3		
0	0.00	0.00	0.00	0.00	0.0000
20	0.14	0.14	0.14	0.14	0.0024
40	0.17	0.17	0.17	0.17	0.0041
60	0.19	0.19	0.18	0.19	0.0063
80	0.20	0.22	0.19	0.20	0.0107
100	0.19	0.21	0.19	0.20	0.0109
120	0.20	0.22	0.19	0.20	0.0116

SD = Standard deviation

**Table D.49:** Apparent permeability coefficient ( $P_{app}$ ) values of FITC-dextran (40 000 Da) applied with different concentrations *Aloe vera* whole leaf extract solutions

Groups	$P_{app}$ values			Average	SD	p-value
	Well 1	Well 2	Well 3			
<b>FD-40 Control</b>	$5.93 \times 10^{-8}$	$6.66 \times 10^{-8}$	$6.32 \times 10^{-8}$	$6.30 \times 10^{-8}$	$3.02 \times 10^{-9}$	-
<b>0.1% w/v <i>A. vera</i> whole leaf extract</b>	$5.68 \times 10^{-8}$	$5.21 \times 10^{-8}$	$5.76 \times 10^{-8}$	$5.55 \times 10^{-8}$	$2.40 \times 10^{-9}$	0.46810
<b>0.5% w/v <i>A. vera</i> whole leaf extract</b>	$6.62 \times 10^{-8}$	$7.41 \times 10^{-8}$	$7.84 \times 10^{-8}$	$7.29 \times 10^{-8}$	$5.05 \times 10^{-9}$	0.21405
<b>1.0% w/v <i>A. vera</i> whole leaf extract</b>	$5.85 \times 10^{-8}$	$6.15 \times 10^{-8}$	$5.62 \times 10^{-8}$	$5.88 \times 10^{-8}$	$2.16 \times 10^{-9}$	0.90932
<b>1.5% w/v <i>A. vera</i> whole leaf extract</b>	$4.63 \times 10^{-8}$	$5.36 \times 10^{-8}$	$4.45 \times 10^{-8}$	$4.81 \times 10^{-8}$	$3.95 \times 10^{-9}$	<b>0.02593*</b>

$P_{app}$  = Apparent permeability coefficient, SD = Standard deviation

Asterisk (\*) indicates statistically significant difference when compared to the negative control ( $p \leq 0.05$ )

## **APPENDIX E**

### **TRANSEPITHELIAL ELECTRICAL RESISTANCE (TEER) VALUES TO CONFIRM MONOLAYER FORMATION IN SNAPWELL® 6-WELL PLATES USED IN CONFOCAL LASER SCANNING MICROSCOPY (CLSM) EXPERIMENTS**

---

**Table E.1:** TEER values (as indication of intact Caco-2 cell monolayer,  $\geq 179 \Omega$ ; Pick *et al.*, 2013:10) before CLSM study with FITC-dextran 4 000 Da in the presence of 0.5% w/v TMC solutions (positive control) and 1.0% w/v *Aloe vera* gel and whole leaf extract solutions

Group	TEER value ( $\Omega$ )		
	Well 1	Well 2	Well 3
<b>Negative Control</b>	615	238	709
<b>0.5% w/v TMC (Positive Control)</b>	617	825	334
<b>1.0% w/v <i>A. vera</i> gel</b>	749	652	866
<b>1.0% w/v <i>A. vera</i> whole leaf extract</b>	680	707	745

**Table E.2:** TEER values (as indication of intact Caco-2 cell monolayer,  $\geq 179 \Omega$ ; Pick *et al.*, 2013:10) before CLSM study with immunofluorescent staining of F-actin with CytoPainter<sup>®</sup> Phalloidin iFluor 488 in the presence of 0.5% w/v TMC solutions (positive control) and 1.0% w/v *Aloe vera* gel and whole leaf extract solutions

Group	TEER value ( $\Omega$ )		
	Well 1	Well 2	Well 3
<b>Negative Control</b>	654	359	751
<b>0.5% w/v TMC (Positive Control)</b>	476	506	667
<b>1.0% w/v <i>A. vera</i> gel</b>	646	835	888
<b>1.0% w/v <i>A. vera</i> whole leaf extract</b>	879	822	986